Fall 12-2009

Detection and Measurement of Water Stress in Vegetation Using Visible Spectrum Reflectance

Arthur Zygielbaum
University of Nebraska-Lincoln, aiz@unl.edu

DETECTION AND MEASUREMENT OF WATER STRESS IN VEGETATION USING VISIBLE SPECTRUM REFLECTANCE

by

Arthur I. Zygielbaum

A DISSERTATION

Presented to the Faculty of

The Graduate College at the University of Nebraska

In Partial Fulfillment of Requirements

For the Degree of Doctor of Philosophy

Major: Geography
(GIS/Cartography/Remote Sensing)

Under the Supervision of

Professor Donald C. Rundquist and Professor Anatoly A. Gitelson

Lincoln, Nebraska

December, 2009

DETECTION AND MEASUREMENT OF WATER STRESS IN VEGETATION USING VISIBLE SPECTRUM REFLECTANCE

Arthur I. Zygielbaum, Ph.D.

University of Nebraska, 2009

Advisors: Donald C. Rundquist and Anatoly A. Gitelson

At any scale, from a single microbe to the planet that nurtures us, water defines our place in the universe. It provides the hydraulic forces needed to give plants structure, and the medium enabling photosynthesis, the basis for most life on Earth, to occur. Knowledge of plant water status is vital to understanding the state or condition of vegetation, information which is essential to disciplines as diverse as agriculture, geography, and climatology. Non-destructive and remote sensing of plant water status allows the gathering of such information across wide geographic extents and over long periods of time. Monitoring vegetation remotely requires an understanding of how reflected light may be used to infer the water status of plants. Several greenhouse experiments were performed using maize (*Zea mays* L.) and soybean (*Glycine max*. (L.) Merr. – hereafter called "soy") to examine changes in reflectance as these plants were subjected to water deficiency and, thereby, to water stress. These tests employed a new experimental design which allowed daily hyperspectral radiometric measurements from intact plants to be compared to representative determinations of relative water content and water potential obtained by destructive measurement techniques. It was discovered that a systematic increase in leaf-level visible light (photosynthetically active radiation – PAR) reflectance accompanied increasing levels of stress in maize, and, when relative water content was below 70%, in soy. This finding, resulting from some yet to be identified change in plant cells or internal leaf structure, is unexpected since there is no absorption of light by water molecules in the PAR spectral region. Despite extensive literature searches, no previous publication of the effect has been uncovered. The increase in PAR reflectance was shown to be useful in estimating the water status of maize, and, when RWC was less than 70%, of soy. More work is needed to determine if this effect can be used to estimate water status from the canopy level or above.

Dedication

This dissertation is dedicated to my wife, Christine Zygielbaum, for her love, help, support, encouragement, and strength. And for sharing the adventure that is my life.

Author's Acknowledgements

This dissertation is the final step in a dream I have had for nearly 35 years, to complete a PhD. I was too distracted by work and life to complete the program I had started nearly four decades ago. Now, with the help and encouragement of close and supportive colleagues and friends, the goal has been achieved. It would be difficult to name all of the people who influenced my academic and career life. So I have decided to name a few who helped me along the way and who took an active role in my degree program at the University of Nebraska-Lincoln. My fear is that I missed someone, because I have been so busy and under so much self-induced pressure. If that is the case, I am deeply sorry.

First, of course, I need to thank my family. Christine Zygielbaum, my wife, is the person to whom this research and this document are dedicated. She has been my steadfast partner in this adventure and has never failed to do what was needed, to encourage when necessary, or to be sympathetic when I had some, usually unfounded, concern. My children, Debby and David, although grown and living their own lives, did not have the benefit of as much of my time as I would have liked to give them. But they expressed their understanding and support as I pursued my goal. I am indebted to my family for allowing me the chance to devote my time to my education and research. No one could ask for a better family. They are truly my closest friends.

Next, I need to recognize the late Dr. Waldo Hamlet Furgason. Dr. Furgason was a professor of zoology at UCLA where I pursued my undergraduate education. He became a good friend and we stayed close until his death in May 1977. Dr. Furgason and I would engage in long discussions about science, its history, and its underlying ethics.

Always encouraging, he was quick to point out a logical flaw and strong in his advocacy of scientific method in the pursuit of truth. He gave me a life-long respect for biology. I would have never have guessed that the end of my formal academic career would cross from "rocket science" and computers back into life sciences.

Dr. Peter Lyman, retired Deputy Director of the Jet Propulsion Laboratory, has been a good friend and colleague for decades. He taught me to think critically, to not accept face value, and to not be afraid of taking an unfamiliar or unpopular path. His encouragement is deeply appreciated. Peter's late first wife, Yvonne, was also someone very special in my life. Her philosophy was to take on problems and not to run from them. If I was griping about something – whether it be work or something personal – her comment always was, "Well, what are you going to do about it?" Thanks, in part, to her influence, I seem to have kept myself busy in many endeavors.

There were five members on my PhD committee. As a group, they were wonderfully responsive and available. They worked well and congenially together. The few disagreements or concerns expressed were quickly settled. Their decisions were always clearly made on the basis of my success as a student and as a researcher. As friends, I always knew I could count on them. It was a privilege and a very deep honor to have their counsel and their support.

Dr. Donald C. Rundquist, committee co-chair, has been a friend and colleague for at least a decade and a half. We met in the process of creating a NASA program to use space data and technology in education. Don is the penultimate educator and the best friend anyone can have. He cares deeply about his students and his field of research. When I asked him about returning to school to pursue a PhD, he never hesitated in

supporting the idea. He helped mold my research and occasionally provided the cautious word or mild rebuke necessary to keep things on track. He and his wife Carol became close friends with Chris and me. They can always be counted on. And they help share the burden when life brings difficult times and saddening events. Without Don's encouragement, friendship, scientific skills, and occasional stubbornness, my research would not have come to fruition and my degree would not have been completed.

Dr. Anatoly A. Gitelson, committee co-chair, is among the most skilled scientists I have ever had the honor of working with. His understanding of scientific principles and the level of knowledge needed to pursue significant research cannot be challenged. He couples his abilities to teach with a quiet sense of humor that makes any interaction a rich experience. Anatoly cares about his students, their education, and their lives. He gave me the technical underpinnings to make my work possible. I will always cherish our many arguments. They were scientific and technical and never personal. But I will never fail to smile and feel good with the remembered sound and image of him saying "No! No! No! . . . . Well maybe." I am indebted to Anatoly for his friendship and for his mentoring. I would be remiss in not mentioning Anatoly's wife, Galina Keydan. Galia's office is close to mine. She took time to ask how I was doing, to question why I looked so tired, and to tell me that I was doing well, but needed to take better care of myself. Galia and Anatoly are life-long and cherished friends.

Dr. Timothy J. Arkebauer, committee member, and I became acquainted when I took his course in plant and water relations. My naïve thought was that a course on how water moved through plants would take, at most, an hour. Tim's skilled and engaging teaching removed that thought very quickly. He took the class through the intricacies,

science, and magic involved in how plants use water. His class caused me to develop an interest in plant water status. The result is this dissertation. Tim is now a colleague and a friend. I never fail to enjoy or to learn from our meetings or lunches. He worked hard with me in the greenhouse to help identify the conditions of the plants and to engineer the experimental processes we used. His love of science in general and his deep knowledge of biology serve him well and made my research a delightful endeavor.

Dr. Merlin P. Lawson, committee member, was introduced to me by Don Rundquist not too long after I moved to Lincoln. He immediately became a friend. Merlin is a master of several fields. His understanding and love for climatology and meteorology are infectious. Merlin's skill as a photographer renewed my interest in that avocation. He is always encouraging, able to poke carefully phrased questions, and ready to answer questions about science or administrative issues. Merlin is a special friend, gifted mentor, and valued colleague.

Dr. Sunil G. Narumalani, committee member, is a talented teacher who taught me about image processing. He encouraged me and occasionally cajoled me. Sunil is good at bringing you back to basics to understand how what you are doing fits into the bigger picture. I appreciate his trust in me as we talked about administrative and career issues. I appreciate his friendship and willingness to do whatever was needed to help me succeed. Any student would be fortunate to have a professor like Sunil. Any person would be fortunate to have a friend like him.

Although I had interactions with many faculty members outside of my committee, there were two who stand out. Dr. Elizabeth Walter-Shea was the first professor I had in my "new" career as a graduate student. She taught me about microclimate, and later,

about solar radiation. I am indebted to her as an excellent teacher and as a scientist. She spent many hours answering questions, making suggestions about my research, and encouraging me when necessary. I am very fortunate to have Betty as a friend and colleague.

Dr. Kenneth G. Hubbard taught a course in the instrumentation of atmospheric research. He gave me an appreciation of the engineering and science involved. He supported me with needed data and advice. Ken is also an inspiring friend. Many years ago, he received a kidney from his wife. Earlier this year his liver failed and he nearly died waiting for a kidney and liver transplant. His courage and the love and support of his wife, Susan, are things that make for epic stories. Whenever I faced a difficult time or felt sorry for myself, thinking of Ken would put my world back into perspective. I prize our friendship.

Not too long after he joined UNL, I met and had a chance to work with the Dr. Prem Paul, the Vice Chancellor for Research. He and his wife Missi became friends with Chris and me. We have shared many good times over the years. They have both strongly encouraged my return to school. Prem was ever saying “stay focused” and “you’re doing great!” The university has done well in research under Prem’s guidance. He has received many accolades, but he always finds time to support people. Whether friends, employees, or colleagues, he is there for them. If there is a problem he can help with, it gets helped. If there is rough spot that needs some motivating language to overcome, Prem is there. I take pride in our friendship.

Dr. Richard Sincovec, ex-chair of the Computer Science and Engineering department, his wife Deanna, Dr. Richard Hoffmann, ex-dean of the School of Arts and

Sciences, and his wife Vicki are four very close friends who also helped make my program successful. Rich and Dick were available to answer questions and to provide scientific, technical, or administrative advice. All four were encouraging and took obvious pleasure in my successes. They occasionally got me away from my computer and reminded me that I had to keep social interactions alive despite the pressure I was under. It will be difficult to repay them for all their kindness and caring.

Now let me turn to the people who worked with me in the field and lab. Dave Scoby is Dr. Arkebauer's technician. He grew the plants I used and took part in the experiments. There never seemed to be a task too hard or too trivial for Dave. I appreciate his knowledge about plants, his hard work and his conscientious efforts on my behalf. Bryan Leavitt, a research assistant in the Center for Advanced Land Management Information Technologies (CALMIT), seemed always available to help me with instruments and to plan research strategies. Bryan's knowledge of the process of doing science was invaluable. He also has a special skill at posing hard questions that lead to more productive and stronger research methods. I am indebted to Bryan for his help and his friendship.

Many other people took time to work with me in the greenhouse or in the field as I pursued my research. Way beyond just physical help, they all asked questions and made suggestions that improved whatever I was doing. Drew Kessler, Paul Merani, Dr. Wesley Moses, Sharmistha Swain, Andy Boateng, Daniela Gurkin, Yi Peng, and Dr. Abby Stillwell, are or were graduate students, who took time out of their busy lives to help me measure plants, drag pots around, and do the many things that were easier with two or more people. I also need to acknowledge Rick Perk, who manages the airborne

remote sensing program for CALMIT, for his friendship, skilled knowledge, and readiness to help. Dr. Tahir Sawar, a visiting professor from Pakistan and Dong Suo, an undergraduate intern from China, contributed selflessly to my work in the greenhouse. All of these people would respond to a phone call and spend hours in a sometimes very hot and very uncomfortable greenhouse or in the very noisy cab of a big machine. Their contributions to the work reported here are manifold and appreciated.

Finally, I would like to thank the people of the UNL Libraries for their ability to provide information, papers, and books whenever I needed them. Through the Illiad system, I could quickly retrieve even obscure and old papers with amazing ease. Just before submitting this dissertation, I found that I had difficulty in obtaining permission to use two drawings from a book. One of the library staff, Paul Royster, created new drawings to use in their stead (Figures 3-1 and 4-1). I appreciate the extraordinary assistance.

To all of you, for helping to make a dream come true, I am deeply grateful.

Arthur I. Zygielbaum

December 4, 2009

Table of Contents

List of Figures

List of Tables

Chapter 1: Introduction

1.0 Chapter Contents

1.1 Chapter Overview

Water defines our place in the universe at any scale, from a single microbe to Planet Earth. It facilitates the chemistry and energy exchange required by all life. Maize, one of the subjects of this dissertation, is over 80% water. The human brain is nearly 70% water. In terms of volume and weight, water is the raw material required in the largest quantity by agriculture (Boyer, 1995). Humans are particularly vulnerable to a lack of water, yet twenty percent of the human population or 1.2 billion people are estimated to live in areas where sustainable water use has been reached or exceeded (World Economic Forum, 2008). Because water is a precious and dwindling resource, great care, based on knowledge, is required to manage and use it efficiently.

Along with sustaining life, water and vegetation influence the climate in which we live. Vegetation accesses water resources below ground, at places normally protected from evaporation, and vents it to the atmosphere through evapotranspiration. This influences the creation of clouds which in turn influences rainfall (Claudio et al., 2005). Hence, vegetation plays an intimate role in the movement of water and in the exchange of energy between land and air (Dekker, 2007). Since vegetation covers about 70% of the

earth's land surface (Jensen, 2007), its participation as a factor in climate and local weather cannot be minimized.

Understanding the water status of plants, the quantity of water in the leaves and the quantity required to support photosynthetic and metabolic processes, is vital to understanding the status of vegetation. This knowledge can be used for activities as diverse as assuring efficient use of water for irrigation, managing water resources for communities, measuring the risk of forest or brush fires, and maintaining the health of ecosystems (Serrano et al., 2000).

Obtaining the data needed to do these things requires sensing technology to monitor water status. The areal extent of vegetation is great, so the cost of providing a sufficient number of local sensors to obtain the needed data is prohibitive. That coupled with the inaccessibility of many vegetated areas requires the use of remote sensing technology to determine water status (Claudio et al., 2005). The research reported in this dissertation is focused toward identifying signatures and patterns in the light reflected from plants that are indicative of plant water status.

Measuring the water status of a plant is a surprisingly complex topic. The status is a combination of the amount of water contained in the plant, the need the plant has for water based on where it is in its life-cycle, and the dryness of the ground and air in which it is living. The amount of water is usually determined scientifically by means of a gravimetric process to determine the plant relative water content (RWC). A plant's need for water is typically ascribed to understanding the leaf water potential measured either through complex instrumentation or a sometimes challenging pressure chamber

technique. None of this technology can directly provide a measure of the water status of vegetation in a large geographic region or in an area inaccessible to researchers.

Remote sensing, which could provide such information, involves the use of electromagnetic radiation reflected or emitted from an object to ascertain its characteristics. Observing the spectrum of light returned from vegetation has been successfully used to determine the concentrations of vital pigments, such as chlorophyll (Gitelson et al., 2003). The effects of water on the reflected spectrum have been studied in an attempt to measure the amount of water in plants. Water causes strong absorption of light in the near and middle infrared (NIR, MIR) portions of the spectrum and causes changes in the level of reflectance throughout the spectrum (Zygielbaum et al., 2009). Attempts to develop indexes based on a mathematical function of the amount of reflected light at various wavelengths for use as a proxy of water status have met with limited success. Most of these efforts have relied upon the absorption by water molecules in NIR and MIR. The results have not achieved the precision measurements necessary to benefit agriculture by detecting early stages of water stress, before the vegetation undergoes irreversible damage.

Thus, the problem driving the current research is lack of a sensitive, accurate, practical, and cost effective technique to estimate plant water status based on measurements of reflected light. This work attempts to develop and test such procedures.

1.2 Determining Water Status of Plants – The States of the Art and Practice

The movement and use of water within plants are, in themselves, surprisingly complex topics. At the simplest level, a plant must extract water from the soil and distribute it throughout its structure. Water is needed for metabolic processes, to

transport nutrients, and to supply the hydraulic pressure needed for plant growth and structural integrity. The plant must control the level of water within its cells and structures despite significant variations in soil and atmospheric conditions. When those conditions become too extreme, the plant cannot maintain a minimum water level and becomes stressed.

Two major characteristics of water in plants are typically discussed in textbooks and literature. The first is in terms of quantity. The second is in the terms of "energy status."

Quantity relates to the amount of water within the elements of the plant. It is described as total water content, water per unit volume, water per unit surface area – equivalent water thickness (EWT), water weight as a fraction of total plant weight, relative water content (RWC), or some variations thereof. EWT is the amount of water per unit leaf area. It is the hypothetical thickness of a single layer of water averaged over the whole leaf area:

$$EWT = \frac{FW - DW}{A} \quad (g\,cm^{-2}) \tag{1-1}$$

where A is the area, FW is the fresh weight of the leaf, and DW is the dry weight. The difference is the water weight. RWC compares the actual leaf water content against the content at full turgor:

$$RWC = \frac{FW - DW}{TW - DW} \tag{1-2}$$

where TW is the weight of the leaf at full turgor. EWT and RWC are prominent in the literature.

Energy status of water in plants is described by analogy to electrical potential and current (Nobel, 1983). Water potential represents the work involved in moving one mole of water at constant temperature and pressure from the conditions at some point in a plant, for example, to a pool of pure water at atmospheric pressure and at some zero reference value for gravity (analogous to zero volts in electricity). Water potential is often measured in units of pressure. The primary contributors to total water potential are hydrostatic or pressure potential (Ψ_P), osmotic potential (Ψ_Π), and gravitational potential (Ψ_g).

$$\Psi = \Psi_p + \Psi_\Pi + \Psi_g \qquad (1\text{-}3)$$

Total water potential varies directly with hydrostatic and gravitational pressures and inversely with osmotic pressure. The difference in water potential between the leaves and roots supports water flow between the two. Primarily because of transpiration, leaves continually lose water. Water loss lowers the hydrostatic pressure and therefore the leaf water potential. Osmotic pressure differences across membranes in the plant also tend to cause the water potential in the leaf to be more negative with respect to the roots.

The closure of leaf stomata, which accompanies water stress, is an attempt by the plant to avoid the loss of water. While this could result in a stabilization of the water potential, the plant increases the solutes in the water within the cells thereby increasing osmotic pressure and decreasing leaf water potential. Closed stomata decrease gas exchange at the leaf surface. This also decreases the amount of the water vapor near the leaf surface. The cooling effects of transpiration are lost causing temperatures to increase. Gross primary production of the plant eventually decreases due to dehydration

effects on the mesophyll cells. Water deficit in the leaves causes a loss of hydrostatic pressure. While normal variations in cell volume, such as diel cycles, can be accommodated by cell wall elasticity, at some point, the cells shrink enough to cause leaf wilt (Taiz & Zeiger, 2006a).

For the purposes here, water stress is considered to be a deficit of available water which causes a decrease in plant growth rate or rate of photosynthesis. Wilting would be an extreme case of water stress. In the literature, water potential is the most often quoted indicator of stress. Relative water content (RWC) is also considered an indicator. Hsiao (1973) defined mild water stress as a lowering of water potential by several bars (one bar is 0.1 MPa) or of RWC by 8-10% below that in a well watered plant. Moderate stress referred to water potential decreasing 12-15 bars (1.2-1.5 MPa) or RWC decreasing by 10-20%. Severe stress was indicated by water potential lowered by more than 15 bars (1.5 MPa) or RWC more that 20%. Desiccation was defined to be the state where more than 50% of the tissue water was removed.

Water potential has limitations as an indicator of water stress. The same tree may have high water potential at its topmost leaves and low water potential at its bottom leaves, but both sets of leaves would be considered healthy and growing. Similarly, water potentials indicating stress in some species do not correlate with stress in others. Some have argued that soil water potential is a good indicator of plant water stress since it is an indicator of the amount of water available to the plant. However, the relative water content of a plant can remain stable despite a decrease in the soil water potential due to water control mechanisms. The case is made that cell elasticity or cell turgor is the real indicator of water status and that RWC is a good proxy for cell turgor (Jones, 2006).

Relative water content and water potential are related in moisture release graphs. The form of the relationship is not linear, is different for differing plant species, and may differ within a species for plants grown under differing environmental conditions (Diaz-Perez, et. al., 1995; Acevedo, et. al., 1979). An example, taken from a paper by Acevedo (Acevedo et al., 1979) is shown below (Figure 1-1). These graphs depict relative water content versus water potential from twice daily measurements for unirrigated sorghum and maize. Note that the same water potential corresponds to differing levels of RWC in each plant, i.e., there is a diurnal hysteresis in the water potential versus RWC relationship.

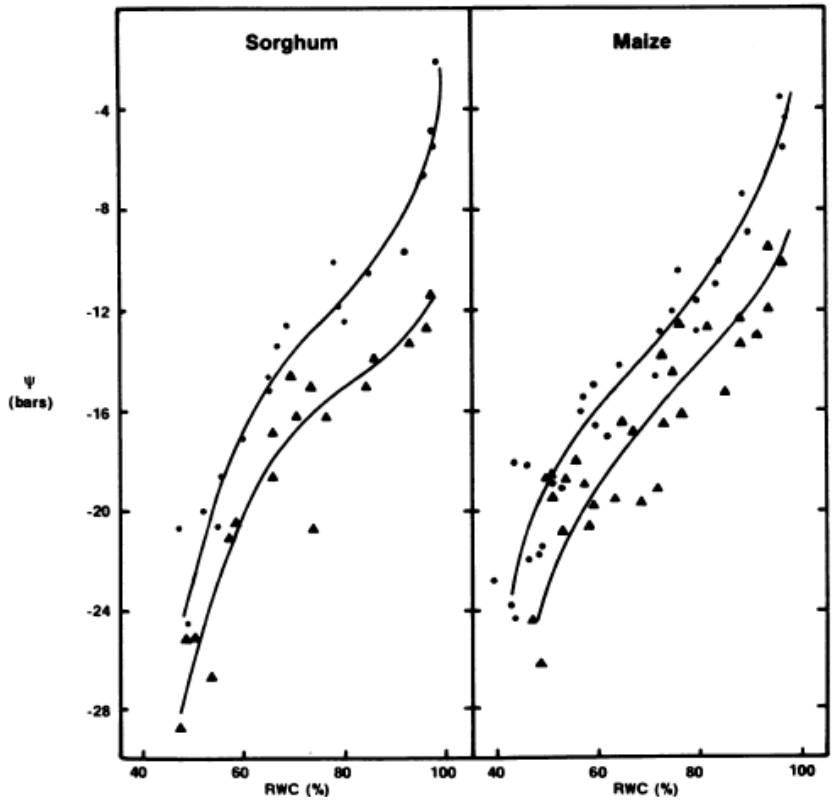

Figure 1-1. Comparison of relative water content and water potential (ψ) measured twice per day in unirrigated sorghum and maize. Points mark the morning measurement; triangles the afternoon measurements. (Acevedo et al., 1979). Copyrighted by and reprinted with permission of the American Society of Plant Biologists.

Without reference to full turgor water potential (Ψ=0), it would be hard to correlate vegetation water content or EWT to levels of stress. However, EWT can provide a good indicator of available fuel for fire potential. If RWC can be retrieved, it would provide a good proxy for turgor pressure and have a non-unique, but determinable, relationship with leaf water potential.

1.2.1 "Ground Truth" Measurements

If changes in water status impart identifiable signatures or changes in characteristics of the reflected light (through changes in absorption efficiency or light scattering), then determination of water status by remote sensing is possible. To be useful, the relationships between these signatures and actual plant water status must be verified. The measurement of actual plant water status, known in the vernacular as obtaining "ground truth," is an important topic. "Ground truth" measurements are the determination of some parameters associated with plant water status by physical or chemical means.

1.2.1.1 Water Content

Retrieval of water content information is usually accomplished by simply weighing leaf samples (whole leaves or leaf punches) to determine the fresh weight. These samples are dried in an oven and weighed again to obtain the dry weight. Sample water weight is the difference between fresh and dry weights. Referring to Eq. 1-2, relative water content is determined by adding an intermediate step where the leaf or punches are placed in water for a period of about 12 hours. These samples take up water during that time to reach full turgor. After their surfaces are quickly dried, the samples are weighed to obtain the full turgor weight. Differencing full turgor weight and the dry

weight yields the full turgor water weight in the leaf. The relative water content is simply the percentage of the original sample water weight compared to the full turgor water weight (Barrs, 1968).

There are many error sources in this process (Barrs, 1968). As soon as the leaf is picked or punches taken, the sample begins to lose water. When the sample is dried, and before it is weighed, it tends to accrete water. The level of error can be 10-20% depending on temperature, humidity, and the length of time the sample is exposed before weighing (Barrs, 1968). Other error sources are more basic: weight changes due to dirt or other contaminants, the difficulty of maintaining a clean environment for weighing, etc.

1.2.1.2 Water Potential

Several instruments are available to determine water potential. The most important are the thermocouple psychrometer and the pressure bomb. Thermocouple psychrometers works by sealing a plant tissue sample in a small chamber with a thermocouple and allowing it to reach equilibrium. At equilibrium, the water potential of the sample is equal to the water potential of air (related to relative humidity). A cooling current is passed through the thermocouple and water condenses on the junction. When the current is shut off, subsequent evaporation cools the thermocouple, inducing current across the junction. The evaporation rate determines the degree of cooling and the magnitude of the current or output signal. The plant sample output is then compared to similar outputs obtained from calibration standards of known water potential. Sensitivity of the measurement to temperature fluctuations is a significant error source. Errors of

0.01 °C can correspond to 5-10% measurement errors. This technique is practical only in a laboratory setting (Taiz and Zeiger, 2006b).

A more common technique is the pressure bomb where an excised leaf is placed within a sealed chamber with its stem exposed to air through a seal. Since the water in the leaf and stem was under tension while the leaf was transpiring, water will be sucked into the leaf when the stem is cut. As pressure is increased in the chamber, water will flow back to the cut end. The chamber pressure at which the water appears at the end of the stem is equivalent to the water potential within the leaf. It is difficult to find assessments of error in pressure bomb measurements. Error sources include crushing the stem and interfering with the free flow of water through the xylem, air leakage around the stem, and the user's ability to distinguish the appearance of water on the cut stem (Jones, 2006; Milburn, 1979).

Stomatal closure can be determined by measuring leaf surface temperature, water vapor pressure near the surface, or stomatal conductance. Such measurements are easily corrupted by air movement. Porometers avoid this problem by measuring the rate of water vapor flow through the stomata. It is difficult to ascertain how accurate they are from the literature. Error sources include the accuracy of ambient relative humidity measurements and the seal between the instrument and the leaf surface (Weatherley, 1966).

1.2.2 Remotely Sensed Measurements

The character of light reflected by leaves is influenced by pigments, internal structure, and water. The spectrum of light can be divided into three major regions: Photosynthetically Active Radiation (PAR), Near-infrared (NIR), and Mid-infrared

(MIR). Light in PAR wavelengths (400 nm to 700 nm), sometimes called the visible spectrum, provides the energy required for photosynthesis in plants. Reflectance in PAR is dominated by absorption by pigments such as chlorophyll. NIR (800 nm to 1300 nm) reflectance is largely influenced by plant cell and canopy structures and to a lesser extent by water. In the MIR (1300 nm to 3000 nm), water absorption dominates reflectance and the structure has a secondary influence.

Most of the light reflected by plants comes from plant structural elements. For example, leaves devoid of pigments reflect in the optical very nearly the same as in the infrared. The air/cell interfaces account for about 80% of the reflectance. Other intracellular interfaces account for about 8% of the reflectance at 800 nm. Most of the remaining reflectance is from the leaf surface (Woolley, 1971). Light entering the leaf is reflected due to the large difference in refractive index between water in the cells and air in the intercellular spaces. It is also scattered by interaction with cell structures with dimensions similar to the light wavelength. Light not absorbed by pigments as it traverses the leaf will reemerge as observed reflected or transmitted light (Gates, 1965).

Pigments such as chlorophyll, anthocyanin, and carotenoids absorb strongly in the blue spectral region (~450 nm), anthocyanin also absorbs in the green (~ 550 nm), and chlorophyll absorbs strongly in the red (~670 nm). The slightly weaker pigment absorption in the green, allows healthy vegetation to show a green color. Pigment absorption is virtually nonexistent in near- and mid-infrared wavelengths. Although water absorption in the PAR region is very weak, water influences leaf reflectance significantly at near- and mid-infrared wavelengths. The direct effect, due to the interaction of light with water molecules, is weak absorption near 970 nm and 1200 nm,

and strong absorption near 1450 nm and 1960 nm. As a leaf is allowed to dehydrate, absorption in these bands decreases and reflectance increases correspondingly.

Secondary effects occur at spectral wavelengths where the water molecule shows little absorption. These effects are thought to result from the influence of hydrostatic pressure or turgor pressure on the shape of the leaf, the characteristics of the internal inter-cellular air spaces in the leaf, and the spacing among leaf elements. As the leaf is dehydrated, absorption in the optical region decreases. The peak sensitivity in terms of change with decreasing water is in the regions near 480 nm and 680 nm. These two peaks correspond to absorption maxima for chlorophyll (Carter, 1991). What appear to be changes in reflectance near 680 nm may, however, actually be changes in chlorophyll molecule florescence as photosynthesis rates are modulated by the amount of available water (Maxwell & Giles, 2000). In any case, the spectral characteristics of a leaf before dehydration and after rehydration are nearly the same. This would argue that the actual amount of chlorophyll was relatively unchanged. The conundrum may be due to changing optical paths as leaf structures shrink and to chlorophyll deterioration in extreme dehydration. In any case, chlorophyll amounts may change due to phenology, local growing conditions, and nutrient levels as well as water status. Therefore, indices based upon apparent correlation with the chlorophyll peaks are suspect.

As water content decreases within a leaf, the reflectance from that leaf changes throughout the PAR, NIR, and MIR spectrum (Figure 1-2). Increased reflectance in the MIR is most likely due simply to the fewer water molecules available to absorb water. The cause for the changed reflectance in NIR is less clear. The weak water absorption lines at about 920 nm and 1200 nm are tied to water molecule density, but the influence

over this region of the spectrum is relatively small. Changes in the PAR related to decreasing water content, clearly visible in Figure 1-2, have been reported in many papers (e.g., Carter, 1991, 1993; Yu et al., 2000; Ceccato et al., 2001; Aldakheel and Danson, 1997). There is very little water molecule absorption in this region so the reason for these changes is not clear. The effect has been ascribed to changes in leaf thickness, decrease in chlorophyll, error in measurement, and changes in shape caused by loss of leaf turgor.

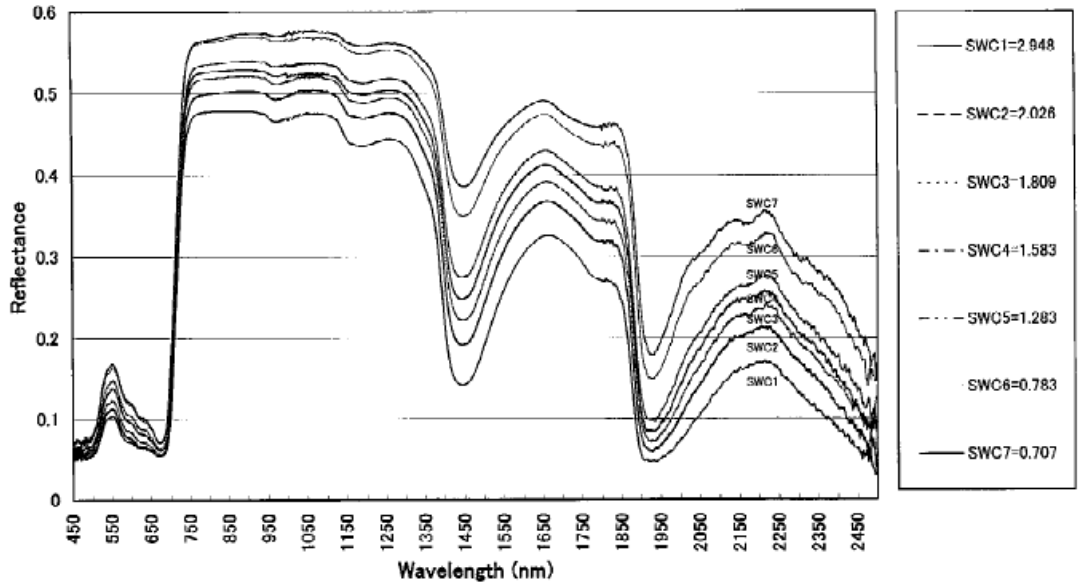

Figure 1-2. Changes in leaf reflectance as water content decreases. Specific water content (SWC), units of kg/kg, relates leaf water weight to leaf dry weight (Yu et. al., 2000). Copyrighted by and reprinted by permission of Springer Publishing.

Various spectral indices have been proposed as proxies for plant water content. Some indices are reported to correlate well with EWT and some with RWC. No literature was found that proposed an index proxy for water potential.

Non-spectral proxies are also suggested. Remotely sensed changes in leaf surface temperature are possible, but suffer from errors due to air movement and the inability to ascertain air temperature and relative humidity remotely. Observation of the thermal IR

bands has also been suggested. However, the many variables in plant characteristics and environmental conditions preclude using infrared thermography for anything other than comparative studies within an image (Jones et. al., 2002).

Because of the strong influence on reflectance by water molecule absorption, most efforts to remotely or nondestructively retrieve water content utilize NIR and MIR wavelengths (Zygielbaum et al., 2009). For example, the Moisture Stress Index (MSI)

$$MSI - {R_{1.6}}/{R_{0.82}}$$

and the Leaf Water Content Index (LWCI)

$$LWCI = \frac{-\ln[1-(R_{1.6}^{D} - R_{1.6})]}{-\ln[1-(R_{1.6}^{D} - R_{1.6}^{FT})]}$$

where $R_{1.6}^{D}$ is the dry leaf reflectance at 1.6 μm (1600 nm) and $R_{1.6}^{FT}$ is the full turgor reflectance at 1.6 μm, have been proposed as proxies using these wavelengths. MSI correlates well with RWC, but the minimum detectable change reported is 50% – far from a desirable 15-20%. MSI appears to correlate with Leaf Area Index (LAI) and only indirectly with water content. The index fails because it does not take into account a base level of reflectance due to the vegetation itself. The LWCI also correlates well with RWC and has good sensitivity but requires specific knowledge of reflectance at two hydration points. Therefore it is not a good candidate for remote sensing applications (Hunt and Rock, 1989). Indices consisting of reflectances at single wavelengths, 1483 nm and 1430 nm, and simple ratios, such as ρ1430/ρ1650, fared no better. Results indicate 20-30% errors in estimation of RWC (Yu et al., 2000).

Indices reported in the literature include the following set (Table 1-1) which was optimized for use with AVIRIS data (Serrano et al., 2000).

Index	Formulation
NDVI	$(R_{895}-R_{675})/(R_{895}+R_{675})$
WI	R_{895}/R_{972}
NDWI	$(R_{857}-R_{1241})/(R_{857}+R_{1241})$
EWT	R_{867} through R_{1049}
WT	R_{867} through R_{1088}
MSI	R_{1599}/R_{819}
NDII	$(R_{819}-R_{1649})/(R_{819}+R_{1649})$

Table 1-1. Spectral reflectance indices and precise AVIRIS bands. (Serrano et. al., 2000)

Of these indices, the Water Index (WI) and the Normalized Difference Water Index (NDWI) provided coefficients of determination (R^2) of 0.88 and 0.86, respectively, against canopy RWC when vegetation coverage was greater than 70%. Correlation coefficients reported were higher than 0.93 ($p<0.001$). Serrano et al. (2000) concluded that either WI or NDWI could be used to recover RWC by assuring that the instrument field of view was characterized by vegetative fraction. Their data sets were sparse, however, and it was difficult to ascertain sensitivity of these indexes to small changes in RWC.

Error sources affecting the accuracy of models and resulting indexes include the variability of water content across species, across growth environments, and across the developmental state of the vegetation. Changes in pigments also mimicked presumed water-change spectral signatures. Insensitivities resulted from plant mechanisms maintaining water levels in leaves despite low soil moisture and the relatively small water level changes that indicated stress.

Despite a modicum of success in the use of indices based on NIR and MIR wavelengths, there are distinct advantages if a model could be found based on PAR wavelengths. Infrared reflected radiation is greatly influenced by plant architecture,

density, and leaf structure. This impacts estimation uncertainty (Zygielbaum et al., 2009). Also, atmospheric attenuation of infrared light is substantially greater than attenuation of PAR (Jenson, 2007). Along with all of these considerations, it is important to note that sensors in the PAR region tend to be cheaper than infrared sensors. They also do not require cooling.

The PAR region was used for the Photochemical Reflectance Index (PRI, Gamon et al., 1992; Thenot et al., 2002). PRI has been investigated as a proxy for water status retrieval. However this index has been shown to be sensitive to changes in chlorophyll, which would confound such use (Thenot et al., 2002).

Inversion of the PROSPECT leaf model (Jacquemoud & Baret, 1990) to determine water content is an interesting investigational approach. PROSPECT is a mathematical model and implementing algorithm for synthesizing leaf spectra. The leaf is represented as a stack of homogeneous plates. The plates are described by a set of parameters including chlorophyll concentration, non-chlorophyll pigment concentration, dry matter concentration, and water content. A structural parameter, "N," is the number of plates involved in the simulation.

Many papers cite PROSPECT. They describe the use of the model to identify biochemical parameter changes or the recovery of water content through iterative inversion. One paper in particular (Aldakheel and Danson, 1997) showed a data set created by observing a leaf dehydrate over several hours. In trying to match the PROSPECT simulation to the real spectra, they discovered that varying the PROSPECT water content parameter alone affected the near- and mid-infrared. Changes in the PAR region were not correctly modeled. As the water content parameter is changed,

PROSPECT models only the direct spectral effects of water absorption and not the secondary effects caused by physical changes. Aldakheel and Danson (1997) varied the "N" parameter in proportion to water content to obtain appropriate changes in the optical spectrum. With this adjustment, the PROSPECT simulation matched their empirical data quite closely. While interesting, there was no follow-up to develop a process to use the PAR reflectance to derive water status.

Although there were many observations of a relationship between PAR reflectance and water status, and despite the advantages in using the PAR spectrum, no paper could be found that quantified the relationship and defined a model to use PAR for the retrieval of plant water status. To the best of our knowledge, the first paper reporting such findings was published by this author and Professors Gitelson, Arkebauer, and Rundquist at the University of Nebraska-Lincoln (Zygielbaum et al., 2009) as a product of the research reported in this dissertation.

1.3 Objectives of Research

The stated goal of the research reported here is to study the leaf optical properties of water-stressed and non-stressed maize (Zea mays L.) and soybean (Glycine max. (L.) Merr. – hereafter called "soy") using reflectance spectroscopy to establish the relationships among PAR, NIR, and MIR reflectance and water stress, and to use those relationships as the basis for non-destructive and remote retrieval of plant water status.

The specific objectives of the research are to:

1. Detect and quantify any systematic relationships between leaf-level PAR reflectance and water stress.

2. Given the existence of such systematic relationships, use leaf-level PAR reflectance to develop techniques, in the form of spectral transformations, for accurately estimating plant water status.

The research proposed is designed to provide new insight into the use of the visible spectrum to determine plant water status. Carefully designed and controlled experiments with maize and soy are the data sources for this research. Analysis of these data will identify statistically significant and repeatable changes to the reflectance spectrum that can be linked to changes in water status. In turn, these will provide the basis to identify models or proxies based on reflected light that can be used to retrieve biophysical parameters, like RWC and water potential.

The proposed research offers a potential for tools that can improve the management of water for crop irrigation. These tools will initially be in the form of sensors that can operate at the leaf-level. Ultimately, if the techniques prove successfully extensible, this work will lead to sensors used from the vantage of aircraft or spacecraft. Such sensors will allow accurate regional or even global mapping of vegetation water status. Beyond this practical use, it should be noted that the physiological and anatomical characteristics underpinning the identified effects will be subjects of speculation and candidates for significant future research. The spectral signatures and patterns upon which any findings are based would certainly result from changes in leaf anatomy and/or physiology driven by water deficit. Photoprotection mechanisms invoked to prevent damage to photosynthetic processes and structures are potential signature sources (Kasahara, et al., 2002; Björkman & Powles, 1984; Long, et al., 1994). Damage to cellular membranes and structures resulting from water deficit and excessive light (Ristic

& Cass, 1992; Utrillas & Alegre, 1997) may also play a key role. It is also possible that changes in dissolved solute concentration, one response to water stress, changes the index of refraction within the cell and thereby the reflectance of light. Because of this physiological tie, the efforts reported in this dissertation may provide new tools to investigate the mechanisms facilitating and protecting photosynthesis in plants.

1.4 Organization of the Dissertation

The organization of this document follows, in general, the progression of the research and analyses performed. Where appropriate, papers submitted and published or submitted and under consideration are included within the chapters.

The experimental design and the methods used for all experiments are the subject of Chapter 2. This covers greenhouse experiments on maize and soy, and field experiments covering maize. Pictures of procedures and instruments are also included. In addition, this chapter includes a summary of software and technique innovations made during this research effort.

Chapter 3 describes observations obtained in greenhouse leaf-level experiments with maize plants. This chapter focuses upon the observations made during several experiments and the findings from subsequent data analysis.

Chapter 4 describes observations obtained in greenhouse leaf-level experiments with soy plants. Analogous to Chapter 3, this chapter includes observations from experiments and findings from subsequent data analysis.

Chapter 5 reports on the retrieval of plant water status from the reflectance spectra measured in the maize and soy experiments.

The concluding chapter, Chapter 6, summarizes the research conclusions and suggests additional research to extend and refine these results.

Published papers, books, and website sources used as references for research and analysis are denoted in the reference section.

Chapter 2: Experimental Design and Methods

2.0 Chapter Contents

2.1 Chapter Overview

Leaf-level spectral observations are a typical starting point in the development of techniques to remotely sense some characteristic of vegetation. Unlike canopy-level observations, leaf-level spectra are not confounded by light reflecting from soil, standing water, barbed wire fence, etc. Leaf-level measurements can also be made without needing to compensate for attenuating effects of atmospheric constituents. Water vapor, for example, absorbs much of the light at the water molecule absorption wavelengths. Calibrating for atmospheric effects takes significant effort. For the first stages of research into reflectance, it makes sense to simplify the effort as much as possible. For these reasons and others, a decision was made to focus the current research on leaf-level analysis.

If one is interested in a leaf-level study of the water status of vegetation, then the plants being observed should have a wide range of water status. Variability in the plant water content, for example, can then be compared with variability in spectral response at many different wavelengths. It is difficult to assure this condition in a field setting. Therefore, initial experiments, and the bulk of the physical research for this dissertation were performed in the Agronomy greenhouse at the University of Nebraska-Lincoln.

Seven greenhouse experiments were conducted. Denoted "Trials," each of these campaigns involved a large number of plants. There were two experimental designs. One, "control versus treated," used on the order of 40 or more plants (the exact number depends on the number of days involved in the experiment) which were randomly placed in two groups: treated (stressed by withholding water) or non-treated (well watered). Measurements of both hyperspectral reflectance and physical relative water content (RWC) were taken on the leaves of the plants. The second experimental design, "sequenced treatment," involved one or more "lines" of plants. There were, for example, seven plants in a line. Each line was treated identically. All plants were well watered until the first day. On the first day, watering was stopped on one plant in the line. On the second day, water was withheld from a second plant, and so on until the end of the trial period. With such an approach, at least one plant was still well watered and the others were unwatered, respectively, for a period of one day, two days, and so on. Hence, on the last day, the line contained several plants with varying degrees of water stress. All measurements were then taken on the last day.

The trials are summarized in Table 2-1. Trial 1 was an attempt to observe a change in relative water content in maize and soy every two hours over the period of a day. The experiment was overambitious and under planned. There were several experimental errors which obscured the results. Therefore, the conditions for and results of Trial 1 will not be discussed as part of the research summary. However, the experiment helped refine the techniques used to obtain data for subsequent trials. In Trial 4, water potential was physically measured. Trial 5 included physical measurements of

Trial #	Plant	Date	Design
Trial 1	Maize & Soy	May 2007	Control vs. Treated. One day observation
Trial 2	Maize	July 2007	Control vs. Treated. All plants treated identically within experiment group. No physical water status measurements.
Trial 3	Maize	Nov. 2007	Control vs. Treated. All plants treated identically within experiment group. Physical RWC measurement on last day.
Trial 4	Maize	April 2008	Control vs. Treated. All plants treated identically within experiment group. Physical RWC measurements made using sampled proxy plants daily.
Trial 5	Maize	Feb. 2009	Control vs. Treated. All plants treated identically within experiment group. Physical RWC and water potential measurements made using sampled proxy plants daily.
Trial 6	Soy	May 2009	Control vs. Treated. All plants treated identically within experiment group. Physical RWC and water potential measurements made using sampled proxy plants daily.
Trial 6A	Soy	May 2009	Sequenced treatment over 5 days on single group of plants. All radiometric and physical measurements (RWC and water potential) made on all plants on last day.
Trial 7	Soy	July 2009	Sequenced treatment over 5 days on four groups of plants. All radiometric and physical measurements (RWC and water potential) made on all plants on last day.

Table 2-1. Trial characteristics.

both chlorophyll concentration and water potential. Ancillary data, including outside and inside greenhouse temperature and humidity and outside visible, NIR and MIR downwelling irradiance, were recorded during each experiment.

Maize was the subject of Trials 2 through 5. For Trials 2 and 3, sixteen maize plants and, for Trials 4 and 5, fifty maize plants (DeKalb DKC 63-46) were grown in a greenhouse (Figure 2-1, left panel). No artificial illumination was used. Seeds were

Figure 2-1. Greenhouse maize and soy experiments (left and right, respectively). Note: the red ribbon on the soy plant used in Trial 7 indicated that this plant would not be watered starting the day of the picture. Orange sticks in both pictures were used to uniquely identify each plant.

planted in a mixture of 1/3 peat moss, 1/3 greenhouse soil (silty clay loam) and 1/3 perlite by volume in single pots. The pot size was 7.6 liters (approx. 0.22 m diameter by 0.20 m height). Fertilizer was applied to ensure nutrient sufficiency. Plants emerged approximately eight weeks prior to initiation of the experiments. Phenologically, the plants were at the V18 to VT stages (Ritchie et al., 1997) during the course of the experiments.[1]

[1] Maize phenology is denoted, in the vegetative stages (as opposed to the reproductive stages) by the number of leaves and whether tasseling has occurred. VE, emergence, is the first stage. When the first leaf is apparent, that is V1, the second, V2, and so on until the 18th leaf, V18. Tasseling is indicated by VT.

Soy was the subject of Trials 6, 6A and 7 (Figure 2-1, right panel). The goal was to compare the spectral responses of a C3 plant (soy) to those from the C4 maize. C3 and C4 denote the two major plant groups, distinguished by different levels of complexity in the photosynthesis process. In this Trial, 6 pots were planted using ¼ peat moss, ½ greenhouse soil (silty clay loam), and ¼ vermiculite by volume. Pot size was about 4.9 liters (0.19 m diameter by 0.21m in height). Three soybean seeds (Pioneer 93M11) were placed in each pot. After the plants emerged, each pot was trimmed to one plant. As before, fertilizer was applied to ensure nutrient sufficiency. Plants emerged about 31 days before testing began. Phenologically, the soy was at R1 in Trials 6 and 6A. The plants had 7 to 8 developed trifoliates during the experiments (Pederson, 2004).[2] Trial 7 was conducted with plants at R^2. They had 11 developed trifoliates.

During Trials 2 through 6, treated plants were not watered during the course of the experiment. The untreated (control) plants were watered daily after reflectance measurements. Sufficient water was applied to assure the soil was at field capacity. Trials 6A and 7 were conducted differently by creating a sequence of plants with varying degrees of water stress ranging from fully watered to highly stressed.

2.2 Measurement Techniques

2.2.1 Spectroscopic Measurements

Reflectance measurements were made primarily using a hyperspectral radiometer (ASD FieldSpec Pro) and a self-illuminated leaf probe. The FieldSpec Pro measures reflectance from 350 nm to 2500 nm. Data were interpolated to 1 nm spectral resolution. Calibration was performed using a 99% reflective Spectralon reference panel. Adaxial

[2] Soy phenology is denoted, in the vegetative stages as VE, emergence, VC, cotyledon, V1, first leaf trifoliate, V2, second leaf trifoliate, and so on until V6, when flowering will soon start. The reproductive stages are designated R1 for the first flower, R2 for the second, etc.

leaf reflectance measurements were made with optically absorbing black foam (spectrally flat 4% reflectance) placed behind the leaf (Figure 2-2). To estimate leaf transmittance and absorption, additional adaxial leaf measurements were made with a white background (Spectralon panel) behind the leaf instead of the black foam (Figure 2-3). The method of calculating transmittance and absorption is discussed below.

Figure 2-2. Reflectance measurement by means of a leaf probe.

For the maize, Trials 2 through 5, the probe was positioned on the leaf approximately 10 cm from the plant stem.[3] Three leaves were measured per plant including the middle leaf ("mid" – most likely to become the ear leaf), the leaf positioned two above the middle leaf ("top"), and the leaf positioned two below the middle leaf ("bottom"). Reflectance was measured on all three leaves. The additional white background measurements for transmittance and absorption were made only on the mid leaf during Trial 7. These measurements were limited to the middle leaf as a way of

[3] Because slight scars, perhaps the result of bleaching from the probe lamp, were seen at some of the leaf measurement sites, the probe position was varied for each measurement.

obtaining representative determinations while limiting the amount of time involved in taking many measurements on a large number of plants.

Figure 2-3. Transmittance measurement by means of a leaf probe.

In soy, Trial 6, the measurements were made on the three leaflets in the fourth trifoliate, approximately the middle leaves on the plant. The middle leaves were arbitrarily selected to provide consistency in leaf position and to, once again, limit the amount of time involved in taking many measurements on a large number of plants. The probe was positioned such that leaf surface filled the field of view of the probe. Readings from the three leaves were averaged to obtain a spectrum representing the plant.

As indicated earlier, an attempt was made to derive transmittance and absorption based on reflectance measurements taken with a black background and a white background behind the leaf. While the analysis seemed compelling, the technique failed in actual practice. For the sake of recording this failure, the reasoning behind the attempt is included here to forewarn other researchers of the difficulties in the approach.

Figure 2-4 depicts the generalized case where there is a reflective material behind the leaf. If the reflectance coefficient of the material is greater than 0, indicating that light is reflected from the material, multiple reflections contribute to the reflectance measurement. After some mathematical manipulation, the infinite series of reflections can be reduced to a single equation for the reflectance:

$$R = \rho_L + \frac{\tau^2 \rho_P}{1 - \rho_L \rho_P} \tag{2-1}$$

where ρ_L is the leaf reflectance coefficient, ρ_P is the panel reflectance coefficient and τ is the leaf transmittance coefficient.

In the case of the original reflectance measurement, using a 4% reflective foam backing, the panel reflectance coefficient can be assumed to be 0. Denoting this reflectance measurement as R_0, and setting ρ_P to 0, it is easy to see that $R_0 = \rho_L$. Conversely, the panel reflectance can be assumed to be 1 for a Spectralon panel. Setting ρ_P to 1 and denoting this reflectance R_1, Eq. 2-1 becomes

$$R_1 = \rho_L + \frac{\tau^2}{1 - \rho_L} \tag{2-2}$$

With a little algebra, one can solve for the transmittance of the leaf:

$$\tau = \sqrt{(R_1 - \rho_L)(1 - \rho_L)} \tag{2-3}$$

Substituting R_0 for ρ_L, the equation for measured transmittance becomes, since the leaf is the only transmittance component:

$$T = \tau = \sqrt{(R_1 - R_0)(1 - R_0)} \tag{2-4}$$

Hence the transmittance can be computed by taking two measurements, one where the leaf is backed with absorbing (black) foam and one where it is backed with a (white) Spectralon reflective panel.

Incident light is reflected, transmitted, or absorbed; therefore, absorption may be calculated from the simple equation:

$$A = 100 - R - T \tag{2-5}$$

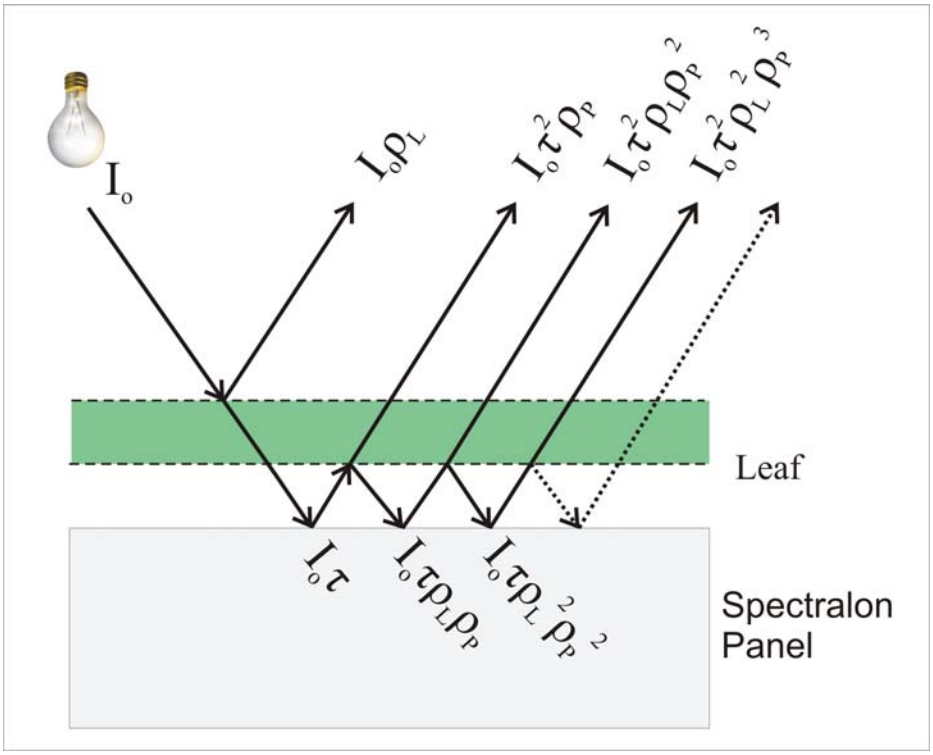

Figure 2-4. Measuring Leaf Transmittance and Absorption. I_o is the incident irradiance, ρ_L is the leaf reflectance coefficient, ρ_P is the panel reflectance coefficient, and τ is the leaf transmittance coefficient.

Despite this analysis, once this technique was tried in the greenhouse, it failed to achieve the expected results. The derived transmittance and absorption were noisy in regions with high absorption. Transmittance should have been small (<1%) in the blue

region because of strong chlorophyll absorption. Non-systematic changes of up to 8% were found after the derivation. One calculation involved in the derivation required subtraction of the pair of reflectances. For most days, this difference was about 0.1% in the blue region. Given that an ASD Field Spec Pro radiometer has a reflectance accuracy of about 0.1% (Kuester et al., 2001), the technique could not have been successful.

2.2.2 Relative Water Content Measurements

A gravimetric process was used to determine RWC. In maize, ten 1.0 cm diameter leaf punch samples were taken from each of the measured leaves (cited above) on each plant. In soy, four punches were made on each of three measured leaves (cited above) providing a total of 12 discs, Figure 2-5. The number of punches was determined by the need to balance getting a reasonable amount of material while minimizing the amount of time spent sampling each plant. These punches were quickly sealed into pre-weighed vials to prevent evaporation of water from the punches. Differencing the filled vial weights from the empty weights provided the fresh weight (FW). The vials were filled with distilled water and refrigerated in darkness at 5 ºC for 15 hours to allow the samples to rehydrate. The punches were then removed from the vials, patted surface dry, and weighed, providing full turgor weight (TW). Next, the punches were placed into open vials and heated in an oven at 105 ºC for 24 hours. Upon removal, the vials were immediately sealed, to prevent accretion water from the air, and weighed. The contents were discarded and the empty vials weighed. The difference between the filled and empty weights provided the dry weight (DW) of the leaf punches. RWC (%) was calculated using the formula:

$$RWC = 100 * \left[\frac{FW - DW}{TW - DW} \right] \tag{2-6}$$

This was used as a proxy for the RWC in all of the plants at each temporal point in the experiment. Due to destructive procedures, sampled plants were discarded.

Figure 2-5. Taking leaf punches.

2.2.3 Chlorophyll Measurements

During Trial 5, additional punches were taken from the "top," "mid," and "bottom" leaves used for RWC determination.

Ten leaf punches from each leaf position on one pair of stressed and non-stressed "RWC" plants were placed in sealed vials, weighed, then ground in an 80% acetone in water solution to destroy the leaf physical structure and extract chlorophyll (a and b) and carotenoids (Lichtenthaler, 1987). The extract solution was placed in a Cary 100 Varian dual-beam spectrophotometer to measure the optical absorption at specific wavelengths (470 nm, 647 nm, 664 nm, and 750 nm). Absorption was, in turn, converted to pigment concentration using equations developed by Porra, et al. (1989). The result was chlorophyll and carotenoid concentration expressed as mg/m^2.

2.2.4 Water Potential Measurements

Water potential was physically measured using a Decagon Devices, Inc., NT-3 nanovoltmeter, and SC-10 10-chamber thermocouple psychrometer, as shown in Figure 2-6. In maize, six 1.0 cm leaf punches were taken from each leaf position on the second pair of RWC sample plants. In soy, the six punches were taken from the same trifoliate as the RWC samples. These were placed into the SC-10 chambers for thermocouple-based measurement of vapor pressure in order to compute total water potential. To determine the osmotic potential in maize, a 30 cm long leaf sample was excised from each leaf position on these plants. In soy, the sample was the portions of the trifoliate leaves remaining after punches were taken. These samples were frozen overnight and then squeezed in order to extract the fluid contained within the plant cells. The fluid extracts were placed into the SC-10 chambers to determine leaf osmotic potential.

Figure 2-6. David Scoby making water potential measurements**.**

Total water potential is the sum of osmotic, pressure, and gravitational potentials. Because osmotic and pressure potentials dominate, gravitational potential is typically ignored in small plants (Milburn, 1979).

Total water potential measurements made during Trials 5, 6, and 7 showed values as low as -2.5 MPa. Corresponding osmotic potential was no lower than -1.6 MPa. Pressure potential can be computed, therefore, simply by subtracting osmotic potential from total water potential. Subtracting -1.6 MPa from -2.5 MPa would indicate a pressure potential of -0.9 MPa. Since pressure potential cannot drop below 0 MPa, either the total water potential measurement or the osmotic potential measurement is in error.

The total water potential measurement is dependent on the small amount of water which evaporates through the leaf surface and closed stomata. It appears that insufficient time was allowed for water vapor equilibrium to be reached within the sample chamber. This was not an issue for the osmotic potential measurement because the extruded liquid sampled from the plant was soaked onto a piece of filter paper which provided a large surface for evaporation. Therefore it is likely that total water potential measurements are in error. Because of this, total water potential and pressure potential will not be presented as part of the observations in Chapters 3 and 4.

2.2.5 Spatial Variability Within Individual Leaves

Because maize leaves are long and narrow, there was concern that reflected light characteristics and the distribution of water may vary along the leaf. During Trial 5 a short experiment was performed to determine the variability of the reflected spectrum and RWC along the leaf. Five control and five test plants were selected at the end of the experiment. Four positions, 15 cm, 30 cm, 45 cm, and 60 cm, from the stem were

marked on the middle leaf of each plant. Spectroscopic measurements were made on both sides of the central rib of the leaf at each of these positions. In addition, one 1.0 cm punch was taken at the site of the measurements. The punches from all of the control plants at each position were placed into a vial. Similarly, the punches from all of the test plants at each position were placed into a vial. These eight sample sets were then used to determine the average RWC distribution along the leaf.

2.2.6 Ancillary Data

Greenhouse temperature and relative humidity were recorded at the time of each reflectance measurement and destructive sampling. The instrument used was a Kestral 3500 "portable weather meter." External data including outside temperature, humidity, and downwelling irradiance were available from the High Plains Climate Center's weather station located approximately 0.5 km east of the greenhouse.

2.3 Experiments

2.3.1 Trials 2 and 3 Descriptions

These multiple-day trials were designed to yield sufficient plant drying to provide the desired wide range of stress. Trial 2 was conducted over five days. Trial 3 was conducted over seven days to assure that reasonably low levels of relative water content (<60%) were attained.

Because variability measures were not available for the spectral characteristics that resulted from water stress, it was not possible to statistically identify an appropriate number of plants to use for the experiment to assure that they represented the characteristics of the plant population. Based on past experience with pigment measurements it was decided to try eight stressed and eight non-stressed plants.

Plants show variable water stress diurnally (Acevedo, et. al., 1979). Having spent the night absorbing water from soil, plants are relatively less water stressed in the morning than in the afternoon. It was hoped that the change in relative water content could be spectrally detected by making measurements about 10:00 am and 3:00 pm.

Physical measurement of RWC is destructive to the leaf sampled. It was not possible, therefore, to perform a hyperspectral observation of a leaf over many days and simultaneously determine its RWC. Hence, it was decided to perform the RWC measurement only at the end of the experiment. The non-stressed plant was kept watered, so its water status should have been relatively unchanged over the course of the experiment. The stressed plant was initially in the same condition as the non-stressed plant. Thus it was assumed that the RWC of the stressed plants started at the level of the non-stressed plant and decreased to that measured in the stressed plants on the last day. What happened in between was assumed, for convenience, to be a linear decrease in RWC. As a consequence, physical RWC measurements were not available for each day of the experiment. It was therefore not possible to carefully compare the spectroscopic measurements to daily RWC determination.

As described above, for each measured leaf, ten leaf punch samples were placed into sealed vials. During Trial 2, the pre-weighed vials were 75% filled with water. The theory was that by placing the leaf punches into water there would be little or no loss of leaf water by evaporation. Unfortunately, water was lost from the vials while punches were being inserted. The resulting fresh weight measurements, and, hence the RWC measurements, were not reliable. The procedure was changed for Trial 3. The vials were not pre-filled with water. It was deemed sufficient to seal the punches into the empty

vials. The vials themselves would contain any evaporated water. This procedure was followed for all succeeding experiments.

2.3.2 Trials 4 and 5 Description

Analysis of Trial 3 data indicated that daily physical RWC measurements were required to understand the observed spectral signatures. The RWC measurements were, by nature, destructive. After sampling, the plant was damaged and could no longer be used for spectroscopic measurements. To obtain a reasonable number of RWC measurements, two randomly selected stressed and two randomly selected non-stressed plants would be destroyed each day. The average RWC measurement for each pair of leaves was used as a proxy for the RWC in all leaves in the corresponding stressed or non-stressed plant group. (Section 3.2 describes the margin of error assumed by use of this RWC proxy.) Enough plants were needed, therefore, to assure that at least eight pairs of stressed and non-stressed plants had been observed spectroscopically each day over the entire seven day experiment despite the destruction of plants. A total of 40 plants were required, as shown in Figure 2-7. Ten additional plants were grown to act as buffer plants at the ends of the rows of plants in the greenhouse. Buffer plants were not measured, and they served only to equalize shading for all the experimental plants.

ASD measurements were made morning and afternoon during Trial 4. Because physical RWC measurements were conducted only in the afternoon, it was decided that no morning ASD measurements would be made during Trial 5. RWC, leaf water potential, and chlorophyll content samples were taken in the afternoon (about 3 pm). The lack of Trial 4 morning physical measurements made these data hard to analyze. Therefore, only afternoon data will be discussed in following chapters.

		Day						
Plant #	C/T/B	1	2	3	4	5	6	7
1	Control	ASD	ASD	ASD	ASD	ASD	ASD	ASD
2	Control	ASD	ASD	ASD	ASD	ASD	ASD	ASD
3	Control	ASD	ASD	ASD	ASD	ASD	ASD	ASD
4	Control	ASD	ASD	ASD	ASD	ASD	ASD	ASD
5	Control	ASD	ASD	ASD	ASD	ASD	ASD	ASD
6	Control	ASD	ASD	ASD	ASD	ASD	ASD	ASD
7	Control	ASD	ASD	ASD	ASD	ASD	ASD	ASD, RWC
8	Control	ASD	ASD	ASD	ASD	ASD	ASD	ASD, RWC, Chl*, Osmo*
9	Control	ASD	ASD	ASD	ASD	ASD	ASD, RWC	
10	Control	ASD	ASD	ASD	ASD	ASD	ASD, RWC, Chl*, Osmo*	
11	Control	ASD	ASD	ASD	ASD	ASD, RWC		
12	Control	ASD	ASD	ASD	ASD	ASD, RWC, Chl*, Osmo*		
13	Control	ASD	ASD	ASD	ASD, RWC			
14	Control	ASD	ASD	ASD	ASD, RWC, Chl*, Osmo*			
15	Control	ASD	ASD	ASD, RWC				
16	Control	ASD	ASD	ASD, RWC, Chl*, Osmo*				
17	Control	ASD	ASD, RWC					
18	Control	ASD	ASD, RWC, Chl*, Osmo*					
19	Control	ASD, RWC						
20	Control	ASD, RWC, Chl*, Osmo*						
21	Test	ASD	ASD	ASD	ASD	ASD	ASD	ASD
22	Test	ASD	ASD	ASD	ASD	ASD	ASD	ASD
23	Test	ASD	ASD	ASD	ASD	ASD	ASD	ASD
24	Test	ASD	ASD	ASD	ASD	ASD	ASD	ASD
25	Test	ASD	ASD	ASD	ASD	ASD	ASD	ASD
26	Test	ASD	ASD	ASD	ASD	ASD	ASD	ASD
27	Test	ASD	ASD	ASD	ASD	ASD	ASD	ASD, RWC
28	Test	ASD	ASD	ASD	ASD	ASD	ASD	ASD, RWC, Chl*, Osmo*
29	Test	ASD	ASD	ASD	ASD	ASD	ASD, RWC	
30	Test	ASD	ASD	ASD	ASD	ASD	ASD, RWC, Chl*, Osmo*	
31	Test	ASD	ASD	ASD	ASD	ASD, RWC		
32	Test	ASD	ASD	ASD	ASD	ASD, RWC, Chl*, Osmo*		
33	Test	ASD	ASD	ASD	ASD, RWC			
34	Test	ASD	ASD	ASD	ASD, RWC, Chl*, Osmo*			
35	Test	ASD	ASD	ASD, RWC				
36	Test	ASD	ASD	ASD, RWC, Chl*, Osmo*				
37	Test	ASD	ASD, RWC					
38	Test	ASD	ASD, RWC, Chl*, Osmo*					
39	Test	ASD, RWC						
40	Test	ASD, RWC, Chl*, Osmo*						
41	Buffer							
42	Buffer							
43	Buffer							
44	Buffer							
45	Buffer							
46	Buffer							
47	Buffer							
48	Buffer							
49	Buffer							
50	Buffer							

Figure 2-7. Plant Utilization Plan. Abbreviations indicate the measurements on each plant. ASD – hyperspectral, RWC – physical RWC, Chl – chlorophyll content by chemical extraction, Osmo – plant total and osmotic potentials. Note that plants used in physical measurements (yellow background) are destroyed in the process. Green backgrounds denote plants involved only in spectroscopic measurements.

2.3.3 Trial 6 Description

Soy was used in Trial 6. The procedures followed were essentially the same as those for Trial 5. Fifty-six soy plants were grown to assure a sufficient number of plants. Twenty-two plants were randomly selected for test plants. Twenty-two of the remaining plants were randomly selected as control plants. No buffer plants were needed since the combination of relatively small plants and relatively large pots minimized the shading of one plant by another. The remaining plants were watered on the same schedule as the control plants but were not used during the trial.

Additional punches were taken from the plants selected for RWC measurements. These samples were used to determine water potential. Because good models were available for chlorophyll estimation based on hyperspectral reflectance, chlorophyll was not measured by extraction (Gitelson et al., 2003).

Following the completion of Trial 6, seven of the extra plants, named a "line" of plants, were used in a special experiment, dubbed Trial 6A. This experiment was designed to make a precise determination of leaf reflectance and transmittance through the use of a Shimadzu UV-2501PC (UV-VIS) recording spectrophotometer. The Shimadzu includes an integrating sphere to capture light scattered hemispherically from the leaf. This is in contrast to the white/black background measurements which lose photons not within the field of view of the leaf probe.

Because the Shimadzu measurement is destructive and the instrument itself bulky and difficult to move, the experiment was designed to have leaf samples at various levels of water deficit available for measurement at a single time. The plants were prepared in the greenhouse in the following manner. One plant was watered every day at 1:00 pm.

The second plant was watered every day except day six. The third plant was watered every day except days five, and six. And so on. The result was a collection of plants ranging from fully watered to a plant with six days of water deficit.

The fourth trifoliate leaves on each plant were spectroscopically measured on the last day with the ASD at the greenhouse. They were then transported to the CALMIT SpecLab where they were spectroscopically measured with the ASD a second time to determine the effect of the move and time differential. Each leaf in the trifoliate was, in turn, punched to obtain RWC samples as described above. Then an approximately 3 cm square section was taken from that leaf for Shimadzu reflectance and transmittance determination. This process was repeated for each leaf of the plant and for each plant. An attempt was made to minimize the time between RWC sampling and the Shimadzu measurement.

2.3.4 Trial 7 Description

Trial 7 was fashioned after the Trial 6A effort described above. Instead of a single line of plants, four lines were used. As in the earlier trial, all plants were well watered at the beginning of the trial. On the second day, watering was stopped on the first plant in each line, on the third day, watering was stopped on the second plant, and so on. At the end of the trial period, at least one plant would still be fully watered while the others would have suffered from one day, two days, three days, etc., of water stress.

During this trial, daily ASD radiometric measurements were made on all leaves in the ninth trifoliate of each plant. (The higher trifoliate was used, as opposed to the fourth trifoliate during Trial 6, because an infestation of white flies had damaged lower leaves.)

On the last day ASD, RWC, water potential, and Shimadzu transmittance measurements were made on all leaves in the ninth trifoliate of all plants.

2.3.5 Sample Size

Trial 4 data were analyzed to verify that eight samples were sufficient to represent the plant population characteristics. The following equation is commonly used to ascertain margin of error, E, in such an assumption:

$$E = z_{\alpha/2} \cdot \frac{\sigma}{\sqrt{n}} \tag{2-7}$$

Where n is the sample size, $z_{\alpha/2}$ is the z value corresponding to the area in the right tail of a standard distribution function, and σ is the standard deviation. The maximum standard deviation among the spectra averaged each day for maize in Trial 4 was 1.9%. For $\alpha = 0.5$, the z value is 1.96. With n=8, the margin of error is 1.3%. Hence, the measurements made are a good representation of the plant population for the species.

In Trial 6, the maximum standard deviation for the test plants was 1.2%. Applying Eq. 2-7, yields a margin of error of 0.8%. Again, the sample set of eight plants is adequate to represent the species population.

The sample size for Relative Water Content measurement was also tested using data from Trial 3. The standard deviation for the RWC measurements was 1.5% and 6.0%, respectively, for the control and test plants. Applying Eq. 2-7, this corresponds to margins of error of 2% and 9%, respectively, for the two samples taken each day from each group. While it would have been prudent to obtain additional RWC samples each day, the logistics of maintaining and measuring a larger group of plants made that

impractical. These levels are adequate to represent the mean value of the larger population.

2.4 Software Developed

A significant amount of software was developed for this effort. Excel was the vehicle for most analyses. Visual Analysis for Applications (VBA) scripts were written for a variety of uses. Figure 2-7 is a screen shot from "C-DAN," the CALMIT Data Analysis program, depicting an example of script developed to process data from raw text

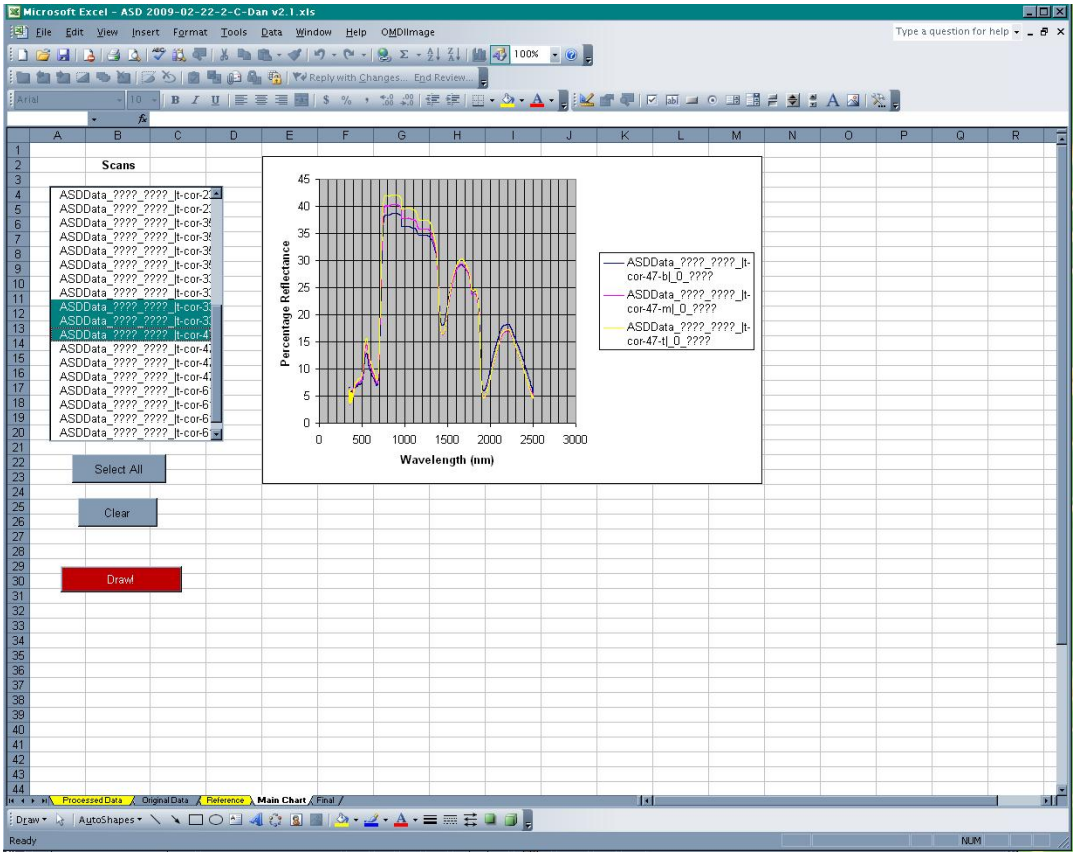

Figure 2-7. Screen capture from "C-DAN."

form into data that could be manipulated within spreadsheets. As shown in this screen, the program also provides a quick look to examine the processed data. Another VBA application used an iterative algorithm to select wavelengths for a spectral index which

minimized the RMSE between the index and physical measurements of a biophysical parameter. Figure 2-8 shows the screen after such an optimization. The selected wavelengths are shown in the upper left of the screen.

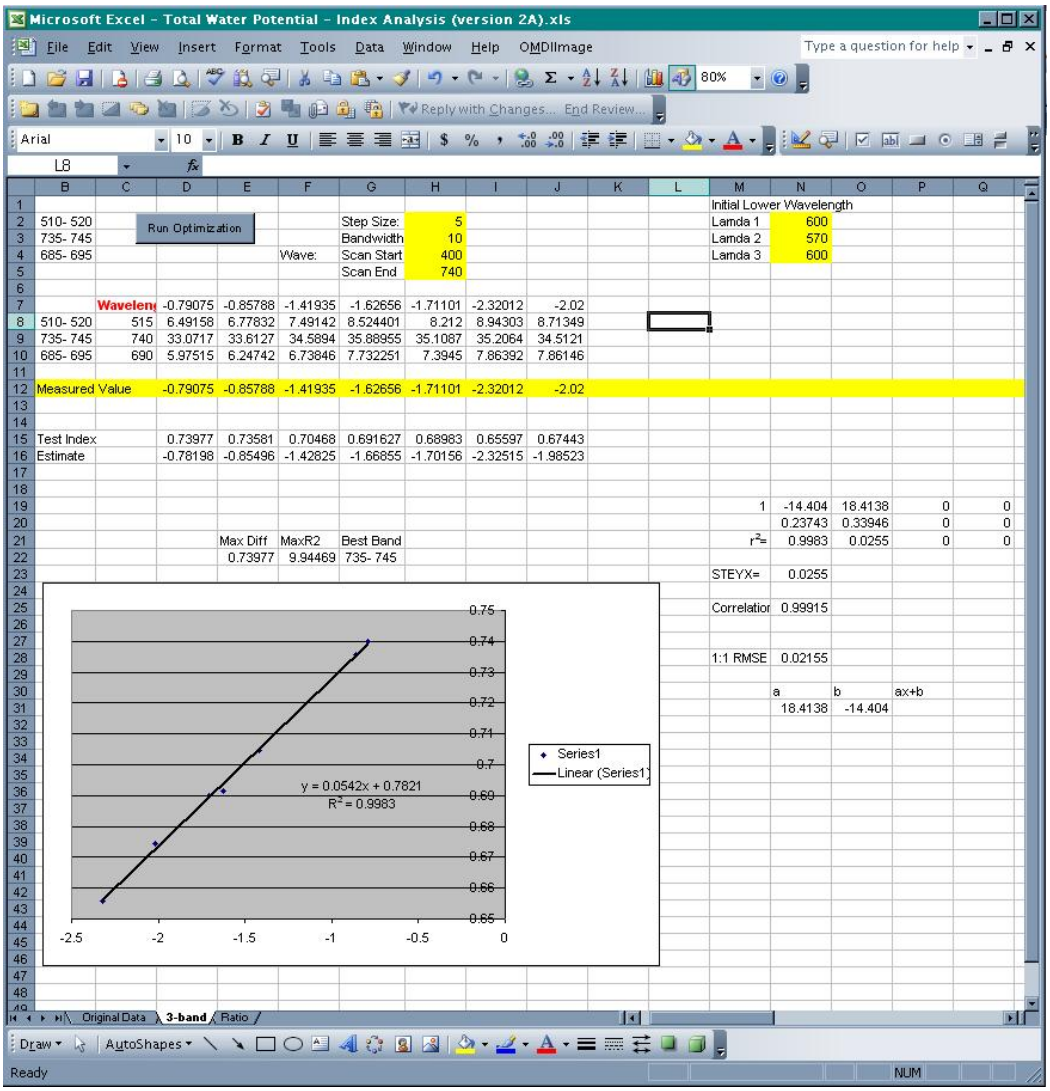

Figure 2-8. Wavelength optimization script.

Several programs were written in Visual Basic (VB) Studio to cope with the large amount of hyperspectral data from each experiment. Trials 4 and 5 involved taking data from three leaves on each of 40 plants once per day for seven days. This is a total of 840 spectra. The data were organized, when taken, by day. They had to be reordered by leaf

so that spectral change over time could be observed. Each spectrum had reflectance values from 2,150 wavelengths. Hence there were 1,806,000 numbers to be rearranged. One VB program automatically reformatted the data sets into leaf by day form. Another program, named "Leaf Analysis," was written to interactively average spectra among the leaf positions and among the days of the experiment. Typically, Leaf Analysis was used to average data each day for each of the leaf positions measured on that day. Averaging removes random reflectance noise and provides an expected reflectance value representative of the larger population of plants. The program presented graphs showing reflectance, inverse reflectance, and a representation of the coefficients of determination (R^2) between any two wavelengths. The latter was used to compare how reflectance at various wavelengths reacted as water content in the leaves changed. Figure 2-9 provides a screenshot of the windows generated when the Leaf Analysis program was applied to data from Trial 4. This software outputs the averaged data as mean reflectance, median reflectance, standard deviation of reflectance at each wavelength, coefficient of variation at each wavelength, and a new data-type, the spectral gradient, to a comma-delimited file. Comma-delimited files are easily imported into Excel.

Spectral gradient is computed by fitting a line through all the reflectance values at each wavelength from each measurement. In essence, a line is fit through the reflectance at 550 nm for the day 1 measurement, the reflectance at 550 nm for the day 2 measurements, and so on for all of the days in the trial period. This is repeated for all other wavelengths. The slope of those lines is the spectral gradient. In other words, the spectral gradient provided the rate of change in reflectance for each wavelength over the trial period. It is an indication how reflectance changed at each wavelength over the

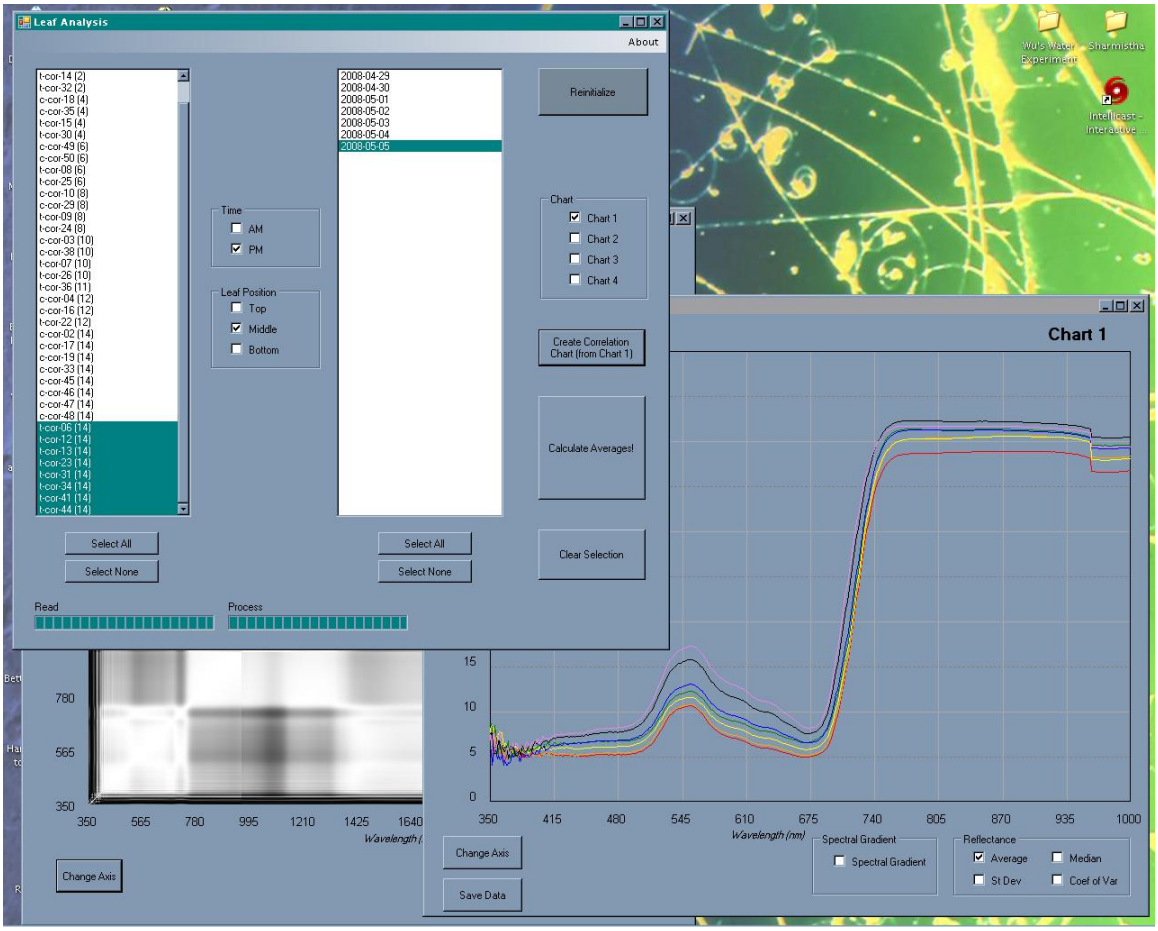

Figure 2-9. Screenshot showing examples of Leaf Analysis program windows.

course of the experiment. An example of a Spectral Gradient, corresponding to the data in Figure 2-9, is shown in Figure 2-10. The plot is scaled so that the maximum computed gradient is set to +/- 1, as appropriate.

Software was also developed to identify the wavelengths that provide the best estimate of RWC or water potential when specific spectral models are used. This program, IndexAnalysis, computes model index values for the reflectances at all possible combinations of PAR wavelengths. Estimated RWC or water content is computed by computing the coefficients of determination for linear and quadratic line fits between the index values and the parameter measurements, and selecting the fits with the highest R^2s.

In addition, noise equivalent (RMSE/slope) is computed to indicate the sensitivity of the index to changes the measured parameter.

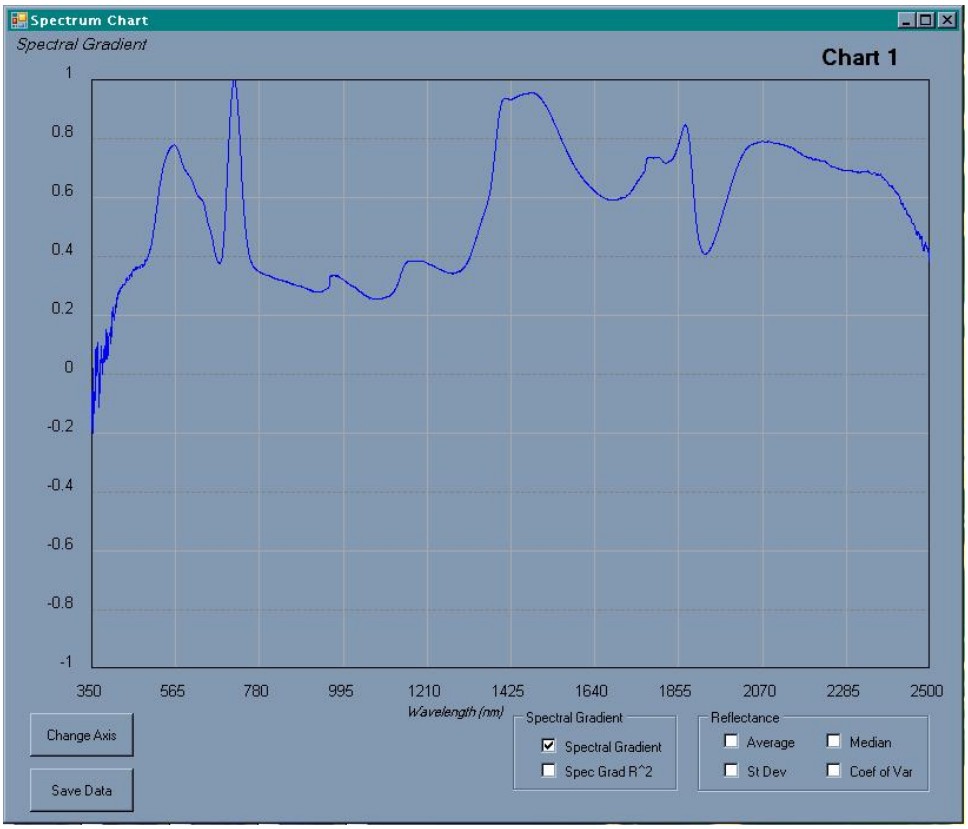

Figure 2-10. Screenshot of Spectral Gradient. This is an example corresponding to the data shown in Figure 2-9.

For a two band model, the software computes two kinds of gray-shaded charts. The first is a "coefficient of determination (R^2) matrix chart" or "R^2 chart" depicting $R^2\{\rho_i \, vs \, \rho_j\}$ where i and j vary from one to the total number of measured wavelengths. The second shows the noise equivalent matrix, $NE\{\rho_i \, vs \, \rho_j\}$. In these charts, white indicates a high value of R^2 (good) or noise equivalent (bad) and black the opposite. Intermediate values are represented by shades of gray. For a three band model, a series of two band charts are presented. Each chart in the series corresponds to a different value

of the third wavelength. The software can create these charts using a variety of models including single band reflectance, two band reflectance ratio, two band normalized difference, two band differenced reciprocal reflectance, and three band. Examples of the

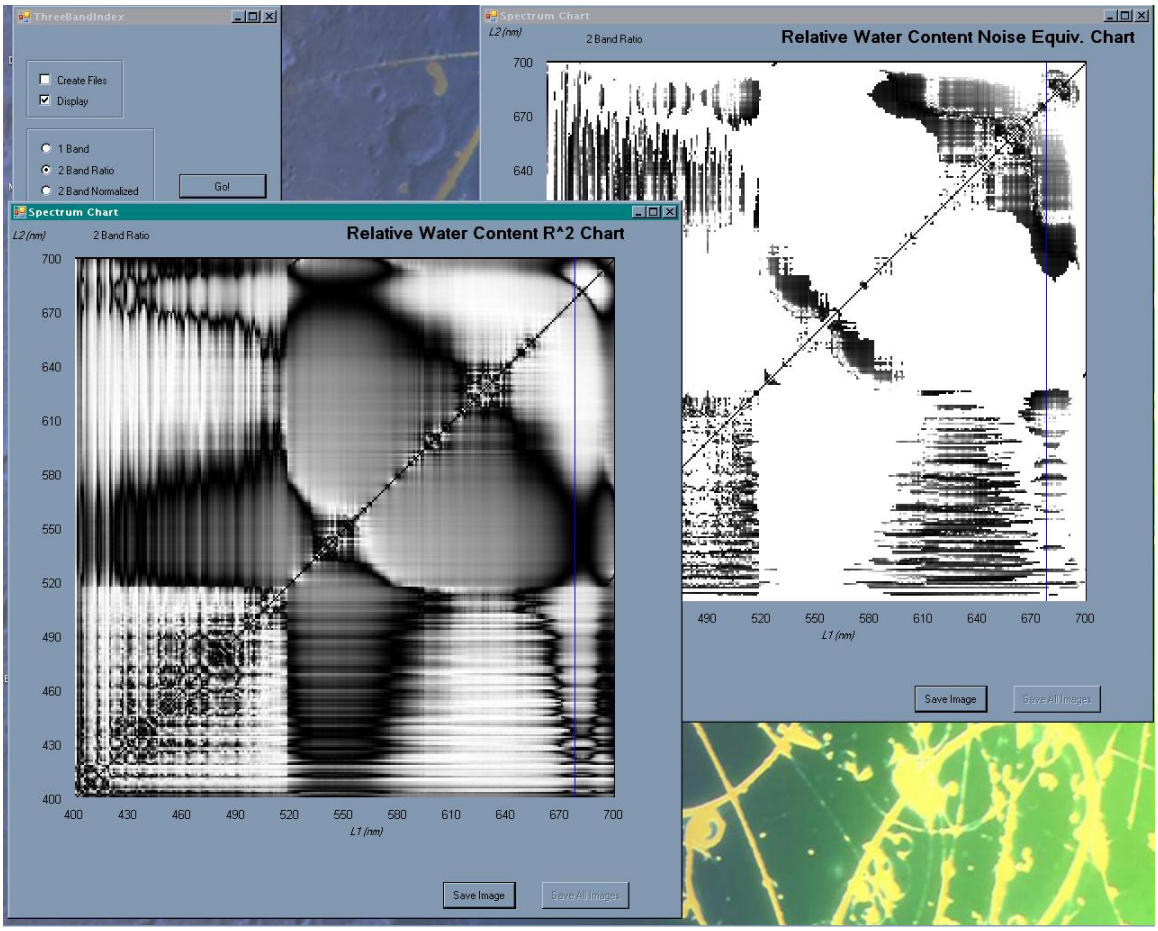

Figure 2-11. "IndexAnalysis" software screenshot. The image in the lower left depicts the coefficient of determination (R^2) matrix chart relating RWC calculated from, in this case, the reflectance ratio model, to that physically measured. The image in the upper right shows the related noise equivalent matrix chart.

R^2 and noise equivalent comparison charts are shown in Figure 2-11. The model illustrated is the ratio $\rho_{\lambda_1} / \rho_{\lambda_2}$. Note the blue line on the noise equivalent image. There is a similar one on the R^2 chart. They mark the positions where a profile is computed by fixing the λ_1 wavelength and varying λ_2. The example profiles are shown in Figure 2-12.

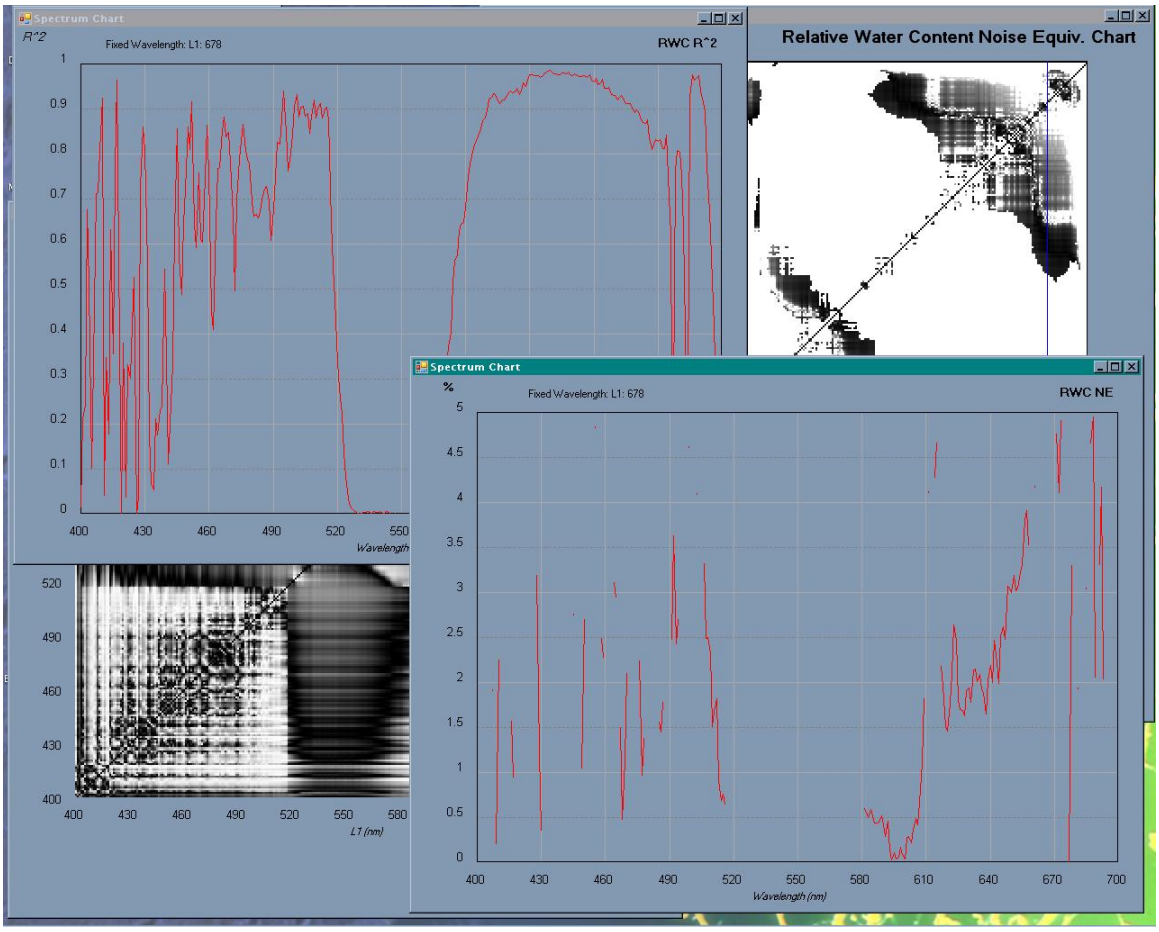

Figure 2-12. "IndexAnalysis" software screenshot showing profiles. Coefficient of Determination and Noise Equivalent profiles computed for the 678 nm wavelength from the data used in Figure 2-10.

2.5 Acknowledgements

Many people helped during the experiments. They were recognized in the acknowledgement section of this dissertation. However, it is appropriate to acknowledge the contributions of the following people to specific procedures described in this chapter. Pigment extraction was performed by graduate students Daniella Gurlin and Yi Peng. Research Technologist David Scoby was responsible for these measurements. The author is indebted to these individuals for the time they spent, the dedication they showed, and the skill they applied.

Chapter 3: Maize Experiments – Observations and Data

3.0 Chapter Contents

3.1 Chapter Introduction

This chapter presents observations and measurements made during water stress experiments conducted with maize. The objective of the chapter is to lay the foundation for the analysis in Chapter 5 of the relationship between water stress and the character of multispectral reflectance in maize.

Maize was selected for the research because it is widely grown as a food product for humans and animals. It has also been exploited in the production of biofuels as alternatives to petroleum. The plant is C_4 which indicates a photosynthetic process well suited to warm, relatively dry climates. When plants grow under conditions of high light intensity, little moisture, and high temperatures, they tend to keep their stomata, the controlled openings that allow gas exchange from the atmosphere to the cells, closed to avoid water loss. This inhibits photosynthesis by causing a decrease in the CO_2 flux into the leaves (McDonald, 2003). Plants such as maize evolved an additional process that fixes CO_2 initially into four-carbon organic acid, which increases the concentration of CO_2 in the bundle sheath cells, thereby compensating for the decreased gas exchanged

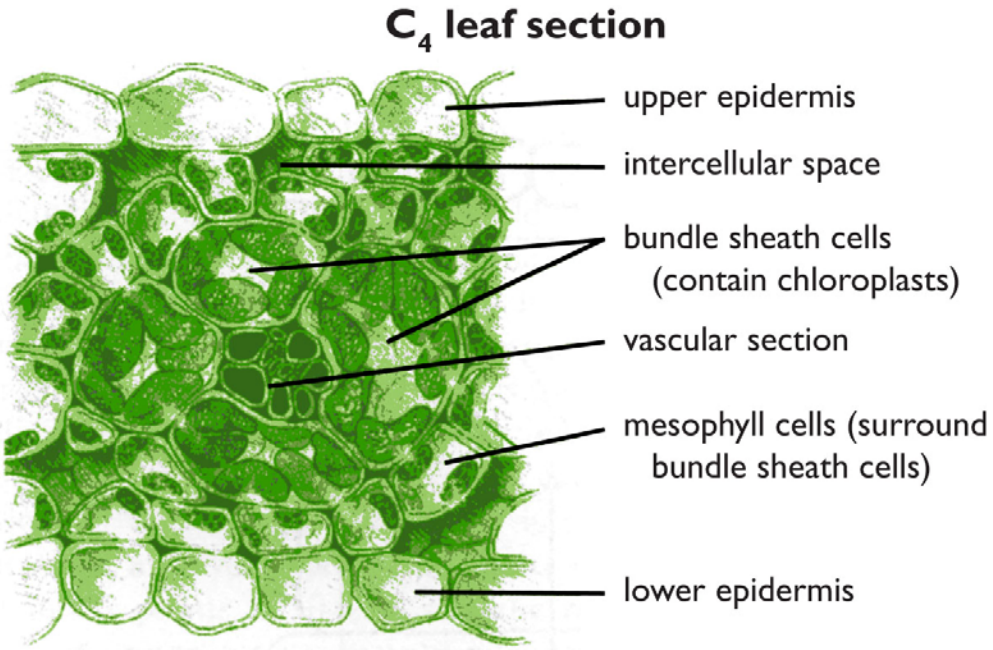

Figure 3-1. C4 leaf diagram. Artwork created and provided by Paul Royster, University of Nebraska-Lincoln Libraries.

caused by the closed stomata. C_4 plants have two types of photosynthetic cells (Figure 3-1), bundle sheath and mesophyll. Both contain chlorophyll-bearing chloroplasts vital to

the cell's production of sugars needed to sustain life and growth. Maize plants were the subjects of Trials 3 through 5.

For each trial, in turn, environmental, direct biophysical and radiometric measurements are presented. The methods used to obtain these data are described in Chapter 2. The amount of data collected during these experiments was quite large. To avoid overloading the reader, the data presented in this chapter are limited to those required to present and explain important observations. As is noted in the text, additional data and detail can be found in Appendix A.

3.2 Trial 3 (Maize – Control vs. Treated)

Research results for Trial 3 are based upon the use of sixteen maize plants; eight for the test group and eight for control. However, the experimental design for Trial 3 was flawed because the biophysical measurements (i.e., relative water content) were taken only on the last day of the experiment due to a poor assumption that the control plant RWC would serve as a good proxy for the test plant RWC on the first day and that the test plants would linearly dry to the RWC found on the last day. While not useful in the sense of obtaining a daily comparison of spectral reflectance and relative water content, the experiment did yield RWC measurements for the eight control and eight test plants on the same day. This, fortuitously, provides a means to understand the statistics of variation in RWC among maize plants and, thereby, to confirm the soundness of the sampling strategy used to obtain comparative RWC measurements in the remaining maize trials.

3.2.1 Statistical Sample Analysis of Relative Water Content

The measured RWC for Trial 3 is shown in Figure 3-2. Control plants yielded a mean RWC value of 98.3% and test plants a value of 57.3%. The standard deviations were 1.5% and 6.0%, respectively, with coefficients of variation (CV) of 1.5% and 10.5%.

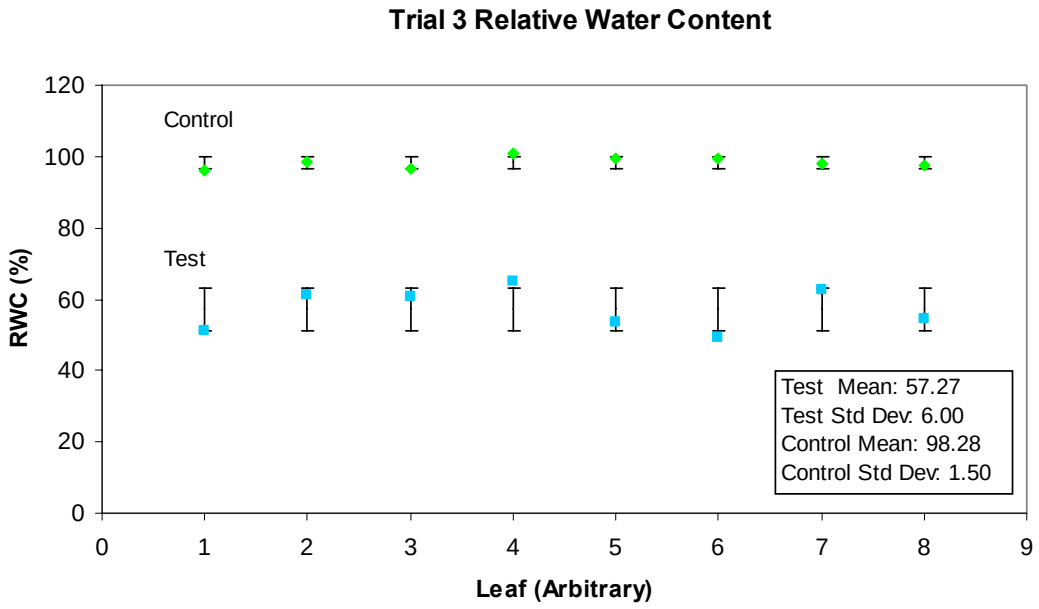

Figure 3-2. Trial 3 Relative Water Content measurements taken on the last day of the experiment.

The variability of RWC in the test plants was greater than that observed in the control plants. The possible reasons are many. The response of each test plant to water deficit could be different based on the peculiar physiology of each plant, nonuniform illumination within the greenhouse, and variation in potting compound causing differing soil water content in each pot. This raises a question about the soundness of the sampling techniques used in later trials.

The sampling technique requires that two control and two test samples were taken each day. Assuming that the Trial 3 statistics are valid for all trials and applying Eq. 2-7

with $\alpha = 0.5$, the margin of error for the RWC measurements is 2% RWC for the control plants and 8% RWC for the test plants. These are the expected errors in making the assumptions that the two samples for each group represent the RWC in the larger population of plants in those groups. Hence, the soundness of the sampling technique is verified.

3.2.2 Radiometric Measurements

3.2.2.1 Hyperspectral Reflectance

Hyperspectral reflectance measurements were made each morning and afternoon during Trial 3 as described in Chapter 2. Because RWC measurements were not available, and because morning and afternoon spectra varied only slightly, only the afternoon determinations will be discussed.

3.2.2.1.1 Variability Over Time

Daily average control middle leaf reflectance spectra are shown in Figure 3-3. For reference, the spectra for all three leaf locations are included in Appendix A, Figure A-1.

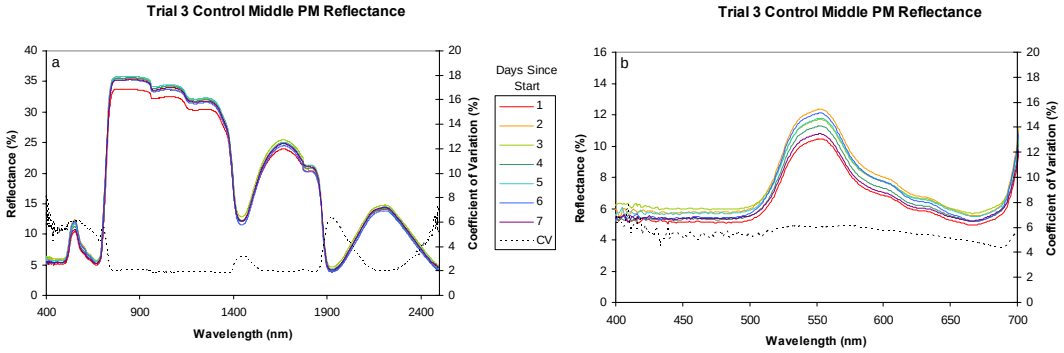

Figure 3-3. Trial 3 daily control middle leaf average reflectance spectra. Panel (a) shows entire measured spectrum. Panel (b) shows only the PAR spectrum.

The coefficients of variation of reflectance were, for the most part, 10% or less throughout the spectrum. The only exception was 14% and 16%, respectively, in top and

bottom leaf CV near the 2400 nm water absorption region. It appears that, except for the variation at 2400 nm, there was essentially no change in reflectance in control plant leaves during the experiment period.

Average daily reflectance spectra for the test leaves are shown in Figures 3-4 and 3-5. The former has multiple plot lines showing how the reflectance spectra changes daily. The latter shows how reflectance at seven specific wavelengths changes each day. Four of the wavelengths represent the major spectral regions collected by the sensor for this project: 600 nm for PAR (or the visible), 900 nm for NIR, and both 1450 nm and 1980 nm for MIR. The two MIR wavelengths are close to water molecule absorption features. (These five wavelengths will be used to represent spectral regions throughout this document.) Examination of these graphs shows that, for the most part, there is a steady increase in reflectance in the PAR and MIR regions with increasing moisture deficit. NIR reflectance appeared to increase between day one and two and then stay relatively constant. In the PAR region, the highest CV values were in the red and blue spectral region. The green region had minimum CV values. To better demonstrate the daily change, test middle leaf reflectance at five wavelengths is plotted in Figure 3-5. Because chlorophyll and carotenoids absorb strongly in blue and chlorophylls absorb in red, any change in reflectance is likely due to a decrease in absorption. Since no systematic increase in reflectance is seen in the control leaf spectra and because the only treatment applied to the test plants is water stress, it can be assumed that the change in reflectance results from increasing water stress in the test leaves.

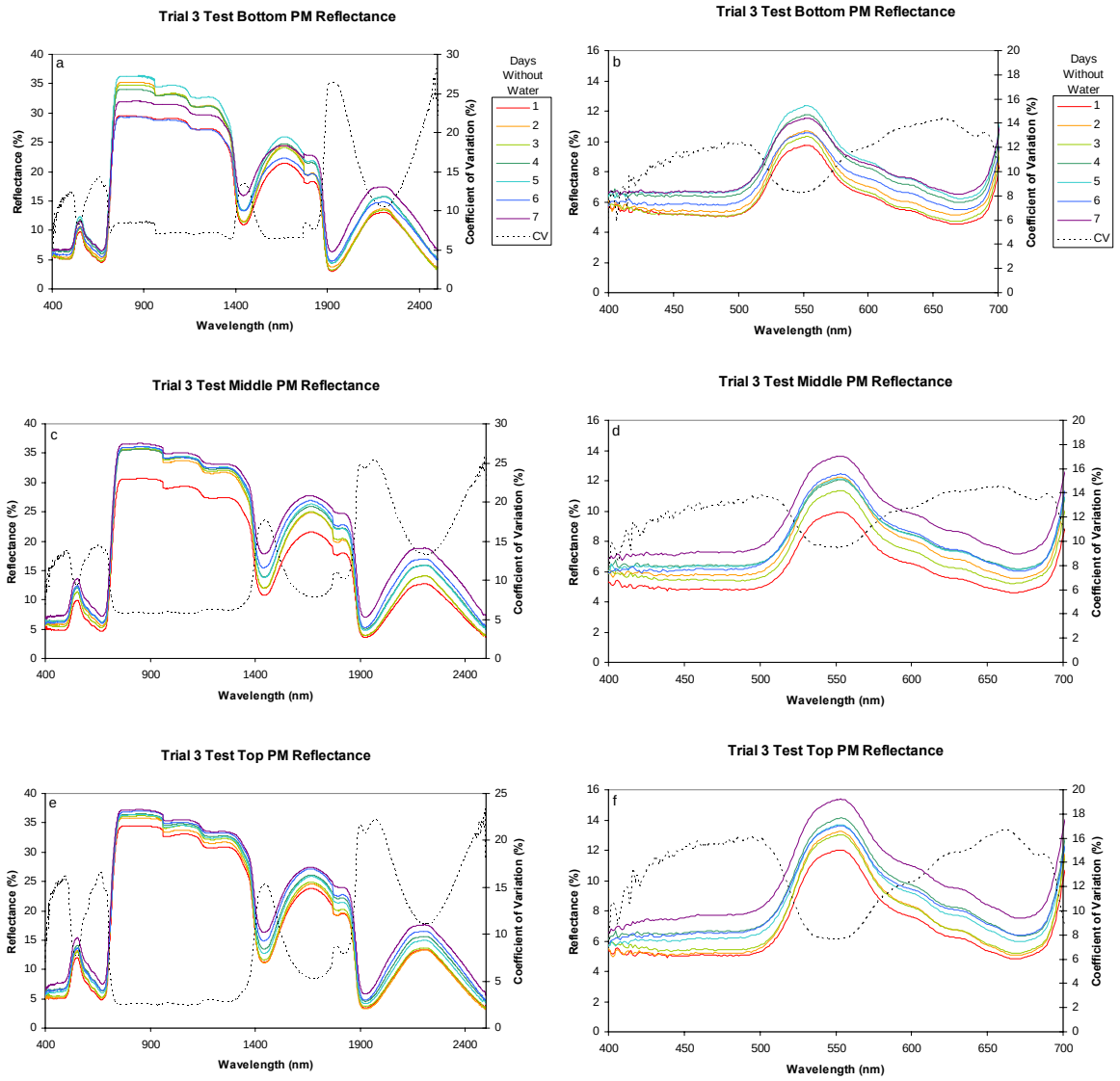

Figure 3-4. Trial 3 daily test leaf average reflectance spectra. Panels (a), (c), and (e) show the full spectrum. Panels (b), (d), and (f) show only the PAR spectrum. Panels show bottom leaves, (a) and (b), middle leaves, (c) and (d), and top leaves, (e) and (f).

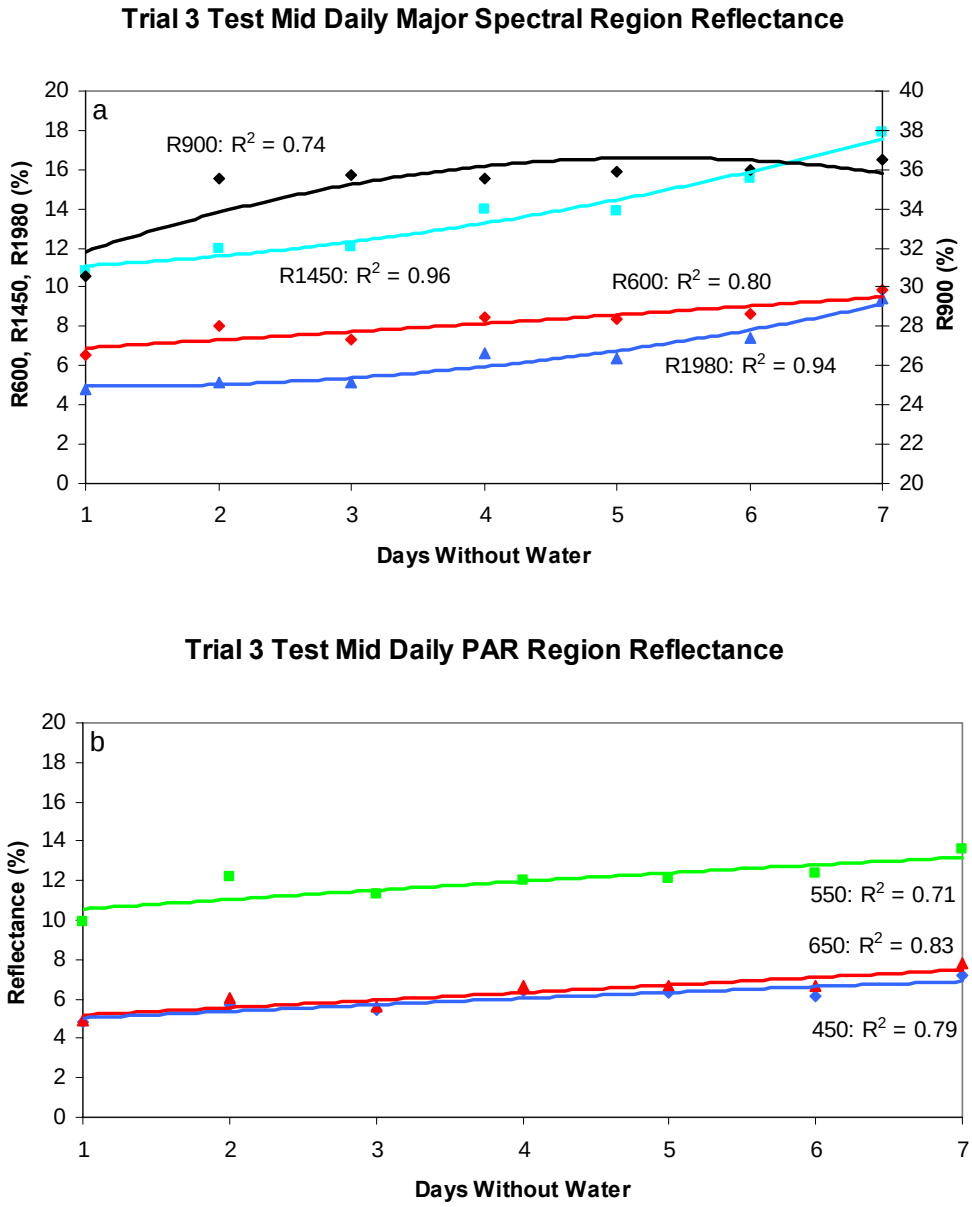

Figure 3-5. Trial 3 test leaf daily reflectance at wavelengths representing spectral regions. Panel (a) shows the major spectral regions. Panel (b) shows the PAR region. Lines are quadratic best-fit.

3.2.2.1.2 Information Content

Remote sensing of biophysical parameters is possible if the reflectance spectrum contains information directly related to these parameters, environmental conditions, and/or other factors of interest. Models used to estimate biophysical parameters are

based on the fact that reflectances in various parts of the spectrum react differently to changes in those parameters. In this section, the information content in the Trial 3 reflectance spectra is discussed. This presentation is more cursory than will be used for the remaining trials since the lack of RWC data reduces the importance of Trial 3 in performing the analysis necessary for proper treatment of this research.

PAR and MIR test leaf reflectance increased over the experiment period. At 550 nm, for example, reflectance changed from 9.9% to 13.6%. At 1400 nm, reflectance increased from 10.9% to 14.4%. The CV in the NIR region was below 6% implying that NIR reflectance was essentially unchanged.

The increases in test leaf PAR and MIR reflectance were closely related. NIR reflectance changes, however, were not strongly related to either of these regions. This can be demonstrated by plotting the coefficients of determination, R^2, of the relationships between reflectances at the characteristic wavelengths identified above. Figure 3-6 depicts the R^2 for these relationships. Control and test leaf reflectances are both included for comparison.

Control leaf reflectance for the selected wavelengths shows high R^2 values only with reflectance in the same specific spectral region. For example, reflectance at 600 nm shows R^2 values above 0.95 with green and red, but values below 0.5 for the rest of the spectrum. Reflectance at the two MIR region wavelengths (1450 nm and 1980 nm) were related to each other, but not to any other wavelengths. Hence, reflectance in each region was essentially independent of that in any other.

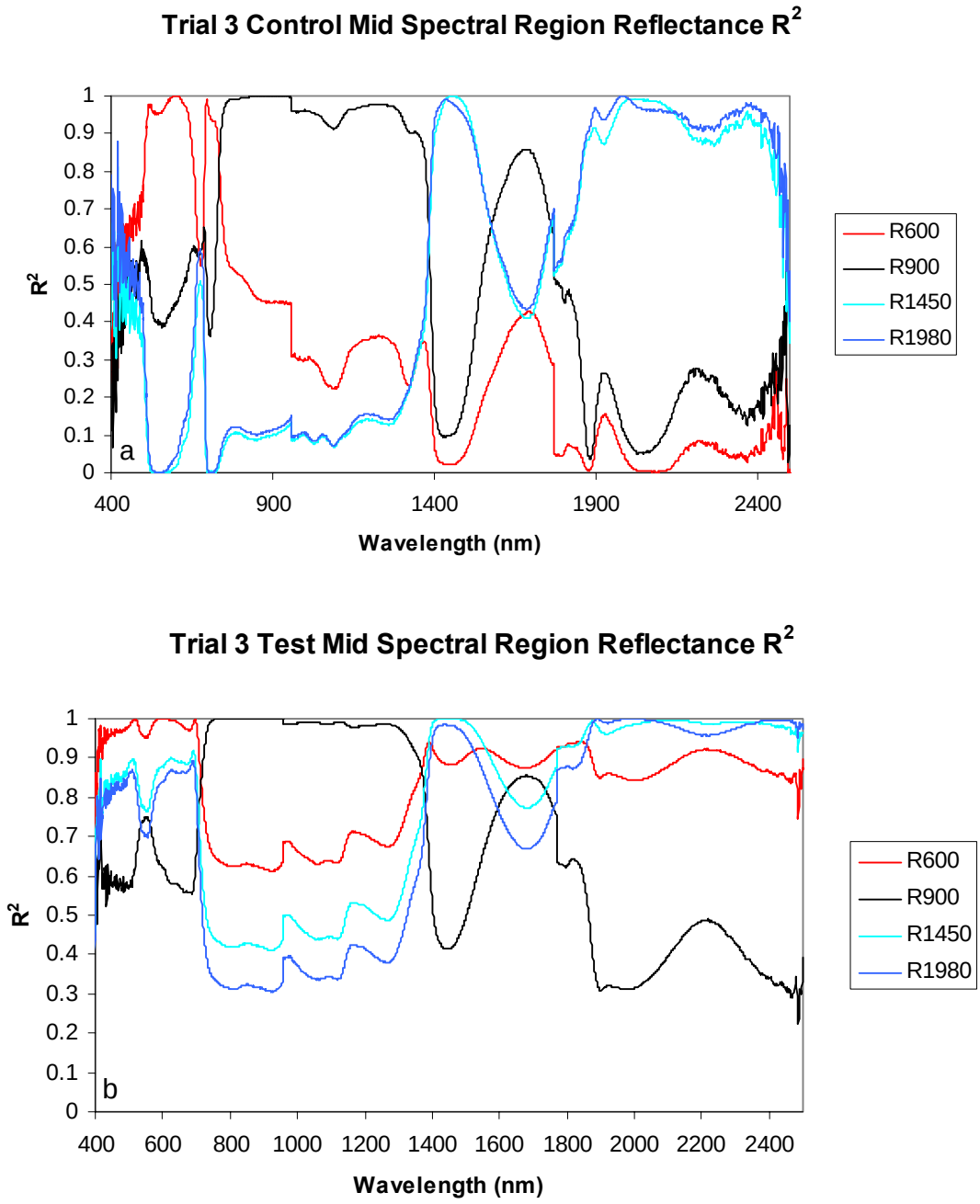

Figure 3-6. Trial 3 strength of the relationships of changes in reflectance at specific characteristic wavelengths against all other measured wavelengths**.** Lines depict R^2 for Trial 3 control leaves, panel (a), and test leaves, panel (b).

Test leaf reflectance was markedly different. Reflectance at 600 nm changed in concert with visible and MIR regions at an R^2 level above 0.85 and presents information very different from that at NIR wavelengths. Examination of Figure 3-6(b) indicates that

NIR reflectance changes were only slightly related to any other part of the spectrum. Over time, and most likely with increasing water stress, the PAR and MIR reflectances change concomitantly.

Increasing MIR reflectance is, likely, related to decreasing amounts of water and, hence, decreased molecular absorption of light in those wavelengths. Since there is no water molecule absorption in PAR, the changes at those wavelengths appear to be caused by some effect related indirectly to the amount of water in the leaf.

3.3 Trial 4 (Maize – Control vs. Treated)

Trial 4 was the first experiment measuring RWC daily through destructive sampling of plants from the control and test plant groups.

3.3.1 Physical Measurements

3.3.1.1 Environment

Exterior temperature, relative humidity, and downwelling irradiance were recorded at the High Plains Climate Center weather station near the greenhouse. Interior temperature and relative humidity were measured just before making radiometric observations. These data are summarized in Figure 3-7.

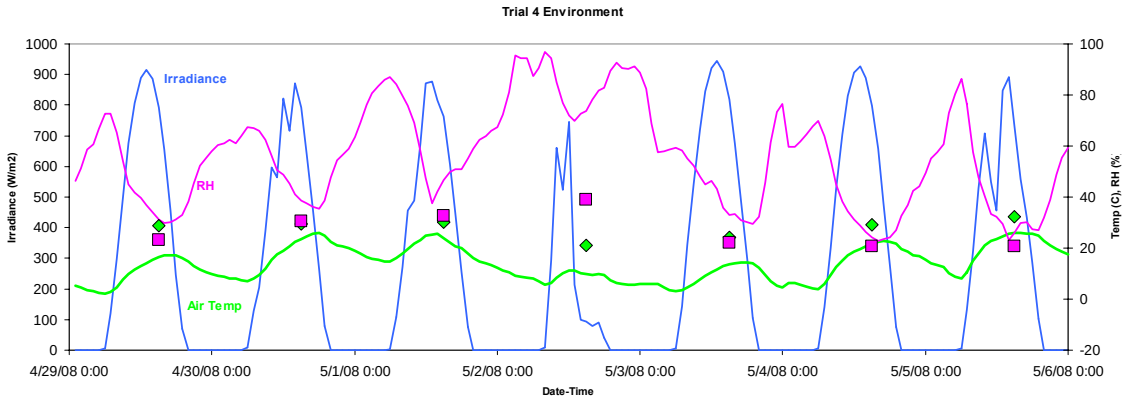

Figure 3-7. Trial 4 environmental conditions. The lines show outside air temperature (green), relative humidity (pink), and downwelling solar irradiance (blue). The temperature and humidity inside the greenhouse at measurement times are shown as diamonds and squares, respectively.

Afternoon temperature averaged about 28 ºC with a standard deviation of 4 ºC. Relative humidity averaged 28% with a standard deviation of 7%. With the exception of a cloudy day, May 2, downwelling solar irradiance at the time of the afternoon measurements was very consistent. If May 2 is included, the average irradiance was 684 W/m^2 with a standard deviation of 262 W/m^2. Excluding May 2 results in an average of 783 W/m^2 and a standard deviation of 30 W/m^2. The importance of this relatively steady illumination will become apparent when the results of Trials 4 and 5 are compared.

3.3.1.2 Relative Water Content

RWC for top, middle, and bottom leaves (defined in Chapter 2) from two randomly selected control plants and two randomly selected test plants was destructively determined each day just after making radiometric measurements. These samples acted as proxies for the RWC in all of the plants at the time of the hyperspectral measurements. A complete summary of the measurements is shown in Appendix A, Tables A-1 and A-2.

The statistics for all sampled control plant leaves (one leaf per position from each of the two sample plants) are shown in Table 3-1. Top and middle leaves had an average RWC of about 96% with a standard deviation of about 2%. The bottom leaves, with an average RWC near 93%, had a higher standard deviation, about 5%. Coefficients of variation were small, 5% or less. Control leaf RWC was essentially unchanged for the period of the experiment.

Leaf	Average RWC (%)	Standard Deviation (%)	Coefficient of Variation (%)
Top	96.0	2.0	2
Middle	96.5	2.1	2
Bottom	93.3	4.6	5

Table 3-1. Trial 4 control plant relative water content measurements.

The test plant leaves showed essentially linear decreases in RWC over the six days of the experiment, as shown in Figure 3-8. Top and middle leaves had a measured RWC (average of two leaves) just below 95% on the first day without watering and about 52% on day six. The bottom leaves began about 91% (average of two leaves) on the first day and 35% on day six. Linear regression best-fit lines indicate that the middle leaves have the smallest daily RWC differences between the two sample leaves. The slopes of fits to the average data points indicate that the top and middle leaf RWC decreased by about 8% per day while the bottom leaf decreased by 11% per day.

3.3.2 Radiometric Measurements

3.3.2.1 Hyperspectral reflectance

As the Trial 4 test plants became increasingly water stressed, the spectrum of reflected light changed dramatically. The systematic increase in reflectance observed during Trial 3 was once again evident.

3.3.2.1.1. Variability Over Time

Trial 4 started with fifty maize plants. Half were water stressed (test plants) and half were well watered (control plants). Since two plants of each group were destroyed each day in determining RWC, eight test and eight control plants remained on the last day of the experiment. The reflectance measurements for each leaf position in the eight test group plants and in the control group plants were averaged to provide a representative spectrum of reflectance.

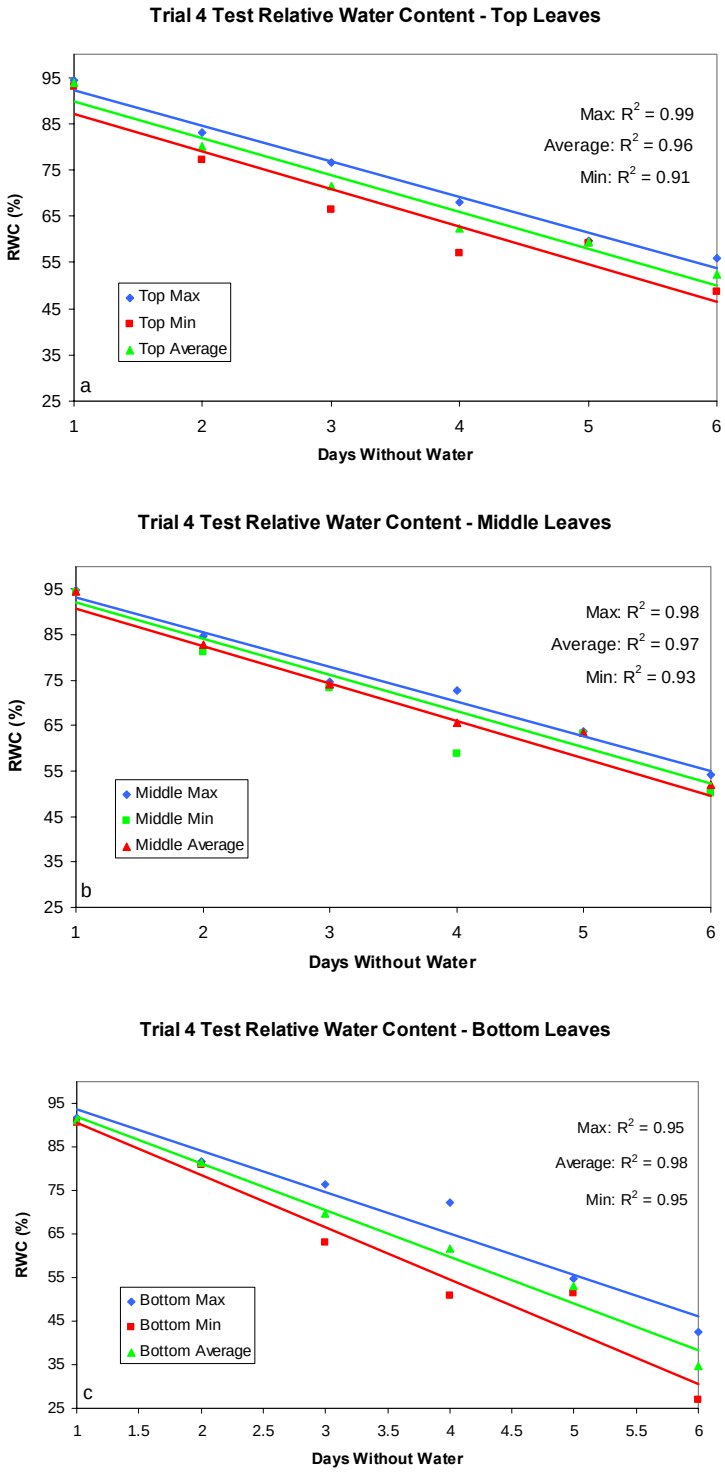

Figure 3-8. Trial 4 measured test leaf RWC. For each leaf position, "Max", "Min", and "Average" indicate the high, low, and average RWC value for the two leaves sampled each day. Lines are best-fit linear regression lines for the high, low, and average values. Top, middle, and bottom leaves are shown in panels (a), (b), and (c), respectively.

Trial 4 average spectra for the control middle leaves are shown in Figure 3-9. The spectra for all leaves may be found in Appendix A, Figure A-2. For all leaf positions, the coefficient of variation of reflectance was below 5% in PAR, below 2% in NIR, and below 5% in MIR. This indicates that the control leaf spectra remained essentially unchanged during the experiment.

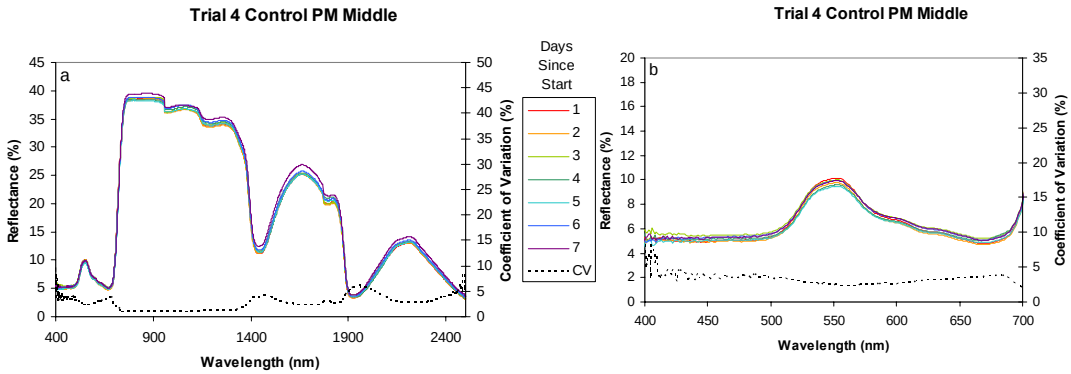

Figure 3-9. Trial 4 daily control middle leaf average reflectance spectra. Panel (a) shows the entire measured spectrum. Panel (b) contains only the PAR spectrum.

Figures 3-10 and 3-11 contain the average daily reflectance for the test leaves. The former shows daily change over the entire spectrum, and the latter shows reflectance change at the seven representative wavelengths identified previously. The test spectra are clearly different from those for the control leaves. As was observed during Trial 3, there appears to be a consistent, nearly monotonic, increase in reflectance across the whole spectrum during the experiment period. Variations in this characteristic among the leaf positions are probably due to different stress levels because of leaf shading as well as physiological and phenological variation among the leaves. The increase in reflectance is in concert with the daily decrease in RWC and corresponding increase in plant water stress. The PAR and MIR regions show this characteristic strongly. NIR reflectance does not. This observation is confirmed by examining the CV lines on the graphs. The

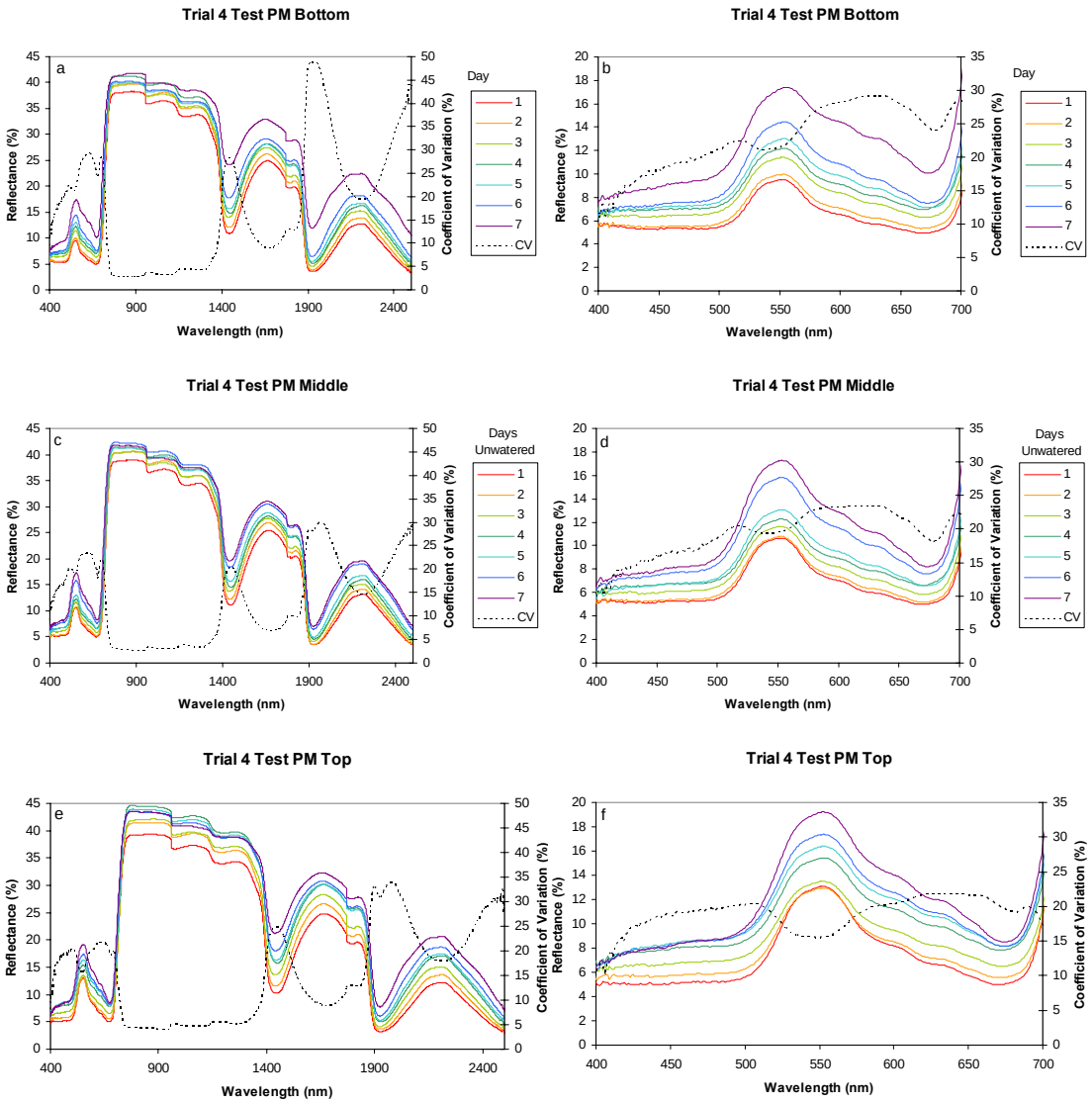

Figure 3-10. Trial 4 daily test leaf average reflectance spectra. Panels (a), (c), and (e) show the full spectrum. Panels (b), (d), and (f) show only the PAR spectrum. Panels show bottom leaves, (a) and (b), middle leaves, (c) and (d), and top leaves, (e) and (f).

charts for each of the leaf positions show the NIR CV to be less than 5%, which indicates that there is no pronounced change in NIR reflectance during the experiment. In general, the CV for all positions showed prominent peaks (CV>25%) just above 1400 nm, 1900 nm, and 2400 nm in the MIR. These are the wavelengths where water molecules exhibit strong absorption. Increasing reflectance at these wavelengths is both expected and consistent with decreasing water content. The bottom leaves showed the greatest

decrease in water content and, therefore, exhibited higher reflectance CV values at these wavelengths.

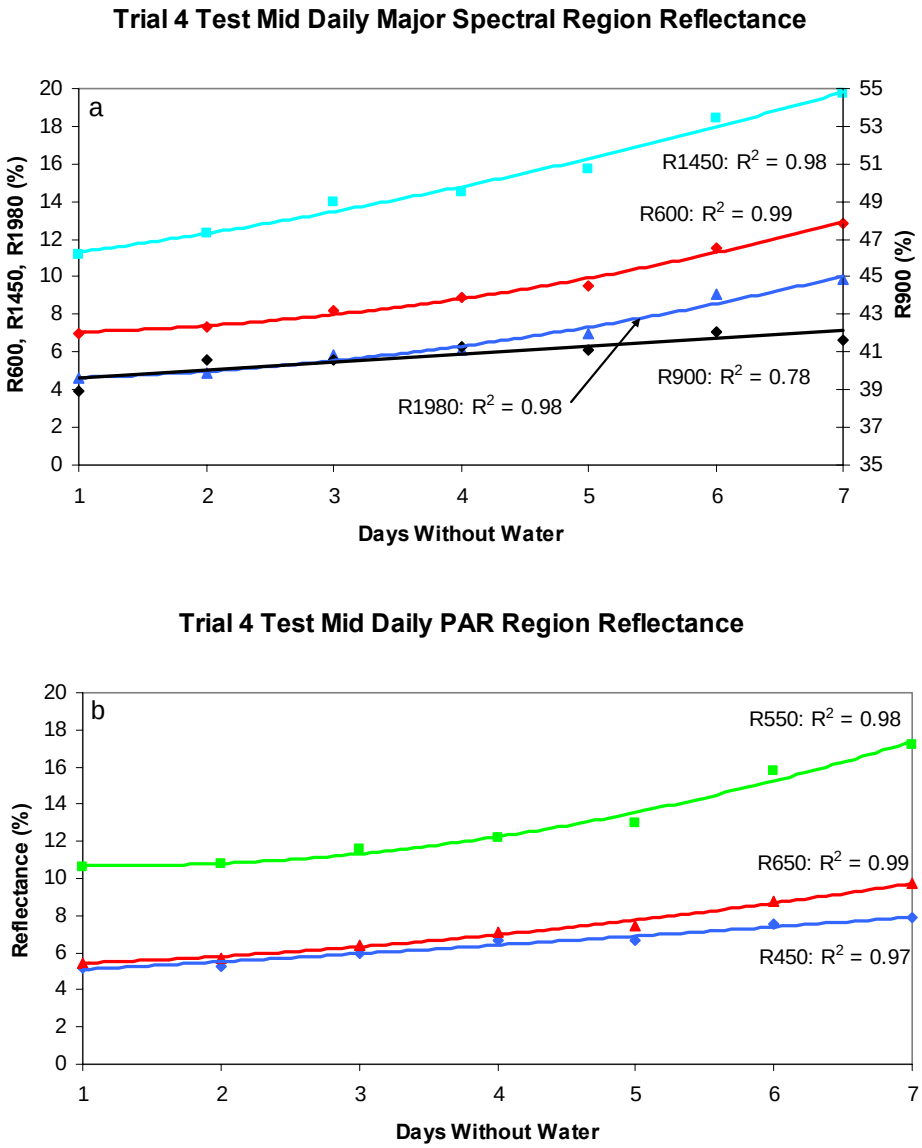

Figure 3-11. Trial 4 test leaf daily reflectance at wavelengths representing spectral regions. Panel (a) shows the major spectral regions. Panel (b) shows the PAR region. Lines are quadratic best-fit.

In the PAR region, CV was between 20% and 30%. Across the PAR range, there was only a small variation in CV. The bottom leaves, again, showed the highest CV, apparently consistent with higher water stress. CV was slightly higher in red and showed

a dip near 550 nm. Pigment absorption (chlorophyll and carotenoids) is extremely high in blue and chlorophyll absorption is slightly weaker in red. Decreasing water content appears to cause decreasing pigment absorption and/or increasing scatter from the leaf structure.

3.3.2.1.2 Information Content

Looking closely at the charts in Figures 3-10 and 3-11, Trial 4 test leaf spectra showed a consistent increase in PAR and MIR reflectance as the experiment progressed and water stress increased. For example, at 550 nm in the PAR region, the middle test leaf had reflectance of about 10% on the first day and 18% on day 7. In MIR, at 1400 nm, the reflectance changed from about 13% to 22%. In both of these regions, the increase in reflectance appeared to be systematically and monotonically related to increasing water stress. NIR reflectance did not exhibit the same characteristics. Although there was variation of NIR reflectance, there was no evident systematic change corresponding to increasing stress. These observations are corroborated by the CV plots in Figure 3-10.

Another way to demonstrate information content of reflectance spectra is to calculate the coefficient of determination (R^2) over time for every wavelength against every other wavelength in the spectrum. The resulting matrix may be denoted $R^2\{\rho_i \text{ vs } \rho_j\}$ where the values of i and j range from one to the total number of wavelengths measured. This, of course, generates a large amount of data. These data can be presented as a gray shaded image where each picture element (pixel) represents an R^2 value for a particular pair of wavelengths. Figure 3-12 introduces a "coefficient of determination matrix chart" or "R^2 chart" corresponding to the Trial 4 control middle leaf spectra. Panel (a) shows

a

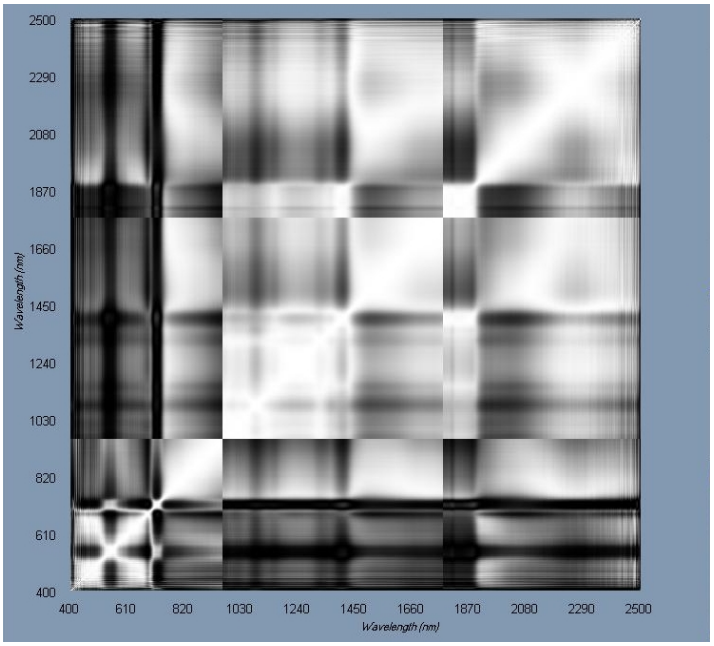

b

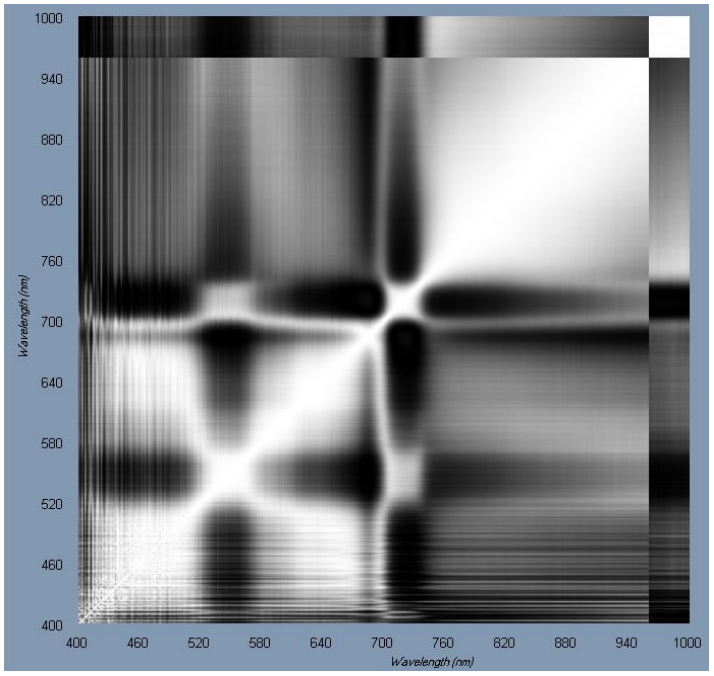

Figure 3-12. Trial 4 control middle leaf coefficient of determination (R^2) matrix charts. Panel (a) indicates the relationship among all measured wavelengths. Panel (b) is limited to PAR and the lower 200 nm of NIR. A white pixel indicates R^2=1. Black pixels indicate R^2=0.

the entire spectrum. Panel (b) shows only the PAR region. The wavelength pair represented by each pixel can be determined by the values indicated on the axes. A white pixel represents a coefficient of determination value of 1 and black indicates 0. These

charts are useful as a qualitative "big picture" view of how reflectance changes at various wavelengths correlate over time. For example, the patterns in these charts show that, except for wavelengths near 550 nm, reflectances for all wavelengths in the PAR are highly correlated. PAR wavelengths are also seen to be uncorrelated with all other regions except for the region just above 1900 nm. Note, also, that changes in green reflectance near 550 nm are unrelated to virtually the entire spectrum except the red edge region around 720 nm. These wavebands are known to be similarly affected by pigment absorption as well as optical scattering in anthocyanin-free leaves (Gitelson & Merzlyak, 1996). The apparent close relationship between reflectances in the blue and the red is due to very strong effect of absorption by pigments in these spectral bands.

To better see these effects, as was shown for Trial 3, Figure 3-13 contains two graphs plotting the R^2 between the seven characteristic wavelengths used previously, versus all other wavelengths. These graphs provide quantitative verification of the observations just made.

The R^2 charts in Figure 3-14 are those obtained from the test leaf spectra. They appear different from the charts in Figure 3-12, thus indicating different information content of reflectance spectra. There is clearly high correlation among reflectances at PAR and MIR wavelengths and weaker correlation between those regions and NIR. A more quantitative representation of these relationships is shown in Figure 3-15. Using the same specific wavelengths specified above, these graphs show the relationship between reflectance at those wavelengths and reflectance in the rest of the measured spectrum.

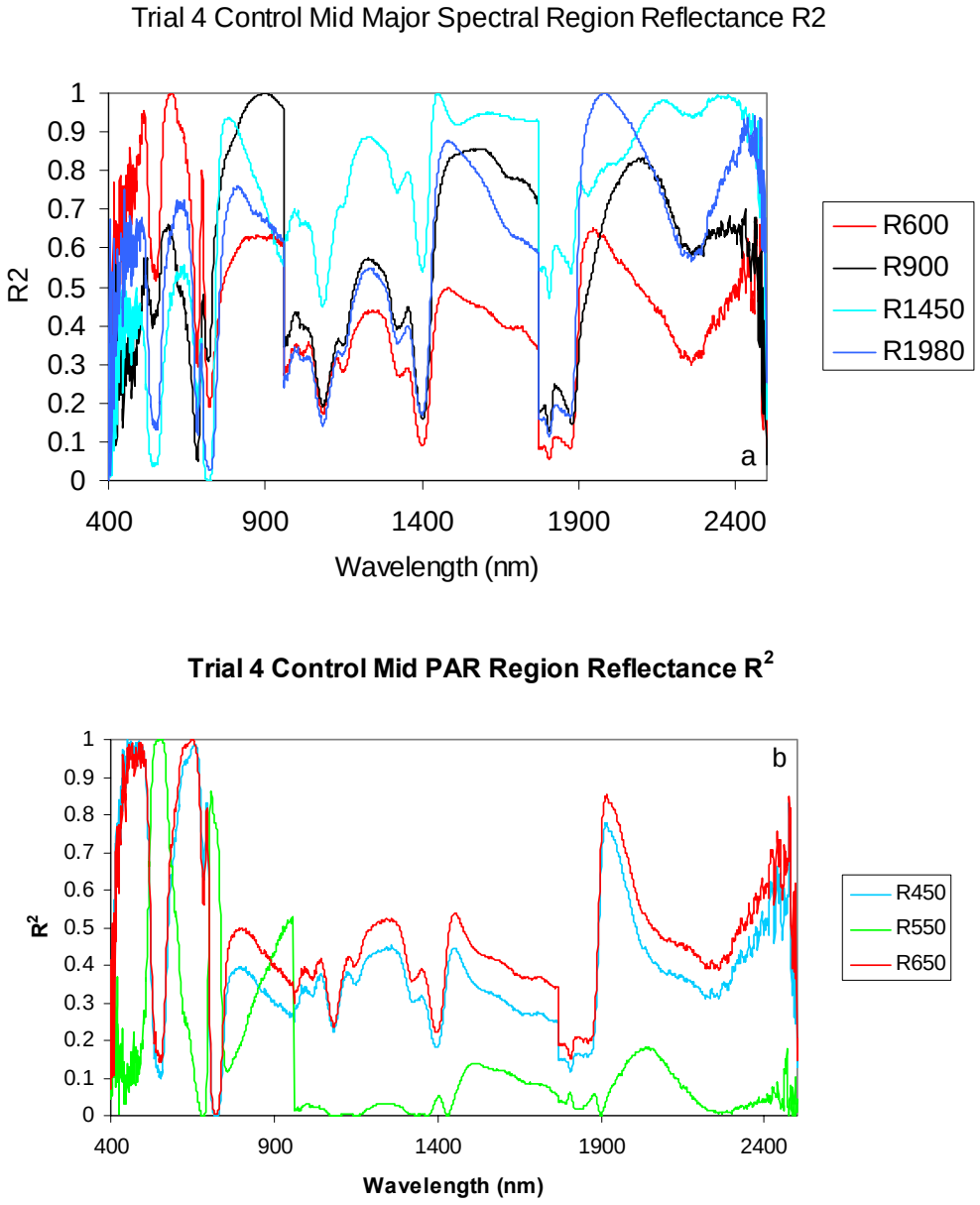

Figure 3-13. Trial 4 control, strength of the relationships of changes in reflectance at specific characteristic wavelengths against all other measured wavelengths. Lines depict R^2 for major spectral regions control, panel (a), and the PAR region, panel (b).

a

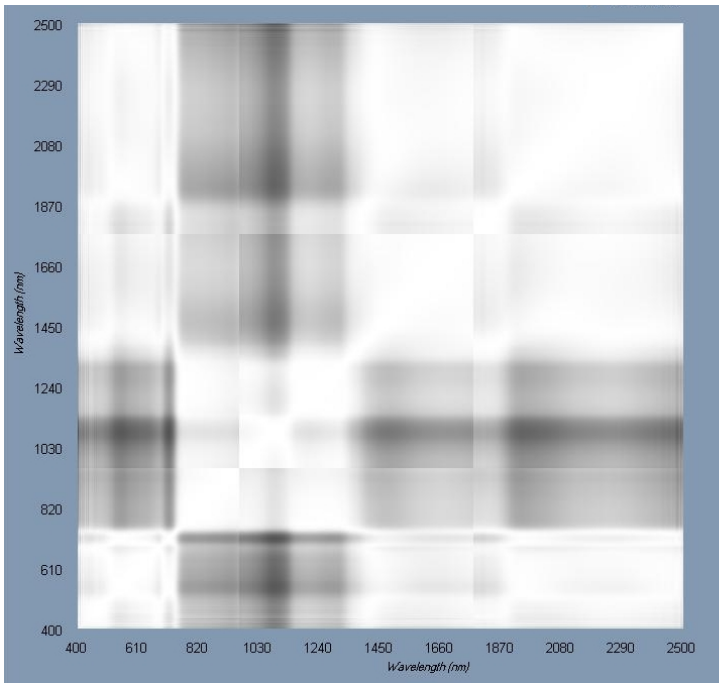

b

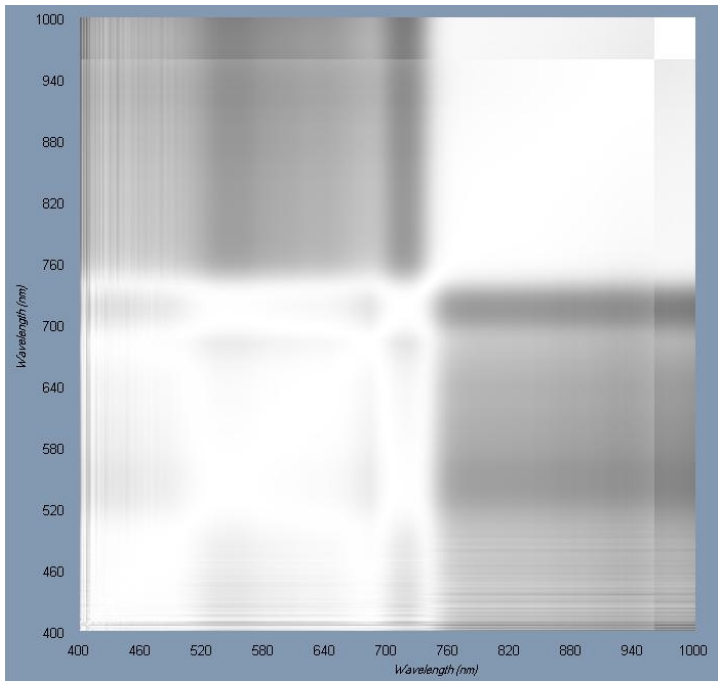

Figure 3-14. Trial 4 test middle leaf coefficient of determination (R^2) matrix charts. Panel (a) indicates the relationship among all measured wavelengths. Panel (b) is limited to near the PAR region. A white pixel indicates R^2=1. Black pixels indicate R^2=0.

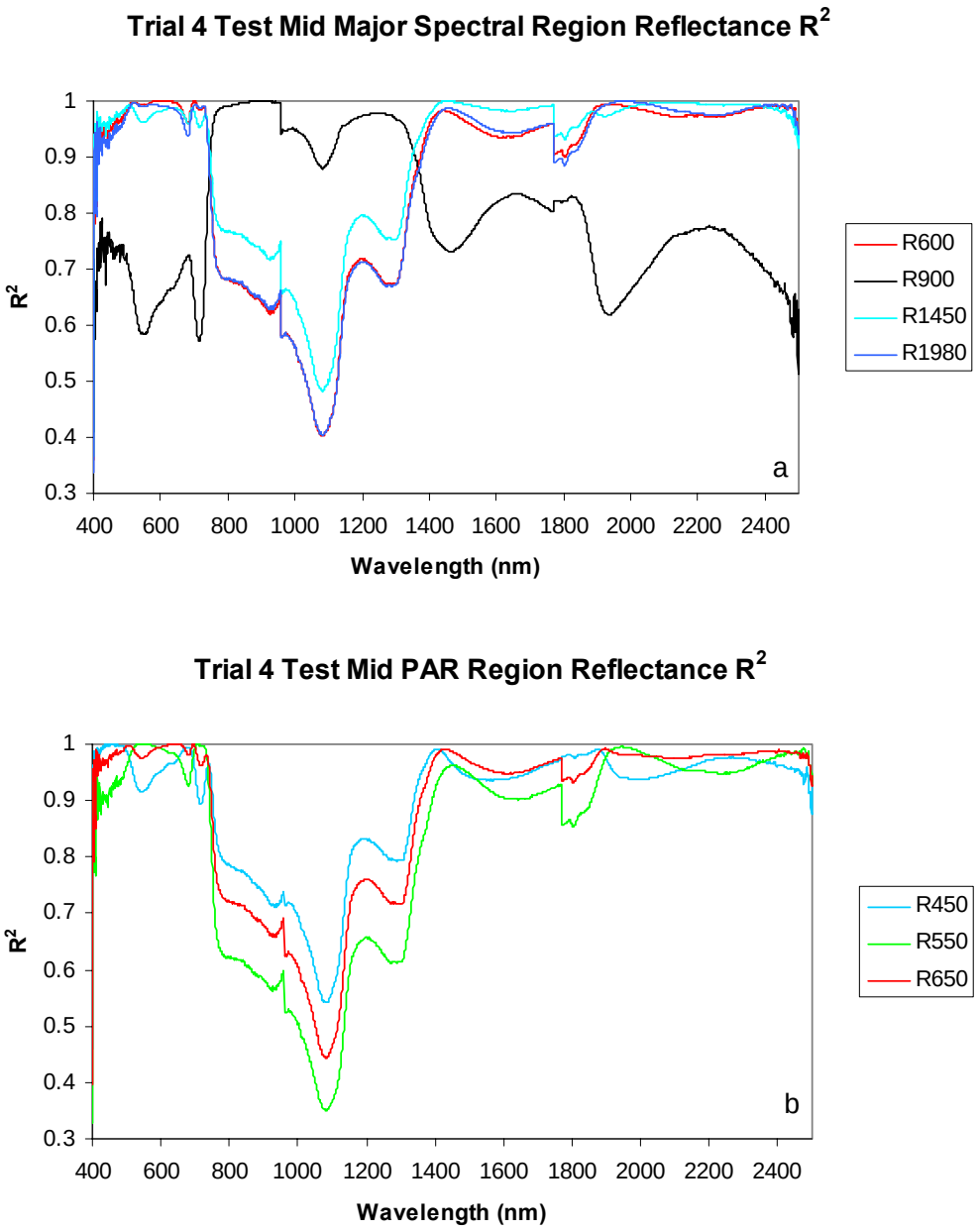

Figure 3-15. Trial 4 test, strength of the relationships of changes in reflectance at specific characteristic wavelengths against all other measured wavelengths. Lines depict R^2 for major spectral regions control, panel (a), and the PAR region, panel (b).

It is readily apparent that PAR and MIR reflectances are highly correlated. Reflectance at 600 nm correlated very strongly with reflectance at 1450 nm and 1980 nm (R^2 is 0.99 and 0.98, respectively). Neither of these regions shows a strong R^2 with respect to NIR. From this, one can conclude, that over time and as water deficit

increases, the reflectances at 600 nm, 1450 nm, and 1980 nm vary similarly. Therefore the reflectance values carry nearly the same information.

One can also observe that blue, green, and red wavelength reflectances correlate very strongly with each other. The only R^2 values below about 0.95 were between green and blue, and between green and red. Even so, R^2 was above 0.9. These observations corroborate what was discussed earlier. Reflectance in the regions of the spectrum where pigments strongly absorb light change similarly as water stress increases.

3.4 Trial 5 (Maize – Control vs. Treated)

Like Trial 4, Trial 5 used destructive sampling of plants to make daily measurements of RWC. In addition, osmotic water potential, total water potential, and chlorophyll content were also determined using the sample plants.

3.4.1 Physical Measurements

3.4.1.1 Environment

As in Trial 4, exterior temperature, relative humidity, and downwelling solar irradiance were recorded. Interior temperature and relative humidity were measured prior to other observations. Figure 3-16 summarizes these data.

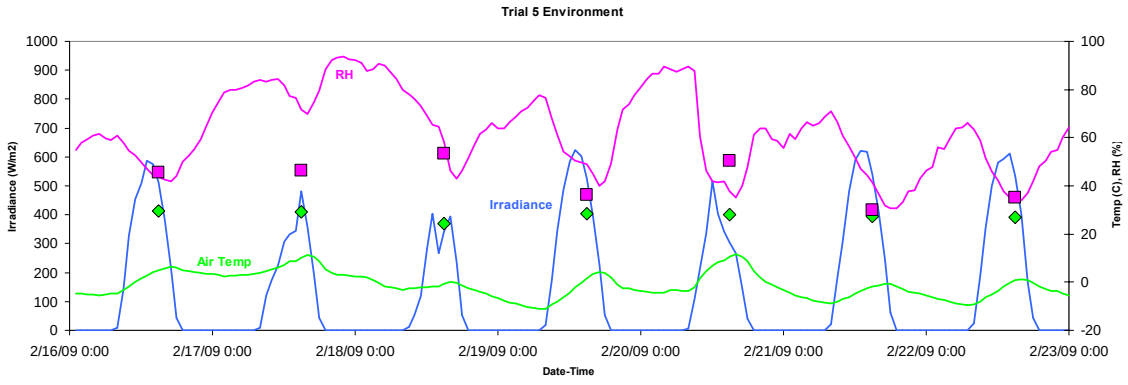

Figure 3-16. Trial 5 environmental conditions. The lines show outside air temperature (green), relative humidity (pink), and downwelling irradiance (blue). The temperature and humidity inside the greenhouse at measurement times are shown as diamonds and squares, respectively.

During Trial 5 the average interior temperature was about 28 ºC with a standard deviation of 2 ºC. Relative humidity was, on average, 42% with a standard deviation of 9%. Downwelling irradiance averaged 463 W/m^2 with a standard deviation of 98 W/m^2. In comparison to Trial 4, the average temperature was the same. Relative humidity was 1.5 times greater. Downwelling irradiance was 60% of that during Trial 4 with a standard deviation over three times greater – 98 W/m^2 vs. 30 W/m^2 (excluding one anomalous day for Trial 4, as described in Section 3.3.1.1).

3.4.1.2 Relative Water Content

Following the experimental design for destructive sampling described in Chapter 2 and used during Trial 4, RWC proxy values were determined for Trial 5. A complete summary of all measurements is shown in Appendix A, Tables A-3 and A-4.

The statistics for sampled control plant leaves (one leaf per position from each of two sample plants) are shown in Table 3-2. All three leaf positions showed an average RWC of about 98%. Standard deviation of the top and middle leaves was about 2%. The bottom leaves showed slightly higher variability – standard deviation of 3%. Coefficients of variation were small. Thus, it can be concluded that the control leaf RWC remained unchanged during Trial 5.

Leaf	Average RWC (%)	Standard Deviation (%)	Coefficient of Variation (%)
Top	97.8	2.0	2
Middle	97.6	2.3	2
Bottom	97.6	3.1	3

Table 3-2. Trial 5 control plant relative water content measurements.

Test leaves, as with Trial 4, showed essentially linear decreases in RWC over the seven days of the experiment as shown in Figure 3-17. However, data for the first and second day of the experiment for the bottom leaves and for one of the two top and middle

leaves appeared to be outliers. For example, the bottom leaf RWC measurements were 113% and 76% on the first day and 134% and 77% on the second day. For the top and middle leaves on days one and two, one leaf was in the expected range above 90% and the second leaf was near 75%. Examination of the measurements showed that the full turgor weight determinations for suspect measurements were very different from the full turgor weights determined for the rest of the leaf samples. Determining the full turgor sample weights is the most error-prone part of the measurement process. The accuracy depends upon effective surface drying of the wet leaf samples without squeezing liquid from inside the samples. These outlying values most likely resulted from measurement error. Therefore, first and second day bottom leaf values and the lower of the middle and top leaf values were ignored in computing RWC statistics.

With that proviso, top and middle leaves had RWC values of 97% and 99%, respectively, on the first day. At the end of seven days, the average (of two leaves) RWC values were 59%, 56%, and 51%, respectively, for the top, middle, and bottom leaves. Linear regression best-fit lines in Figure 3-17 indicate that the middle leaves have the smallest daily RWC differences between sample leaves. Since data for the bottom leaves started on day 3, it is difficult to compare this position with the others. The slopes of the average best-fit lines show a daily decrease in RWC of about 7% for each leaf position.

Leaves in this experiment were less stressed than those in Trial 4. After six days without water, Trial 4 leaves were approximately 10% lower in relative water content than those in Trial 5. The differences between the maximum and minimum RWC values for each leaf pair were also smaller in Trial 5, as can be observed by comparing Figures 3-17 and 3-8. Trial 4 average differences were 9%, 4%, and 6% for the bottom, middle,

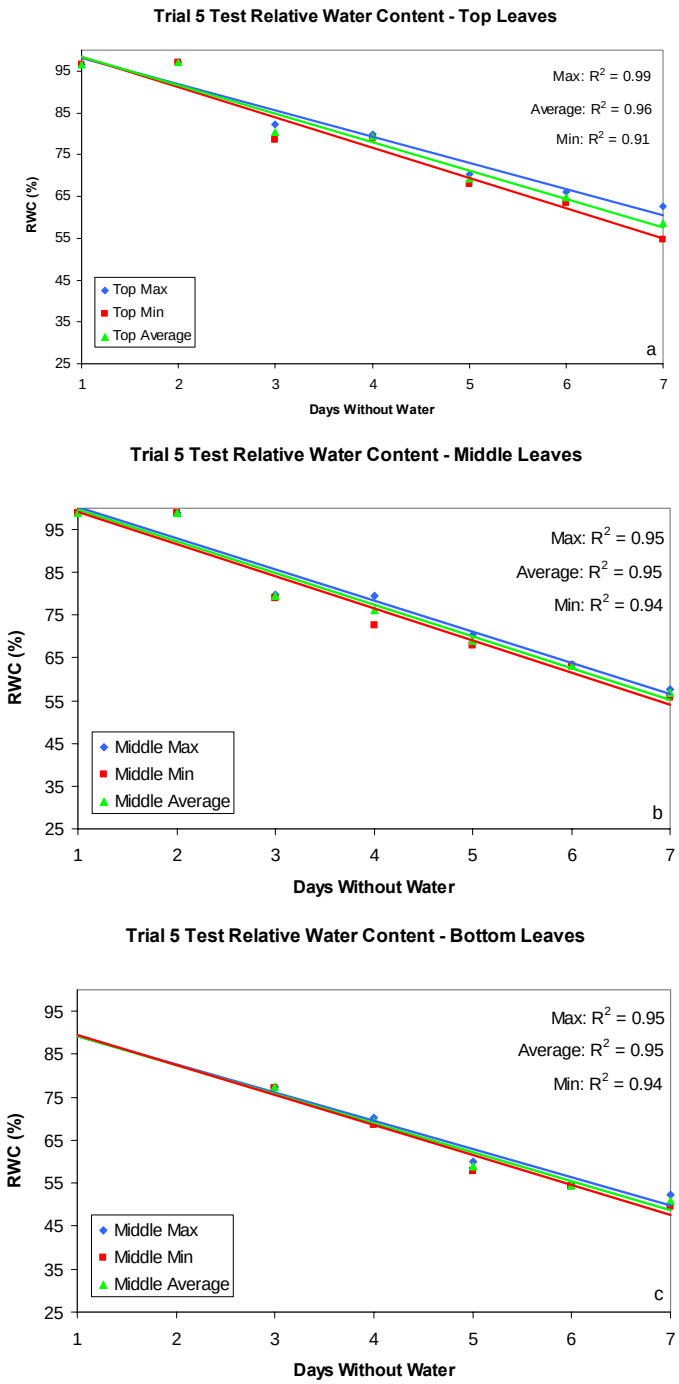

Figure 3-17. Trial 5 measured test leaf RWC. For each leaf position, "Max", "Min", and "Average" indicate the high, low, and average RWC value for the two leaves sampled each day. Lines are best-fit linear regression lines for the high, low, and average values. Top, middle, and bottom leaves are shown in panels (a), (b), and (c), respectively. Clearly erroneous data have been excluded as explained in the text.

and top leaves, respectively. For Trial 5, the average differences were 1%, 2%, and 4% for the same leaf positions.

3.4.1.3. Water Potential

Water potential was measured during Trial 5 using one of the two top, middle, and bottom leaves selected for destructive RWC determination (details are in Chapter 2). Osmotic water potential is plotted versus day from the start of the experiment in Figure 3-18 for both test and control leaves. This measurement provides insight into the state of plant cells. Low osmotic potential indicates that solute concentrations have increased in cell in order to increase osmotic pressure and bring more water into the cell (Jones & Turner, 1978; Milburn, 1979). Because only one measurement was made for each plant group on each day, error bars are not available.

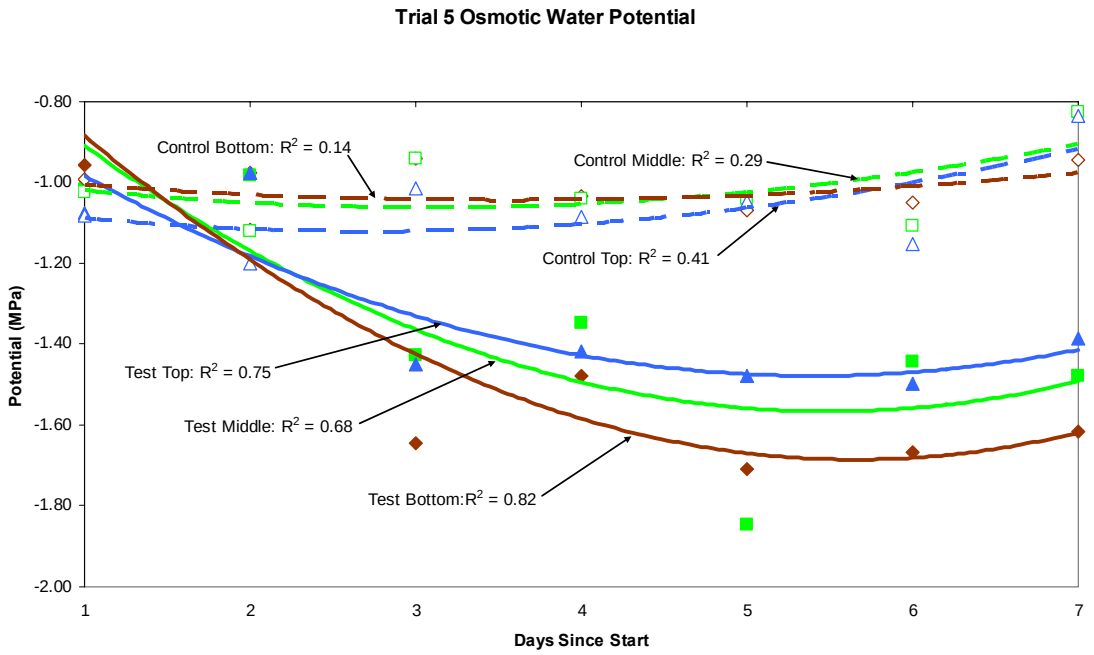

Figure 3-18. Trial 5 osmotic water potential vs. day from start of the experiment. Open symbols indicate control leaf water potential. Closed symbols indicated test leaf water potential. Top, middle, and bottom leaves are indicated, respectively, by a triangles, squares, and diamonds. Lines are quadratic regression best-fits to each data set: solid lines indicate test data and dashed lines indicate control data. Coefficients of determination are shown for all lines.

From Figure 3-18, it can be deduced that all control leaves were at a relatively constant osmotic potential. Coefficients of variation were, calculated to be 10% or less. Therefore control leaves showed little change in osmotic potential over the course of the experiment.

Test plant leaves showed decreasing osmotic potential from day one to the third day following the start of the experiment. After day three, osmotic potential remained relatively unchanged. The CV values, from days three to seven, for the top, middle, and bottom leaves were 5%, 13%, and 3%, respectively. This leveling-off of osmotic potential probably indicates that the leaf has reached a limit in the amount of solutes available to adjust osmotic pressure (Morgan, 1984).

3.4.1.4 Chlorophyll Content

Chlorophyll content was measured by chemical extraction during Trial 5. The process is described in Chapter 2. Figure 3-19 shows the change in total chlorophyll (*a* and *b*) content over the period of the experiment for control and test plants, respectively. The control plants showed increasing chlorophyll content appropriate for healthy, growing plants. The test plants showed an increase in chlorophyll content, similar to that in the control leaves for the first three days and then declining levels for the remaining four days.

Chlorophyll content will be revisited in Chapter 5. Understanding the influence of chlorophyll content on the reflectance spectrum is an important consideration in developing a model to use as a proxy for water status.

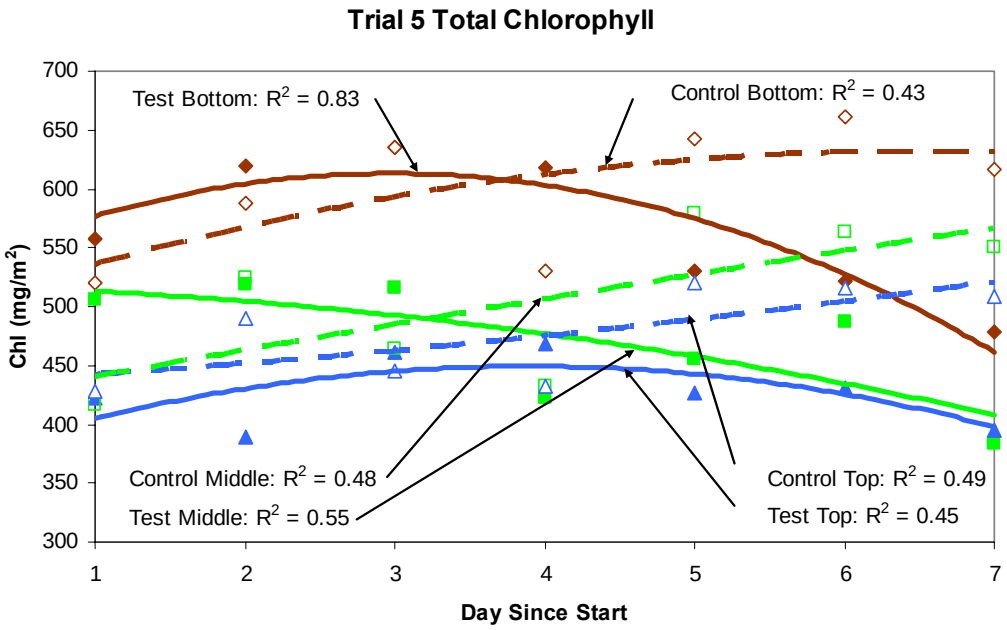

Figure 3-19. Trial 5 measured chlorophyll content vs. day from start of the experiment. Open symbols and dashed lines denote control leaf measurements. Closed symbols and solid lines denote test leaf measurements. The lines are quadratic regression best-fit.

3.4.2 Radiometric Measurements

3.4.2.1 Hyperspectral Measurements

Hyperspectral measurements on the first day of the experiment were flawed because incorrect calibration values were input to the ASD Hyperspectral Radiometer, which caused erroneous reflectance values. However, because the calibration equations were linear between 400 nm and 970 nm, it was relatively simple to compensate for this error. Compensating for the error in the remaining portion of the measured spectrum, 970 nm through 2500 nm, was not possible because of the mathematical complexity of determining corrections based on higher order calibration equations. Therefore, reflectance values are shown only for 400 nm to 970 nm on day one of the experiment. Correct calibration values were applied on succeeding days.

3.4.2.1.1 Variability Over Time

Figure 3-20 contains the Trial 5 control middle leaf reflectance spectra. Spectra for all three control leaf positions are included in Appendix A, Figure A-5. As with Trial 4, the control plant bottom and middle leaves showed little variation in reflectance, although reflectance of the top leaves appeared to have a little more variability. CV of reflectance (Figure 3-20 and A-5) was below 10% for all leaf positions at every wavelength. Once again, this implies that there was virtually no change in reflectance for the control leaves over the period of the experiment.

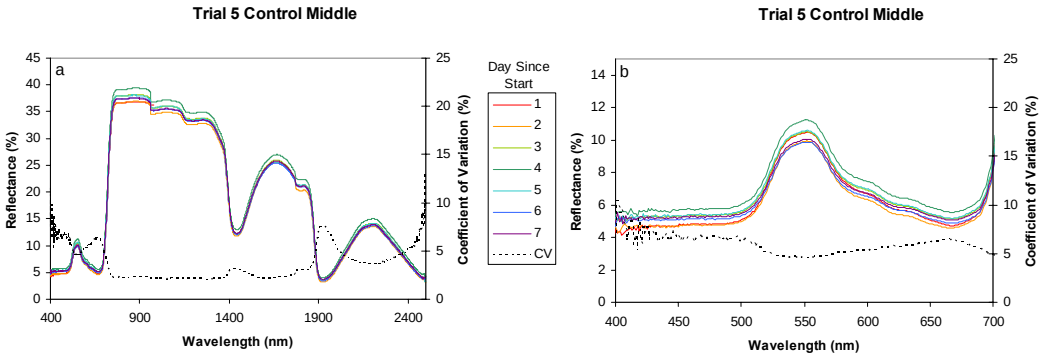

Figure 3-20. Trial 5 daily control middle leaf average reflectance spectra. Panel (a) shows the entire measured spectrum. Panel (b) contains only the PAR spectrum. Only 400 nm to 970 nm reflectance is shown for day one.

Figures 3-21 and 3-22 contain the test leaf reflectance spectra. Like the earlier trials, the reflectance for the test leaves showed an increase over time. Reflectance in the PAR and MIR regions appeared to increase with time after watering stopped but reflectance in NIR did not. CV of reflectance was similar in shape to those for Trial 4. The NIR region reflectance showed CV values well below 10%. All leaves showed increases in CV at the same wavelengths in the spectrum, in PAR near 530 nm and 640 nm, in MIR above 1400 nm, 1900 nm, and 2400 nm. The bottom leaf showed slightly higher peaks of CV than the other leaves. Overall, the peaks of CV were 5% to 10%

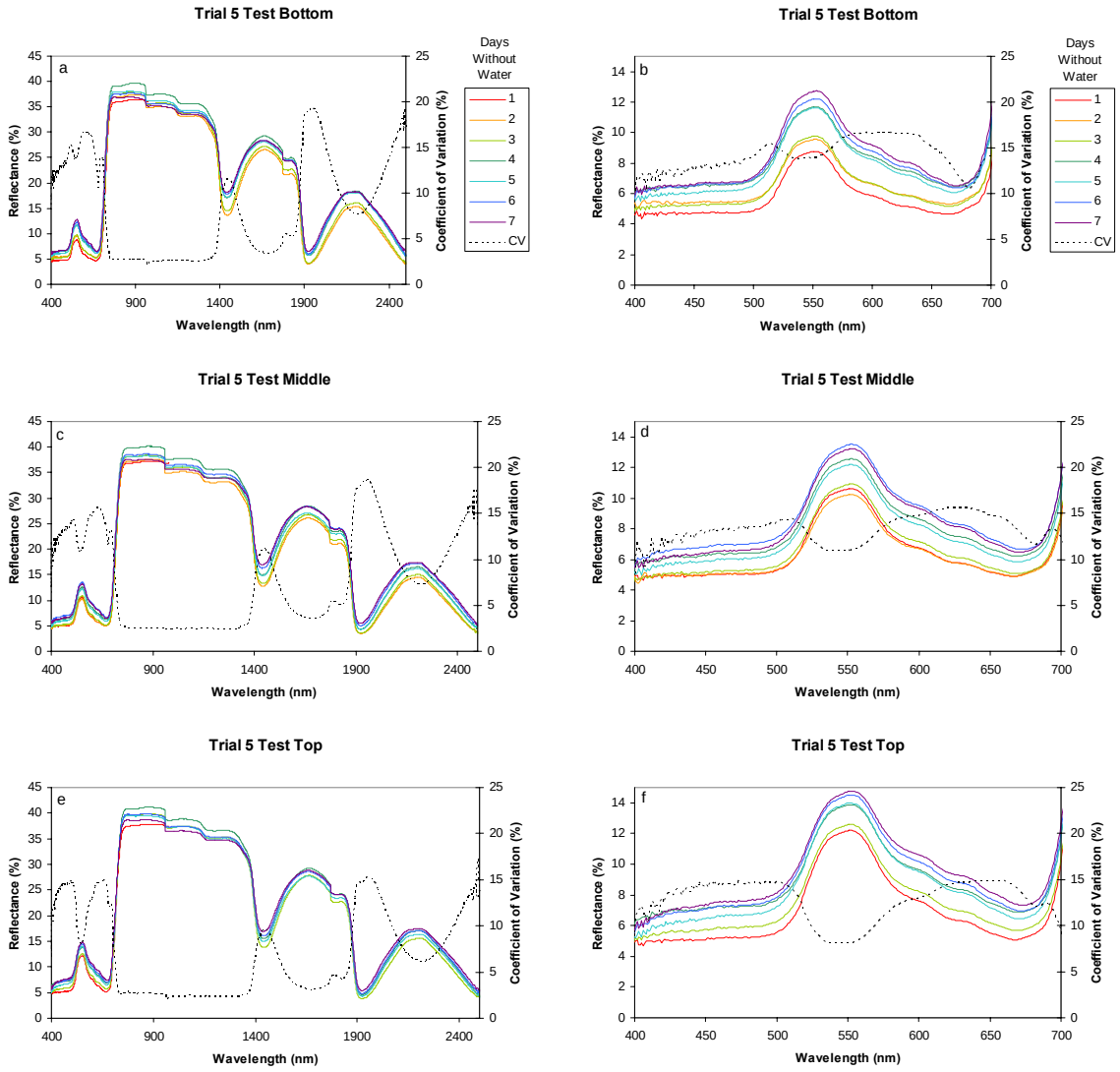

Figure 3-21. Trial 5 daily test leaf average reflectance spectra. Panels (a), (c), and (e) show the full spectrum. Panels (b), (d), and (f) show only the PAR spectrum. Panels show bottom leaves, (a) and (b), middle leaves, (c) and (d), and top leaves, (e) and (f). Only 400 nm through 970 nm are shown for day one.

lower than those in corresponding days in Trial 4.

Trial 4 spectra showed a consistent increase in reflectance in the PAR and MIR regions over time. The reflectance of leaves at each day in these regions is higher than the reflectance the day before. The reflectance change in Trial 5 was not as consistent. For example, the reflectance in PAR region on days two, five, and seven was slightly less than those on the preceding day. The explanation appears to be related to the

environment. As can be observed by comparing the relative humidity and irradiance values in Figures 3-7 and 3-16, Trial 4 was conducted during fairly uniform weather conditions. In contrast, there was higher variation in illumination and relative humidity during the seven days of Trial 5.

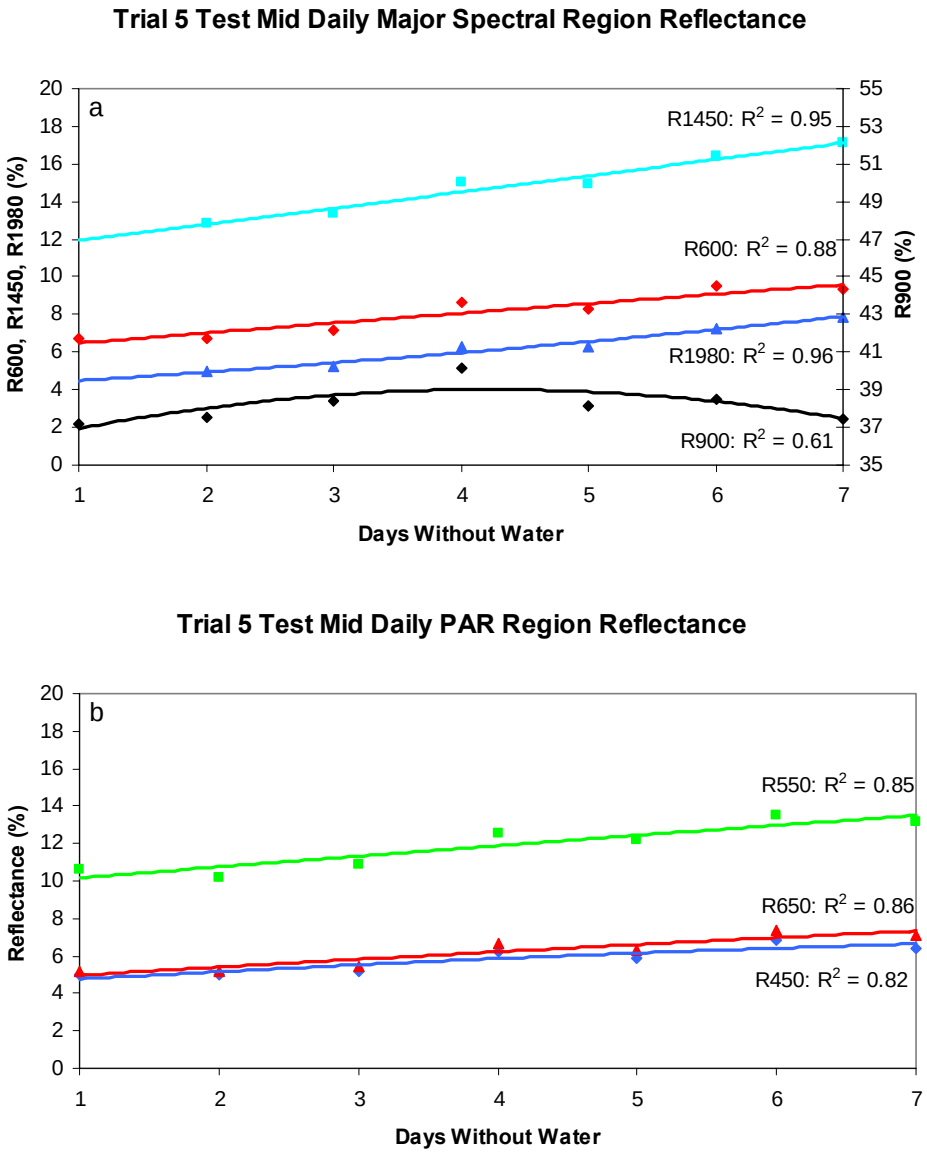

Figure 3-22. Trial 5 test leaf daily reflectance at wavelengths representing spectral regions. Panel (a) shows the major spectral regions. Panel (b) shows the PAR region. Lines are quadratic best-fit.

One interpretation is that decreasing illumination, increasing relative humidity, or both, caused less water loss from the plant. If less water was lost, then the plant would have an opportunity to replenish its water content by drawing more water from whatever remained in the potting soil. Hence, the Trial 5 plants could show a slight reduction in water stress during the day prior to the three apparently inconsistent spectral measurements.

3.4.2.1.2 Information Content

As was observed in Trials 3 and 4, Trial 5 PAR and MIR reflectance increased similarly throughout the experiment. Changes in NIR did not appear closely related to the other two regions. The discussion on CV in the previous section corroborates these observations.

R^2 charts for Trial 5 control leaves are shown in Figure 3-23. For the control leaves, the PAR region appeared to correlate well with all regions except that near about 1400 nm to about 1700 nm. Within the PAR, reflectance near 550 nm and 720 nm did not correlate well with other wavelengths. Other than those areas, the reflectance in the whole PAR region reacted similarly over the experiment period.

Once again, examination of specific wavelengths in each spectral region and within PAR helps to clarify the relationships. Figure 3-24 contains graphs plotting the relationship (R^2) between specific wavelengths representing the major spectral bands, and the PAR region, versus all other wavelengths. In general, reflectance at all of the selected specific wavelengths is strongly related to all other wavelengths (R^2>0.7). The exceptions are near the green absorption minima at 550 nm, the red edge at 715 nm, about 970 nm, and about 1750 nm. The first two may be related to small random

a

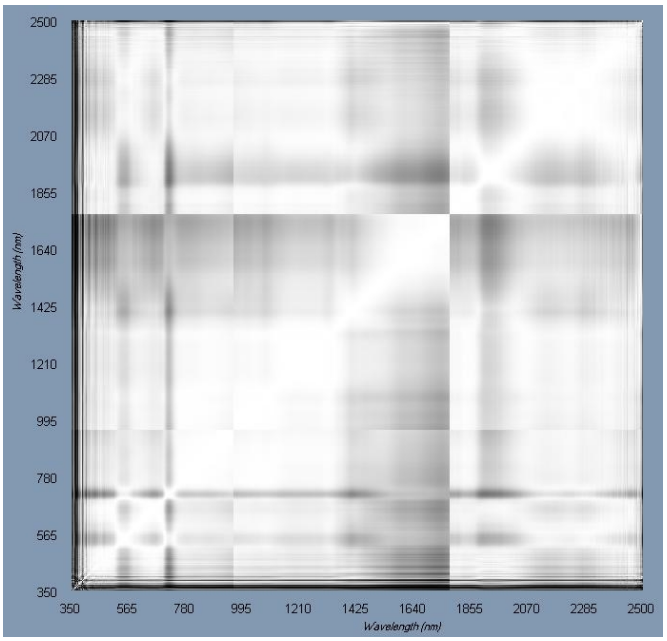

b

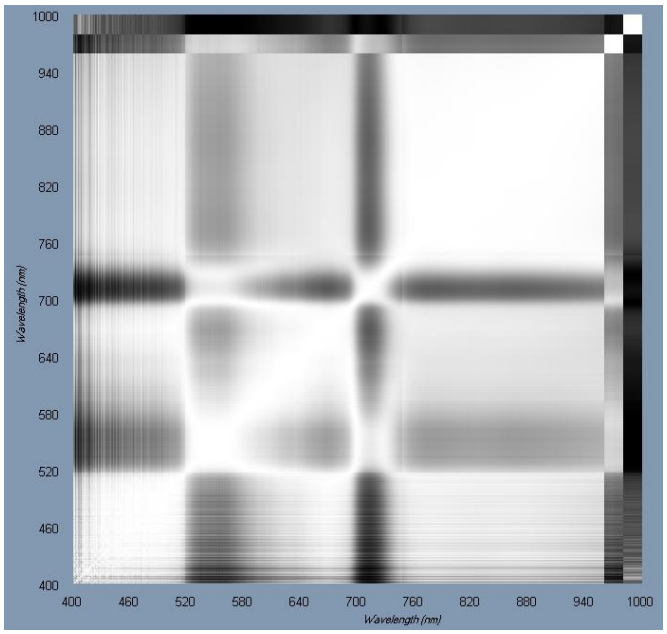

Figure 3-23. Trial 5 control middle leaf coefficient of determination (R^2) matrix charts. Panel (a) indicates the relationship among all measured wavelengths (day two through seven only because of calibration error). Panel (b) is limited to near the PAR region (all days). A white pixel indicates R^2=1. Black pixels indicate R^2=0.

differences in chlorophyll among the control leaves. It is possible that the latter two are due to structural scattering that is largely unrelated to other plant constituents such as

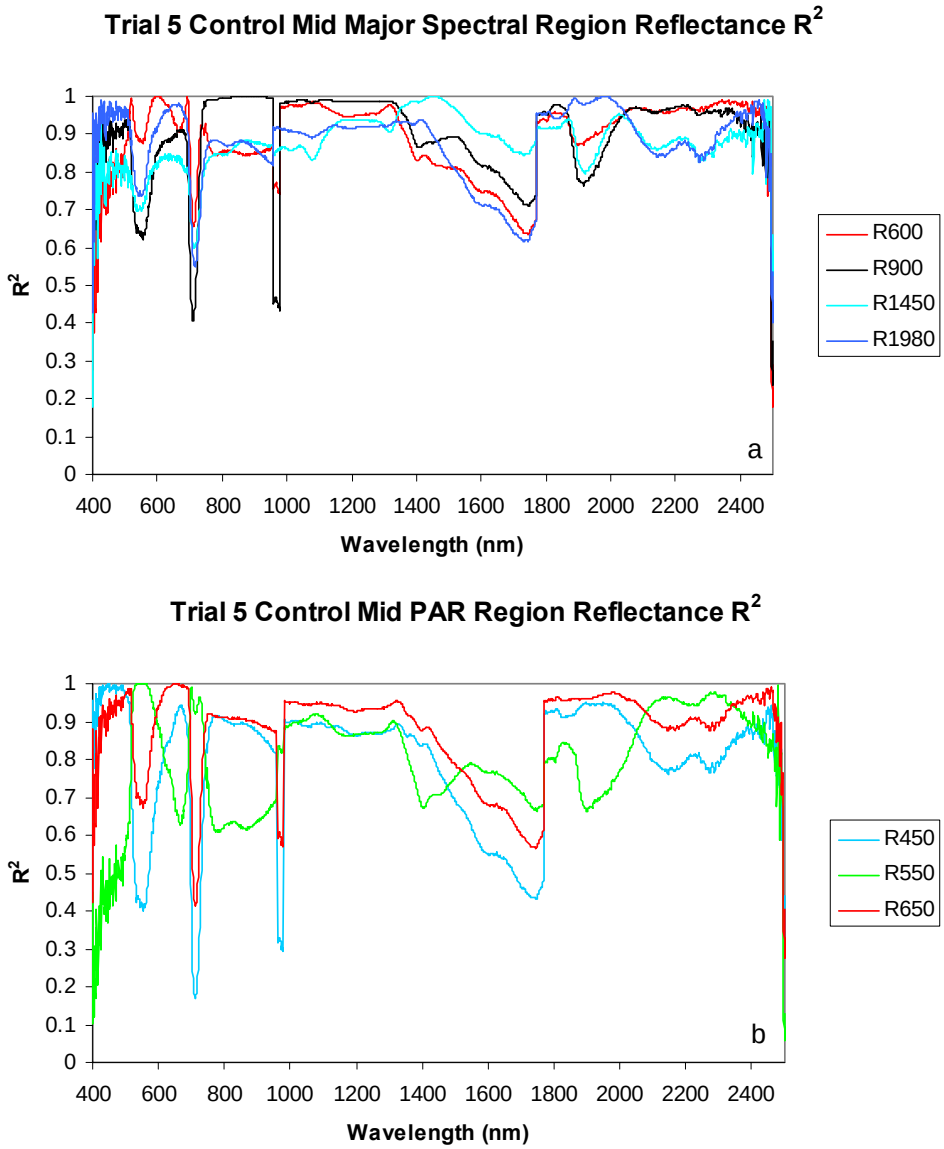

Figure 3-24. Trial 5 control leaf strength of the relationships of changes in reflectance at specific characteristic wavelengths against all other measured wavelengths. Lines depict R^2 for major spectral regions control, panel (a), and the PAR region, panel (b).

pigments or water content. Trial 4 R^2 values (Figure 3-13) averaged near 0.55 for all selected wavelengths. In Trial 5, the average was about 0.9. The reason for this difference is not known. It is not likely to be caused by environmental factors. More

importantly, given the small variation in reflectance overall, it is difficult to suggest any systematic causes.

R^2 charts for test leaves are in Figure 3-25. The test leaf reflectance, similar to Trial 4, showed strong correlation between PAR and MIR. NIR reflectance did not correlate to reflectance in the other two regions. Within PAR, all wavelengths were strongly correlated with each other. There appeared to be smaller R^2 values among those areas showing weaker correlation in Trial 5. This was evidenced by the blacker features at similar wavelengths in comparison to Trial 4 (Figure 3-14).

Graphs plotting R^2 for specific wavelengths against all other wavelengths in the spectrum are shown in Figure 3-26. Like Trial 4, NIR did not correlate strongly with any other region, PAR reflectance correlated strongly with MIR reflectance, and all wavelengths within the PAR correlated well with all other PAR wavelengths. Reflectance at 600 nm had R^2 values above 0.98 with all other PAR wavelengths and greater than 0.85 throughout MIR. However, R^2 values with the NIR are as lows as 0.1. As before, there appears to be a strong relationship between water content, evidenced by the water molecule absorption wavelengths, and PAR reflectance.

Unlike Trial 4 (Figure 3-15), areas with weaker correlations showed much smaller R^2 values. For example, NIR minimum R^2 was about 0.4 at 1450 nm in Trial 4. In Trial 5, the R^2 was 0.0. It was noted earlier that the change in reflectance during Trial 5 was not as consistent as that observed during Trial 4. At least some of this was attributed to greater variation in the environment. It is possible that this effect contributed to lower R^2 values by obscuring the weaker correlations.

a

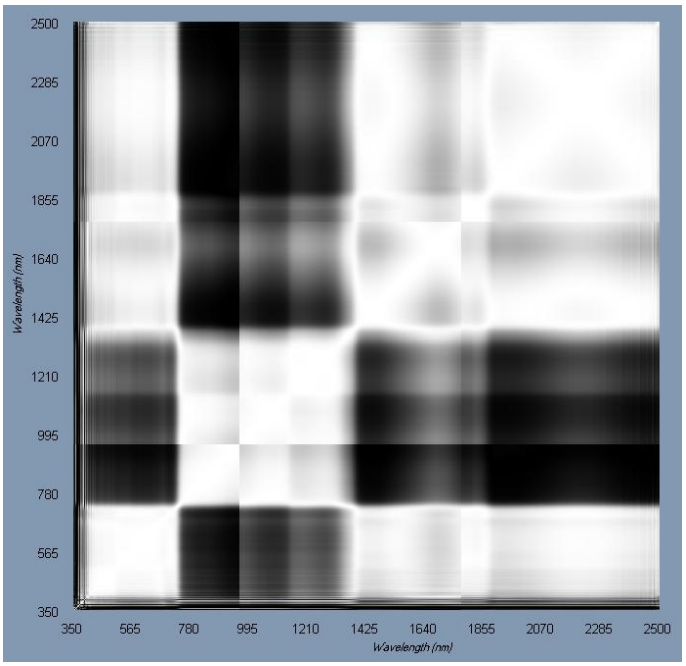

b

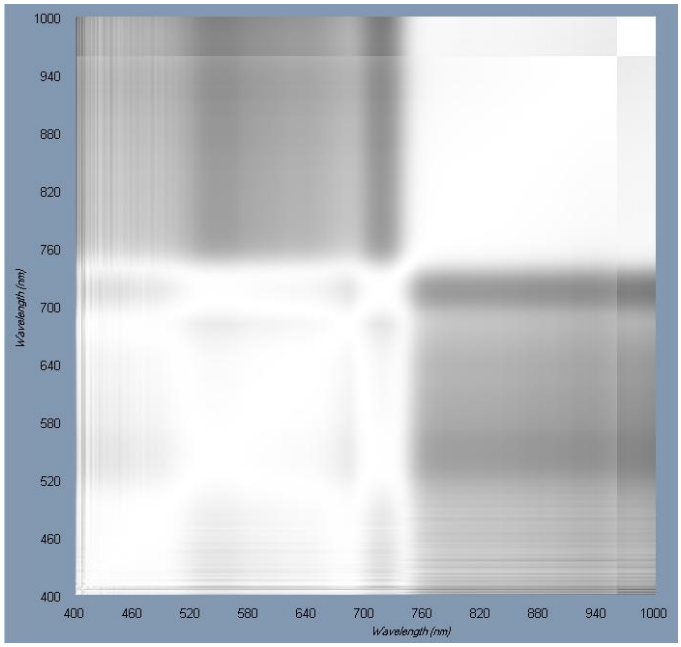

Figure 3-25. Trial 5 test middle leaf coefficient of determination (R^2) matrix charts. Panel (a) indicates the relationship among all measured wavelengths (day two through seven only due to calibration error). Panel (b) is limited to near the PAR region (all days). A white pixel indicates R^2=1. Black pixels indicate R^2=0.

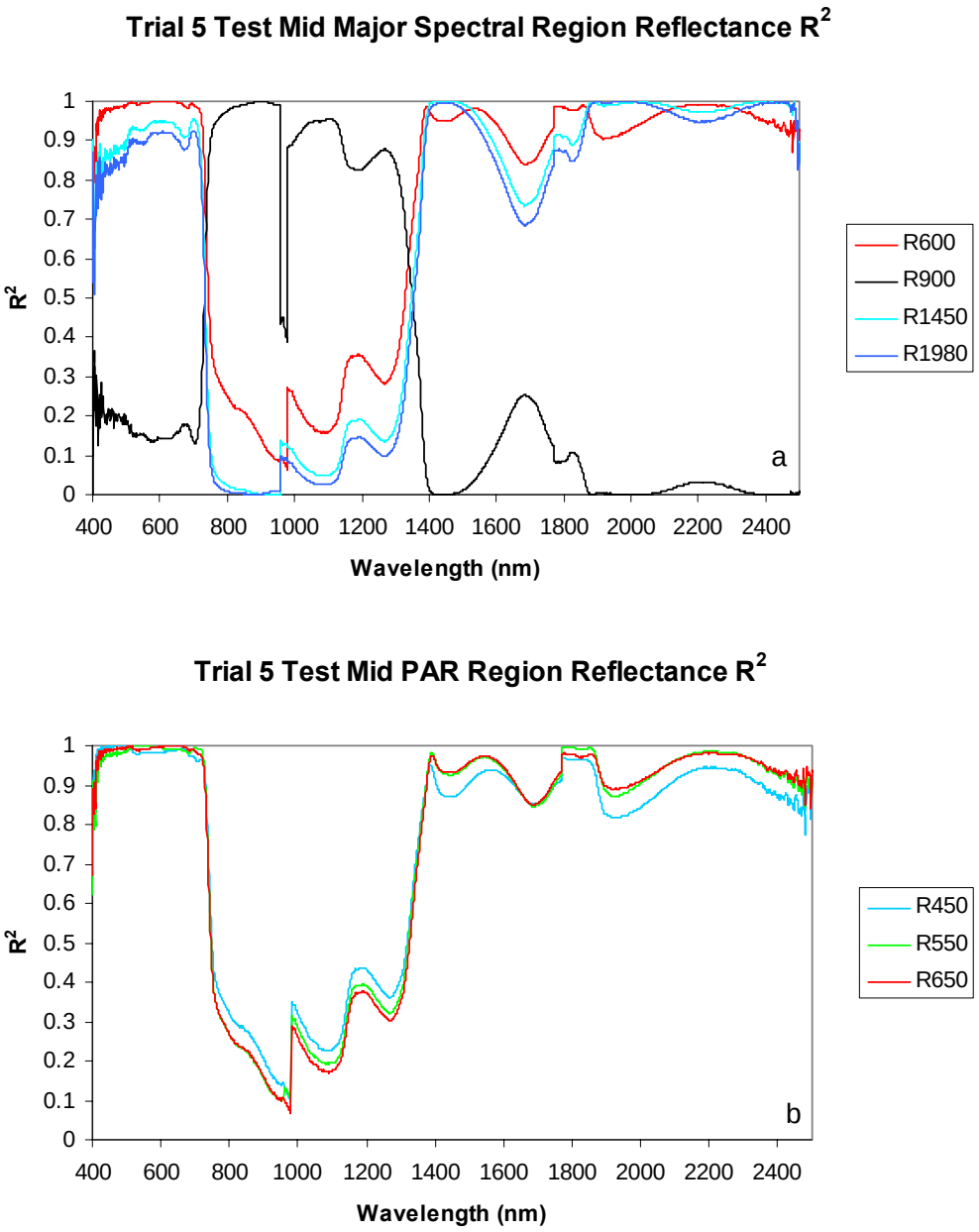

Figure 3-26. Trial 5 test leaf strength of the relationships of changes in reflectance at specific characteristic wavelengths against all other measured wavelengths. Lines depict R^2 for major spectral regions control, panel (a), and the PAR region, panel (b).

3.5 Leaf Surface Variability Experiment

During Trials 3, 4, and 5, measurements were made approximately 2 cm from the stem on top, middle, and bottom leaves. Some concern was expressed that there may be variability caused by the position at which the ASD probe was placed on the leaf. To

understand the impact of sample positioning on leaves, an experiment was performed at the end of Trial 5. As described in Chapter 2, measurements were made twice at four positions on each of the middle leaves. The results are plotted in Figure 3-27(a). Control reflectance was virtually unchanged along the length of the leaf. Test reflectance varied by a small amount, on the order of one percent. However, the standard deviation error bars suggest that the probable change in reflectance was slight. For comparison, the measured relative water content is shown in Figure 3-27(b). Control plant RWC dropped by about 2% over the length. The test plant RWC decreased by 7%. The actual Trial 5 ASD probe position was much closer to the stem than 15 cm for all measurements. From this, it can be concluded that spatial variation had little or no impact on the Trial 4 or 5 experiments.

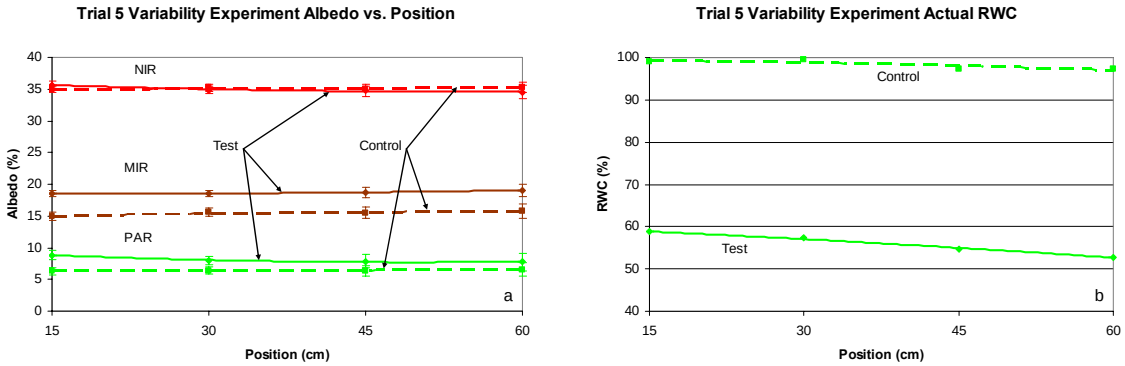

Figure 3-27. Spatial variability experiment. Panel (a) graphs albedo vs. leaf position for PAR, NIR, and MIR albedo. One standard deviation error bars are displayed at all points. Quadratic regression best-fit lines are shown to connect points. Panel (b) shows the physically measured RWC at each leaf position.

3.6 Chapter Conclusions

The principal findings from the research summarized in this chapter are as follows:

1. **Over three independent experiments, it was shown that maize leaf reflectance in PAR and MIR increases over time for plants deprived of water.** No such systematic effect was observed in maize control leaves. It was also found that PAR reflectance and MIR reflectance changed almost synchronously. As mentioned above, MIR reflectance is affected strongly by water absorption. There is little or no absorption of light in the PAR region by water. It may, therefore, be assumed that a secondary effect, associated with the onset of moisture deficit, is causing the change in PAR reflectance. Because there was relatively less variability in green light reflectance, compared to the stronger chlorophyll and carotenoid absorption wavelengths in the blue and chlorophyll absorption in the red, this effect is probably due more to a change in absorption by leaves.
2. The experimental design using RWC determination on randomly selected plants as proxies for the larger plant population was validated. The results of Trial 3 showed this statistically. Consistency of reflectance increase over the three trials along with a concomitant decrease in RWC showed this by inference. In addition, a special experiment performed during Trial 5 showed that there was little, if any, error introduced by inadvertent and unavoidable variation in the position at which measurements were made on the leaves.

Chapter 4: Soy Experiments – Observations and Data

4.0 Chapter Contents

4.1 Chapter Introduction

This chapter presents observations and measurements made during water stress experiments conducted with soy. The objective of the chapter is to lay the foundation for the analysis in Chapter 5 of the relationship between water stress and the character of multispectral reflectance in maize.

In Chapter 3, maize was described as a C4 plant, which includes those plants using a particular photosynthesis process well suited to warm, dry climates. In contrast, most plants in the world (about 95%) use a more primitive photosynthetic process known as C3. C3 plants thrive in temperate climates. As shown in Figure 4-1, C3 plants have

chloroplasts in their mesophyll cells and not in their bundle sheaths. Note the specialized palisade layer of almost columnar mesophyll cells which underlie the upper epidermis. This layer may play a significant role in differentiating reflectance between water-stressed C4 and C3 plants. The photosynthetic rates of C3 plants are also substantially lower than those in C4 plants. It is thought that C4 plants evolved after C3 plants because among plant families, there are no families that consist only of C4 plants (McDonald, 2003). Soy is a well-known and important C3 crop plant. It provides food, in the form of its beans, as well as oil used for a variety of purposes. This plant was the subject of Trials 6 and 7.

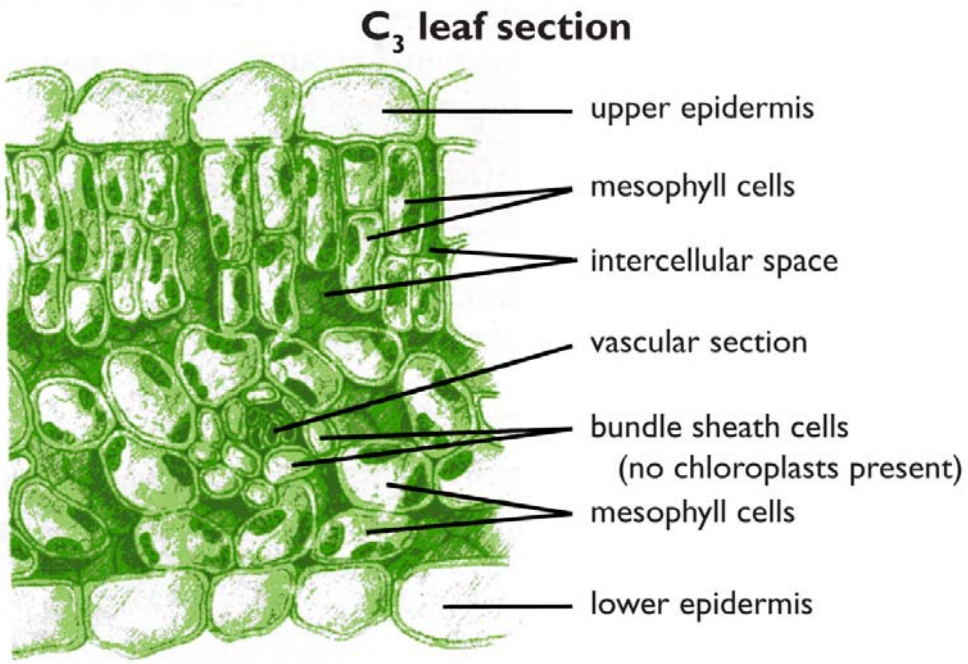

Figure 4-1. C3 leaf diagram. Artwork created and provided by Paul Royster, University of Nebraska-Lincoln Libraries.

The two experiments performed with soy had different designs. As described in Chapter 2, Trial 6 was similar to the design of the maize experiments where plants were randomly assigned to control and test groups. In Trial 7, there were four "lines" of plants. In each line, one plant was watered for the full period of the trial. A second plant

was not watered after the second day; a third plant was not watered after the third day; and so on until each line represented plants having a gradient of water stress.

Each trial is described below, in turn. Direct biophysical, environmental, and radiometric measurements are also presented. Similar to the maize experiments, direct biophysical measurements included RWC and water potential. Environmental measurements included temperature, relative humidity, and irradiance. Radiometric measurements included reflectance and transmittance.

4.2 Trial 6 (Soy – Control vs. Treated)

As described in Chapter 2, Trial 6 involved forty-four plants randomly divided into two equal groups: control and test. Control plants were watered every day following the experiment measurements (approximately three pm). Test plants were unwatered for the entire experiment period. Two control and two test plants were randomly selected each day for destructive determination of physical parameters. Measurements used all three leaves at the fourth trifoliate position, near the center of the plant.

4.2.1 Physical Measurements

4.2.1.1 Environment

During Trial 6, downwelling solar irradiance was continuously recorded. (Unlike other trials, as explained in Chapter 2, irradiance measurements were made inside rather than outside the greenhouse.) Interior temperature and relative humidity were determined daily prior to other measurements. Figure 4-2 summarizes these data.

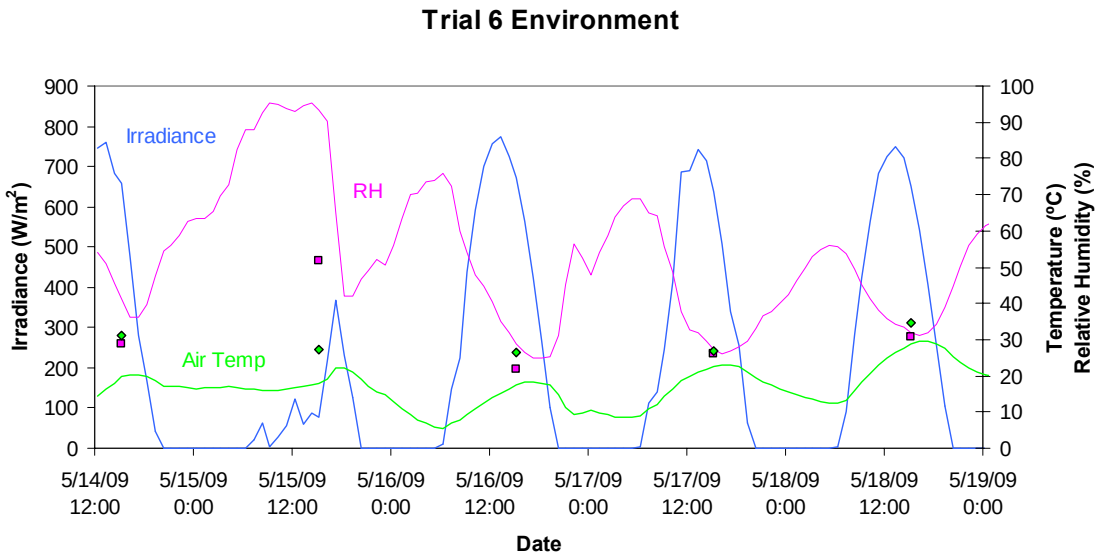

Figure 4-2. Trial 6 environmental conditions. The blue lines show downwelling irradiance. The temperature and humidity inside the greenhouse at measurement times are shown as diamonds and squares, respectively.

The average temperature during the experiment was 29 ºC with a standard deviation of 4 ºC. Relative humidity averaged 32% with a standard deviation of 12%. Irradiance at the time of the other physical measurements averaged 540.0 W/m^2. The standard deviation for irradiance was 259.5 W/m^2. This rather large variation is caused by the very cloudy sky on the second day of the experiment. If the data for that day is ignored, the average relative humidity and irradiance become 27% and 655.8 W/m^2, respectively. Their standard deviations drop, respectively, to 4% and 14.3 W/m^2.

4.2.1.2 Relative Water Content

Destructive sampling was used to determine RWC. Two control and two test plants were randomly selected each day. Four 1-centimeter disks were punched from each leaf in the fourth trifoliate (yielding a total of 12 discs per plant) after reflectance measurements were made on those leaves. Using the technique described in Chapter 2,

RWC was determined for each set of leaves. The complete results are shown in Appendix A, Tables A-6 and A-7.

The control leaves had an average RWC of 91.7%. The standard deviation was 3.6%. The coefficient of variation of RWC was 3.9%. Thus, it can be stated that there was virtually no change in control leaf RWC over the period of the experiment.

Figure 4-3 contains plots of RWC versus time for the maximum, minimum, and average of the two daily leaf samples. Looking just at the plot points, average RWC was 92.7% after the first day without water, 95.8% on the second day, and dropped to 66.2%

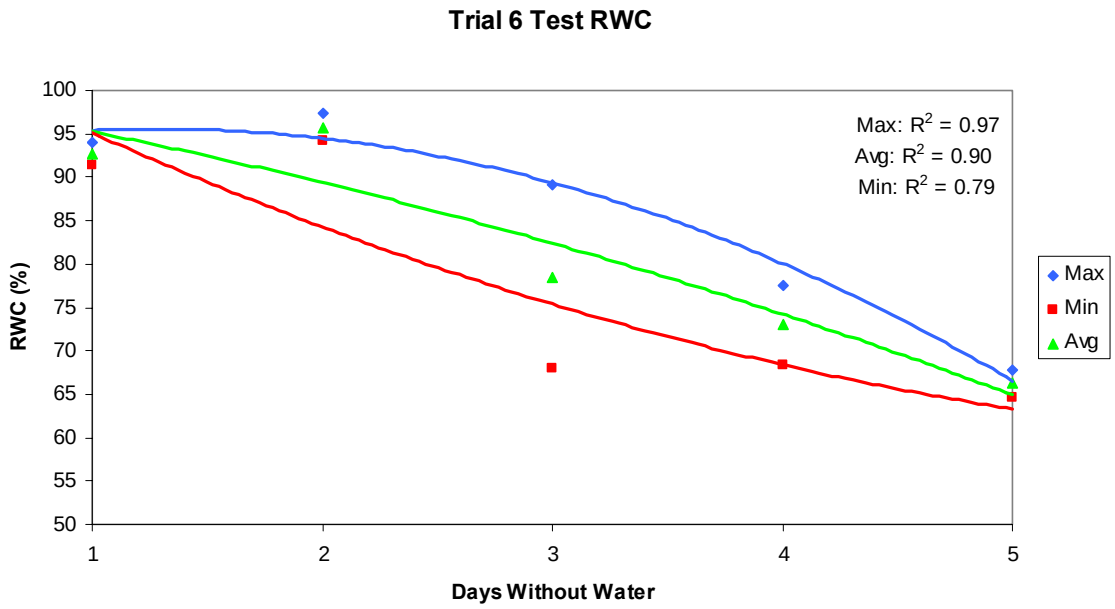

Figure 4-3. Trial 6 measured test leaf RWC. "Max", "Min", and "Avg" represent the maximum, minimum, and average values for the leaves sampled from two plants each day. Lines are best-fit quadratic regression lines for the high, low, and average values.

on day five. The increase in RWC on day two is similar to that seen with maize when there was a reduction in irradiance. From Figure 4-2, it can be seen that day two was a very cloudy day, which may have given the plant a chance to recover additional water from the potting soil while the leaves were at minimal stress. There were no obvious

indications to explain the increased spread in the values obtained on days three and four. Overall, the average decrease in RWC was 7.6% per day.

4.2.1.3 Water Potential

Control leaf osmotic potential remained relatively constant, near -1.2 MPa, through the experiment, as shown in Figure 4-4(a). Osmotic potential for the test leaves, shown in Figure 4-4(b), appeared to remain level for the first two days, about -1.1 MPa, and then decreased to an average value of -1.7 MPa on day five. Again, it appears that that plant stress was eased on day two. The decreased osmotic potential indicates that the cells in the test leaves were responding appropriately to a water deficit. Note the similarities in the plots between the test leaf osmotic potentials and those for RWC in Figure 4-3. Increasing water stress is clearly shown in both graphs.

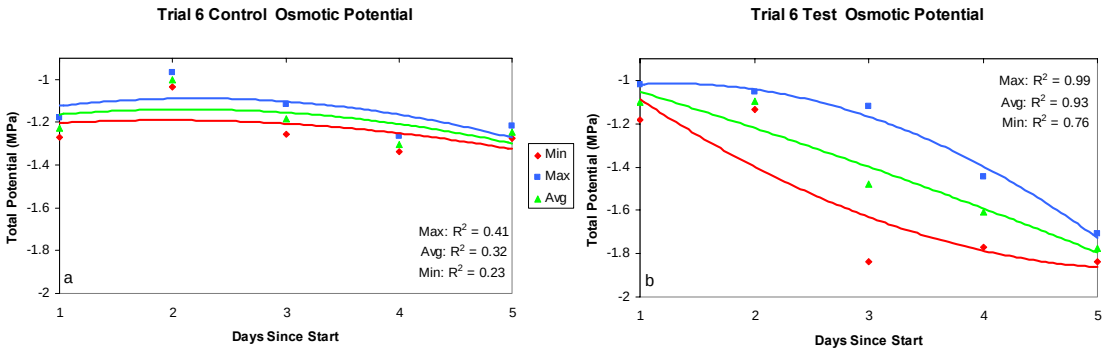

Figure 4-4. Trial 6 Osmotic Potential. Control and test leaf osmotic potential are shown in panels (a) and (b), respectively. Each point represents the maximum ("Max"), minimum ("Min"), or average ("Avg") value for the leaves of two sampled plants. Lines are quadratic best-fit lines.

4.2.2 Radiometric Measurements

Hyperspectral measurements were made each afternoon. As was done in Chapter 3, this section presents reflectance over time, information richness in comparing reflectance in one part of the spectrum against another.

4.2.2.1 Hyperspectral Reflectance

4.2.2.1.1 Variability Over Time

Control plant reflectance spectra are shown in Figure 4-5. Each plotted line represents an average of 15 plant reflectance measurements and each plant reflectance measurement is the average of the three leaflets in the fourth trifoliate. Hence, the average control leaf reflectance includes individual spectra from 45 leaflets.

The coefficient of variation of reflectance over the experiment period for the control plants is quite small for most of the spectrum. Above 520 nm, it is well below 5%. Below 520 nm, CV reaches about 15% at 400 nm. Reflectance itself shows what appears to a systematically increasing reflectance below 520 nm over the experiment period. There appears to be no systematic change in reflectance above 520 nm. The reason for the reflectance increase in the blue region for control plant leaves is unknown. (The test plant data do not show this signature.)

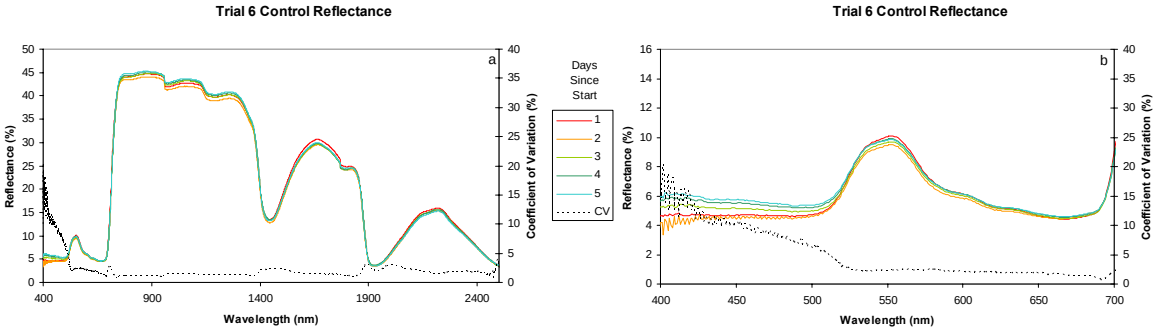

Figure 4-5. Trial 6 daily average control leaf reflectance spectra from the fourth trifoliate leaves from 15 plants (total of 45 leaves. Full spectrum and PAR spectrum are shown in panels (a) and (b), respectively.

The test plant leaf spectra, Figures 4-6 (daily reflectance spectra) and 4-7 (reflectance at specific wavelengths) show considerable variation. CV over the experiment period reaches a peak of 21% near 600 nm, 700 nm, and 1450 nm. The

region from 1900 nm to 2000 nm and the region above 2400 nm have CV peaks above 30%. Within the PAR region, CV was near 20% from 580 nm to 640 nm and there was very little variation below 500 nm (<10%). The NIR reflectance showed virtually no variation (CV < 5%) over the period.

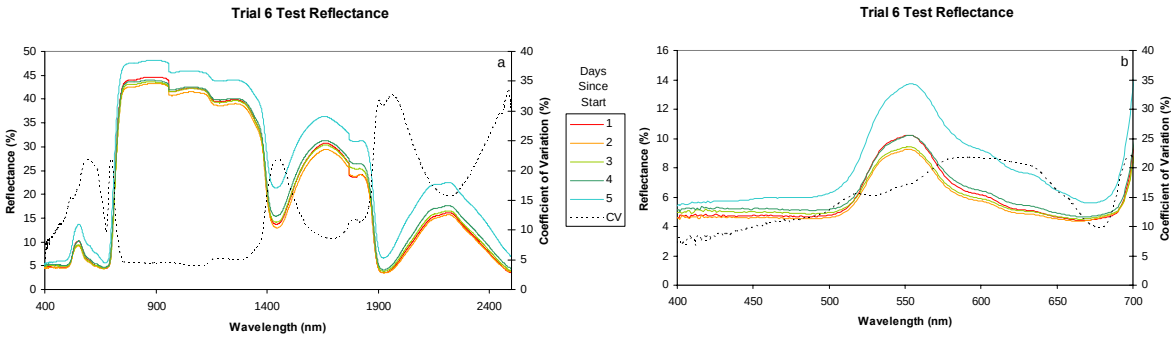

Figure 4-6. Trial 6 daily average test reflectance spectra from the fourth trifoliate leaves of 10 plants (total of 30 leaves). Full spectrum and PAR spectrum are shown in panels (a) and (b), respectively.

As shown in Figure 4-7, overall reflectance on the first day was higher than that observed on day two. At 550 nm, for example, reflectance was about 10.2% on day one. On day two, reflectance dropped to about 9.2% and then increased each day until it reached 13.6% on day five. The decrease in reflectance on day two may be related to the postulated decrease in water stress due to the cloudy day, discussed in previous sections. On the second day, the lower light levels may have subjected the plant to less stress and decreased photosynthetic production and evapotranspiration. Lower evapotranspiration water loss would give the plant a chance to replenish leaf water from that which remained in the potting soil.

4.2.2.1.2 Information Content

"Coefficient of determination matrix charts" or "R^2 charts" were introduced in Chapter 2. Figure 4-8 contains an R^2 chart for Trial 4 control leaves. From this chart, it can be seen that reflectance in the blue range from 400 nm to 520 nm correlates quite

closely with the NIR spectral region ($R^2 > 0.7$) as well as with reflectance in the red region (620 nm to 670 nm). The green region shows moderate correlation (R^2 0.7 to 0.9) to the MIR region near the water absorption features near 1400 nm and 1900 nm as well as near 1800 nm where there is no absorption feature.

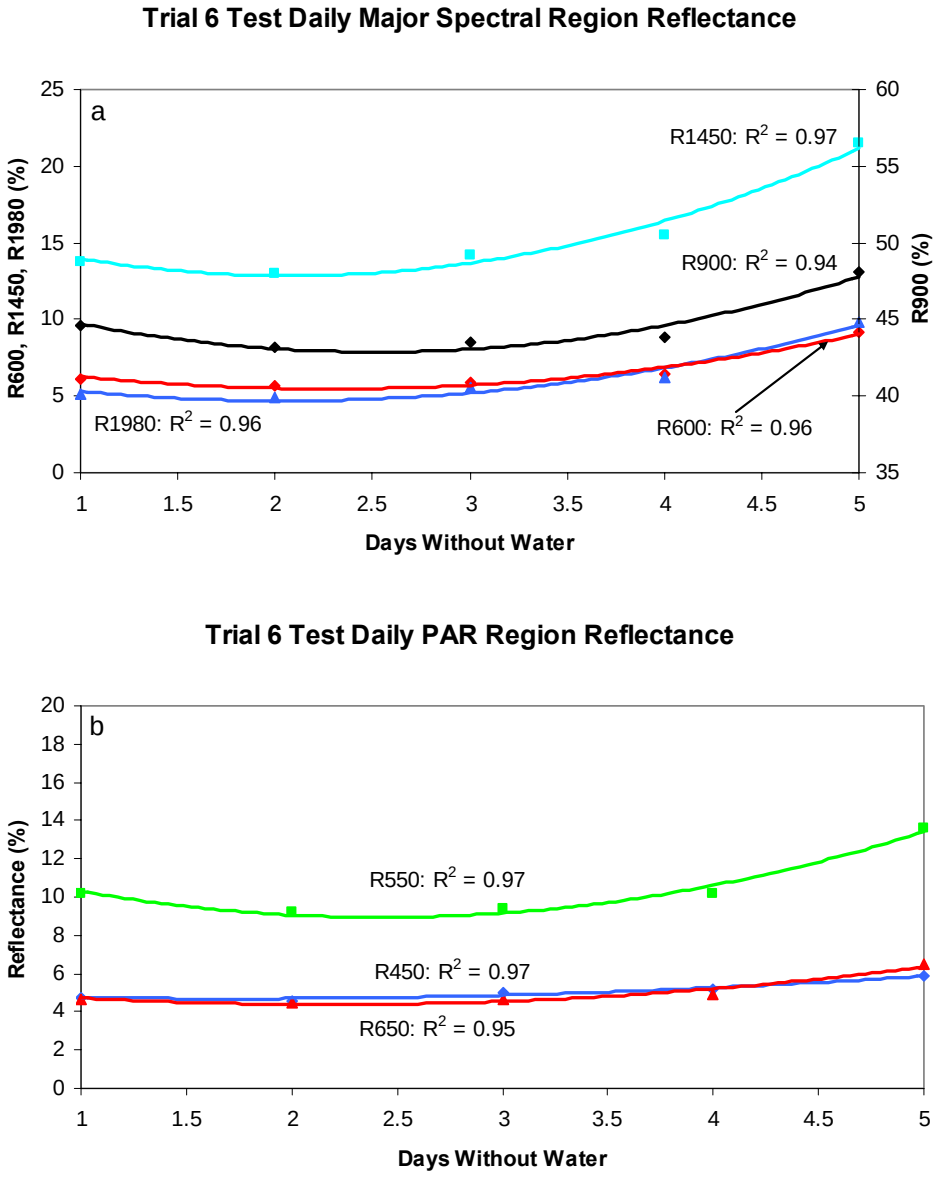

Figure 4-7. Trial 6 test leaf daily reflectance at wavelengths representing spectral regions. Panel (a) shows the major spectral regions. Panel (b) shows the PAR region. Lines are quadratic best-fit.

a

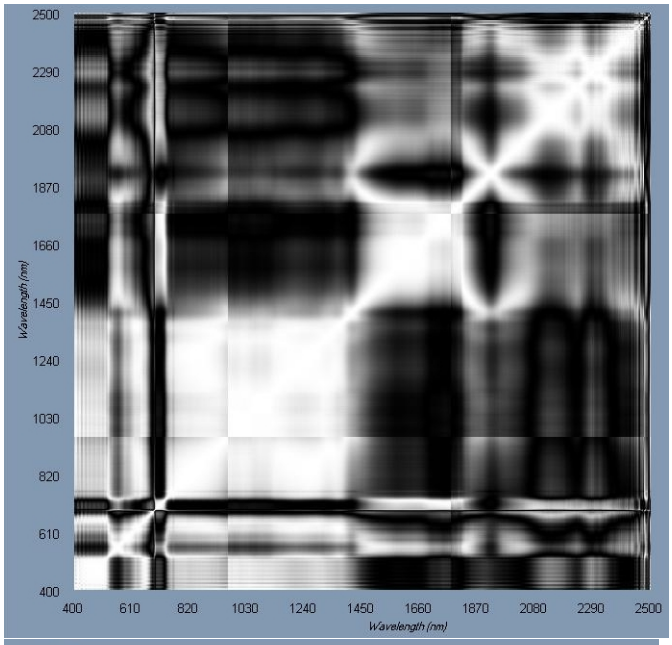

b

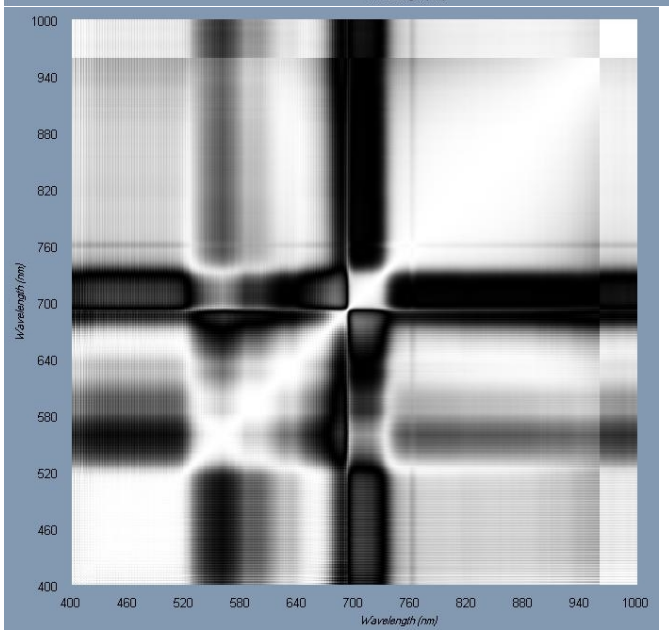

Figure 4-8. Trial 6 control leaf R^2 matrix charts. These charts show the strength of the relationships among the reflectances at each wavelength measured. Panel (a) shows the full spectrum. Panel (b) shows just the PAR spectral region up to 1000 nm.

As was done in Chapter 3, reflectance at seven wavelengths will be compared to reflectance at all other wavelengths to better see the relationships. Figure 4-9(a) shows the R^2 relationships among the reflectance at wavelengths representing each major spectral region and major water absorption wavelengths with all other wavelengths.

Figure 4-9(b) shows the same for three wavelengths representing the PAR. The observations noted in the previous paragraph are corroborated by these charts.

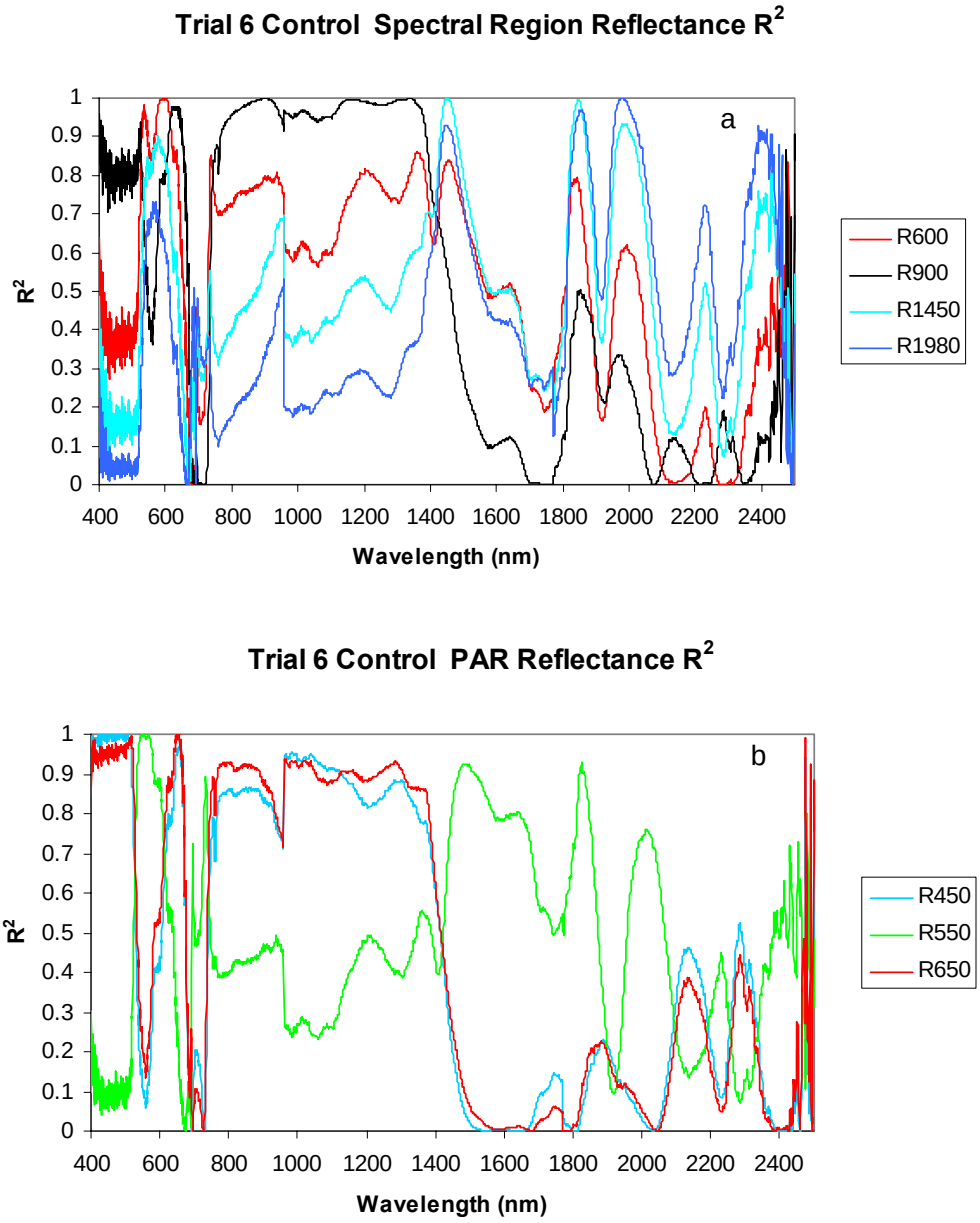

Figure 4-9. Trial 6 control leaf strength of the relationships of changes in reflectance at specific characteristic wavelengths against all other measured wavelengths. Lines depict R^2 for major spectral regions for the control, panel (a), and the PAR region, panel (b).

The test plant R^2 charts were very different (Figures 4-10 and 4-11). Reflectance at virtually all pairs of wavelengths correlate strongly (R^2>0.9). The areas showing lower

a

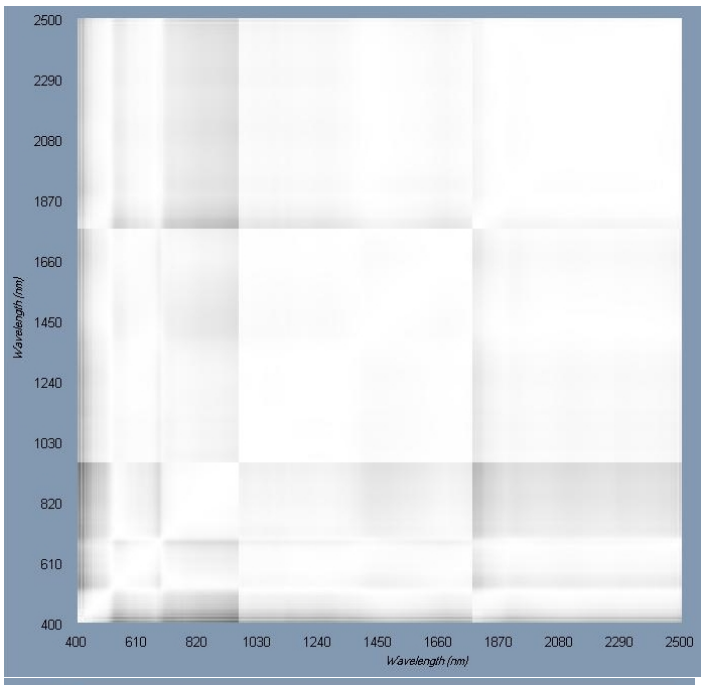

b

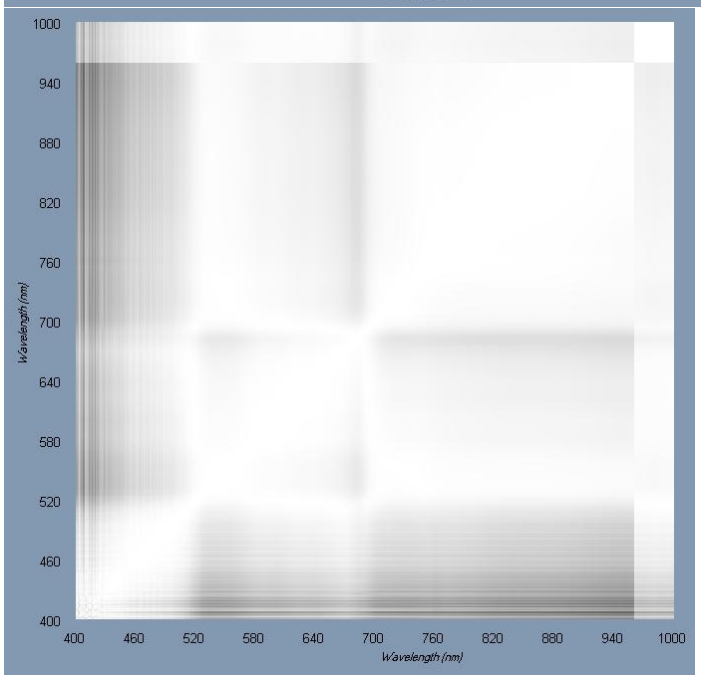

Figure 4-10. Trial 6 test leaf R^2 charts. These charts show the strength of the relationships among the reflectances at each wavelength measured. Panel (a) shows the full spectrum. Panel (b) shows just the PAR spectral region up to 1000 nm.

R^2 are 400 nm to 450 nm versus 530 nm to 630 nm ($R^2 \sim 0.8$), 400 nm to 500 nm versus 700 nm to 950 nm ($R^2 \sim 0.8$), and 530 nm to 580 nm versus 1770 nm to 1820 nm

(R^2 ~0.8). This implies that reflectance at all wavelengths tends to vary similarly as the leaf water status is degrading.

Based on the consistent and high levels of correlation, it can be concluded that little information is available by comparing reflectance at different wavelengths.

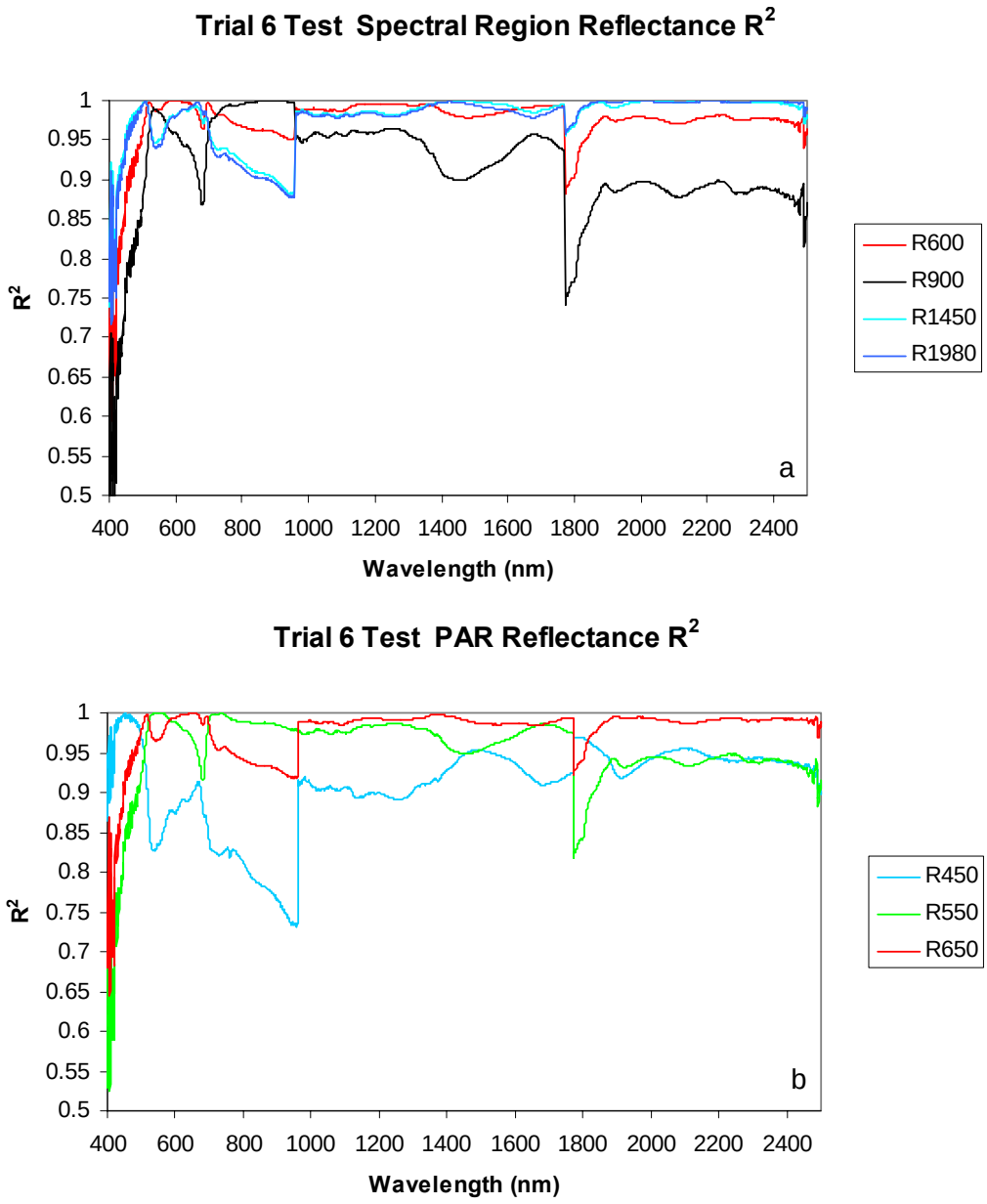

Figure 4-11. Trial 6 test leaf strength of the relationships of changes in reflectance at specific characteristic wavelengths against all other measured wavelengths. Lines depict R^2 for major spectral regions, panel (a), and the PAR region, panel (b).

4.3 Trial 7 (Soy – Sequenced Treatment)

Trial 7 employed a different experimental design from that used in Trials 4, 5, and 6. The design concept was tested in a small experiment after Trial 6 as described in Chapter 2.

Four "lines" of plants, each consisting of six plants, were kept well watered until the beginning of the experiment. On the first day, all plants were watered except one in each line. Those four plants were not watered for the remainder of the experiment. On the second day, a second plant in each line became unwatered. On the third, a third plant in each line became unwatered, and so on. The intent was that at the end of the experiment period, six plants in each of four lines spanned the range from unwatered to watered every day for the six days. When the experiment was conducted, the trial was stopped on the fifth day because the unwatered plants had reached very low levels of RWC (<50%).

Daily ASD reflectance measurements were made on the leaves at the ninth trifoliate on each plant. The ninth trifoliate was used (as opposed to the fourth trifoliate in Trial 6) due to a white fly infestation that made lower leaves unusable. On the last day, day five, Shimadzu transmittance measurements were made on those same leaves followed by destructive RWC and water potential measurements on the plants from two of the lines.

A mesh screen was placed around all of the plants in this trial in an attempt to slow the drying of the plants. This mesh reduced the illumination reaching the plants by about 50%.

4.3.1 Physical Measurements

4.3.1.1 Environment

External solar irradiance along with greenhouse temperature and relative humidity were continuously recorded during Trial 7. Figure 4-12 plots the measurements obtained. Temperature at the time of the hyperspectral reflectance measurements averaged 26.8 ºC with a standard deviation of 3.5 ºC. Humidity was slightly more variable, averaging

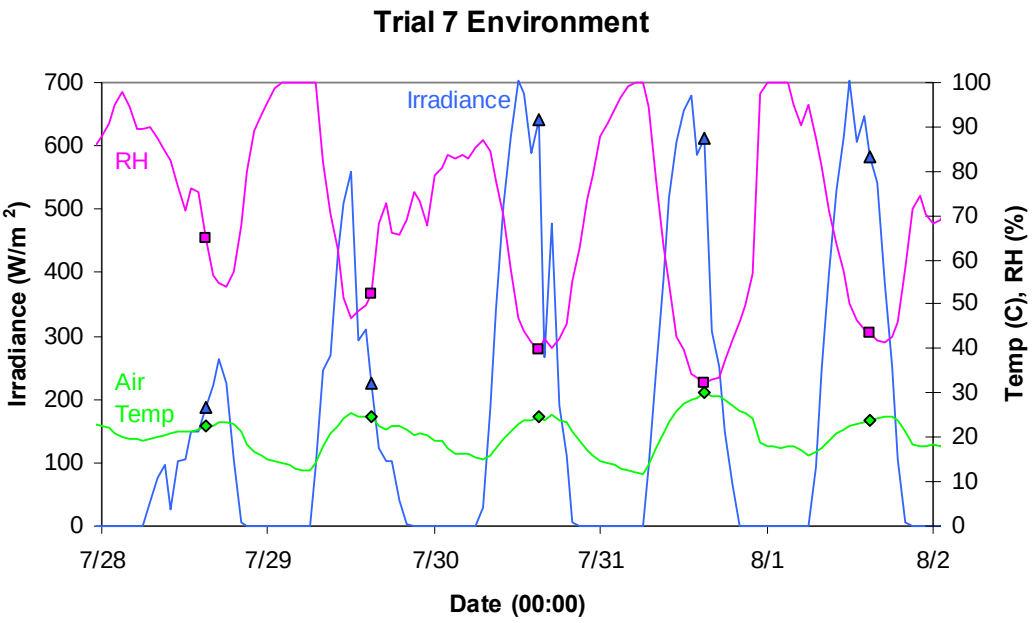

Figure 4-12. Trial 7 environmental conditions. The blue, pink, and green lines show downwelling solar irradiance, greenhouse relative humidity, and greenhouse air temperature, respectively. The temperature, humidity, and irradiance at hyperspectral measurement times are shown as diamonds, squares, and triangles respectively. Note that a mesh screen reduced the illumination reaching the plants by about 50%.

48.2% with a standard deviation of 12.7%. Irradiance showed substantial change during the experiment. The measured irradiance increased from 188.5 W/m^2 on day one to a peak of 640.7 W/m^2 on day three. The average irradiance was 460.8 W/m^2 with a standard deviation of 216.9 W/m^2.

As mentioned above, an attempt was made to slow the rate of drying of the plants by shading the plant lines with a mesh screen. This reduced the level of illumination that reached the plants by approximately 50% from the measured values.

4.3.1.2 Relative Water Content

This experiment involved four lines of plants. At the end of the experiment, each line had plants that had been unwatered for one, two, three, four, and five days. Plants from two of the lines were destructively sampled, following reflectance measurements, to determine relative water content. Hence, there were two measurements made for each level of water deficit. The measurements were made by punching twelve samples (four samples from each of the three leaflets at the ninth trifoliate) from each plant. The maximum, minimum, and average RWC determinations for the pair of plants on each day are plotted in Figure 4-13. Plants showed a fairly consistent decrease in RWC from about 85% on the first day through 42% on day five.

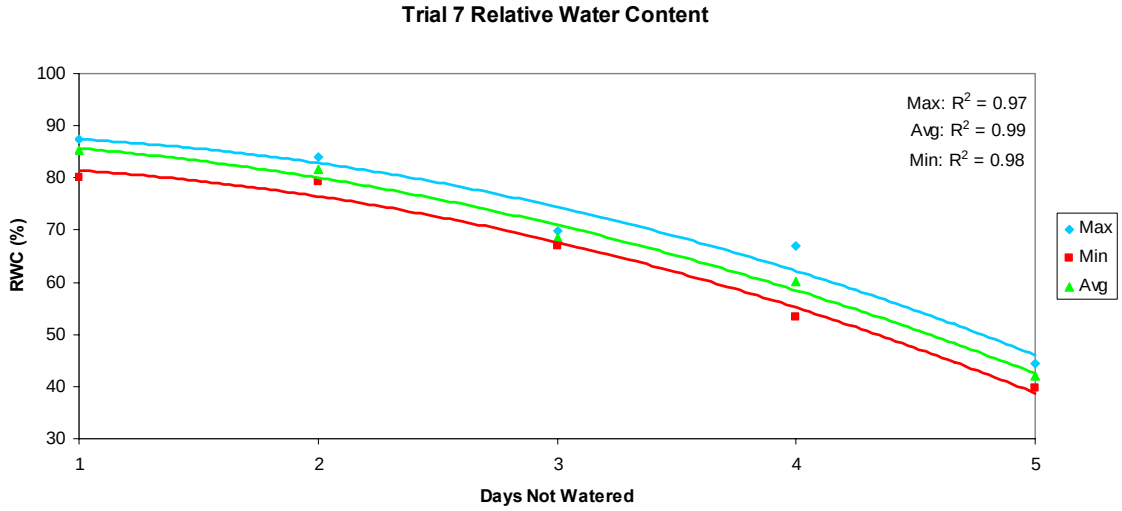

Figure 4-13. Trial 7 measured leaf RWC. "Max", "Min", and "Avg" represent the maximum, minimum, and average values for the leaves sampled from two plants at each water stress level. Lines are best-fit quadratic regression lines for the high, low, and average values.

4.3.1.3 Water Potential

Osmotic potential was measured from the same leaves used for RWC determination. The results are plotted in Figure 4-14. The measured value on day one was about -1.35 MPa. This decreased slightly to -1.40 MPa on day two. The value dropped steadily to -2.94 MPa on the last day. Looking back to Trial 6, the highest osmotic potential was -1.10 MPa. This indicates a higher initial level of water stress during Trial 7.

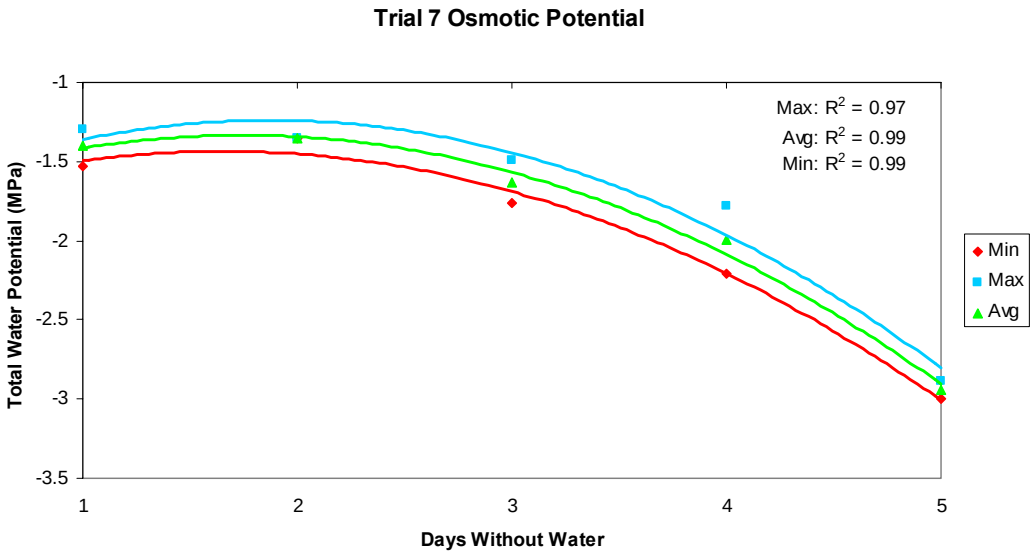

Figure 4-14. Trial 7 Osmotic Water Potential. Each point represents the maximum ("Max"), minimum ("Min"), or average ("Avg") value for the leaves of two sampled plants. Lines are quadratic best-fit lines.

4.3.2 Radiometric Measurements

4.3.2.1 Hyperspectral Reflectance

Hyperspectral reflectance was measured every day on the leaves of the ninth trifoliate on each plant. The resulting data set can be examined in several different ways. Looking only at the last day, the plants in each line should present the reflectance spectra of leaves ranging from fully watered through five days without water. Examining just the

"always watered" plants and the "unwatered since day one" plants in each line, results in a rough equivalent to the control and test leaf grouping in earlier experiments. It is also possible to increase the number of leaves observed for each day of stress by grouping the reflectance spectra from plants in each line having the same number of days without water (for example the first day's spectra for plants not watered the first day plus the second day's spectra for the plants not watered starting the second day, and so on). These three groupings will be shown in turn. In the following discussion, "stress level" is defined as the stress induced by the number of days the plants were not watered.

Figures 4-15 and 4-16 show the spectra taken on the last day. Each plotted line is an average of the leaves from plants unwatered the same number of days. Because there were four lines of plants, each spectrum represents the average reflectance from three leaflets on each of four plants (12 leaflets total). As can be seen by examining the plot, reflectance appeared to increase steadily, except for the leaves unwatered for three days. At 550 nm, for example, reflectance increased from day one to day two, then decreased on day three, and again increased on days four and five.

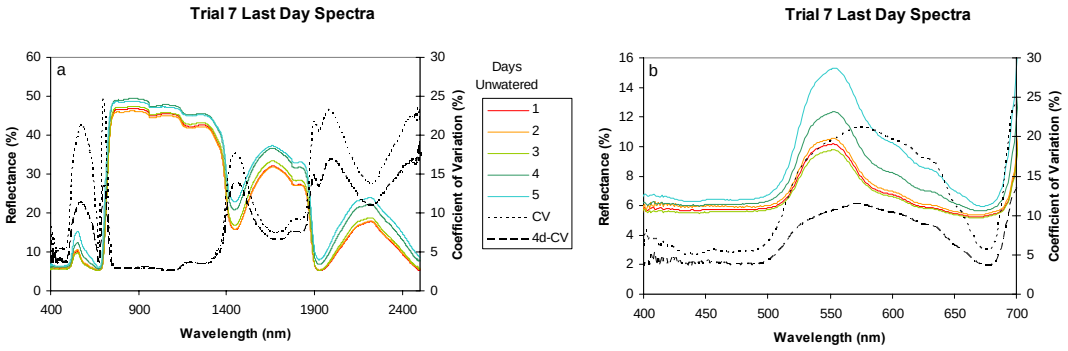

Figure 4-15. Trial 7 reflectance spectra taken on all plants on the last day of the experiment. "CV" designates the coefficient of variation for all five stress levels (days without water). "4d-CV" designates the CV for the first four levels of stress (unwatered for one, two, three, or four days). Panel (a) covers the entire spectrum. Panel (b) shows only the PAR portion of the spectrum.

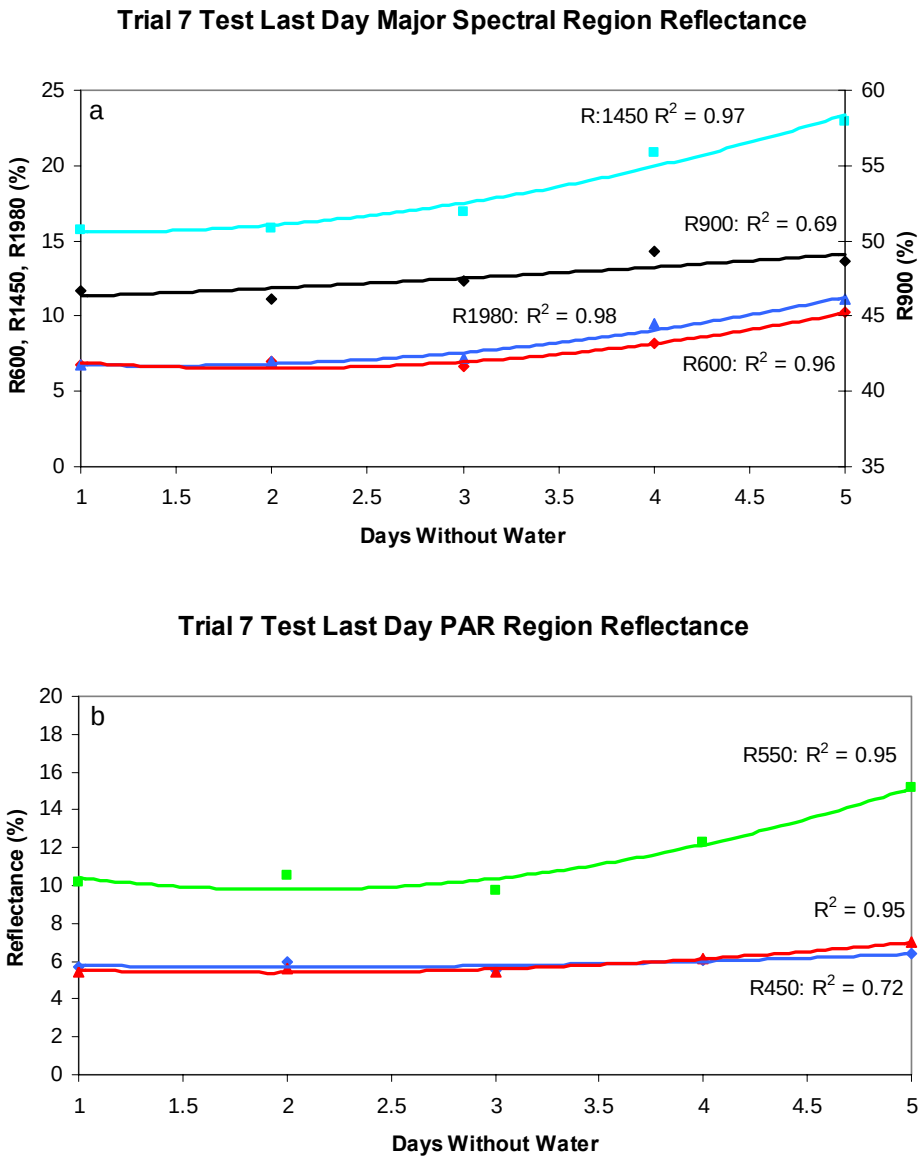

Figure 4-16. Trial 7 last day reflectance at wavelengths representing spectral regions. Panel (a) shows the major spectral regions. Panel (b) shows the PAR region. Lines are quadratic best-fit.

Two CV curves are plotted in Figure 4-15. One includes all five stress levels. The second was plotted to show variation over the first four days when RWC was greater than 60%. CV for all five stress levels shows variation near the water absorption features at about 1400 nm (17%), 1900 nm (23%), and above 2400 nm (23%). Peaks also occur in the PAR at the red edge, 700 nm (24%), and about 590 nm (21%). Similar peaks

occurred in the CV derived for leaves stressed four days or less. The magnitude of the peaks was considerably less (14% near 1400 nm, 17% near 1900 nm, 17% above 2400 nm, 13% near 700 nm, and 11% near 590 nm). The CV in the NIR was below 5% indicating no pronounced variation in that part of the spectrum. This confirms, as one can also observe in the reflectance lines, that reflectance changed only a small amount for plants stressed less than four days.

To make a comparison to the test and control groupings used in previous trials, one can view, respectively, those plants not watered after the first day, and those plants watered every day. Figure 4-17 contains plots for those plants. The CV for those plants watered every day, Figure 4-17 panels (a) and (b), was less than 10%, and was virtually uniform across the spectrum. Therefore there is no significant variation in these "control" plants. For the "test" plants, those not watered since the first day of the experiment, Figure 4-17, panels (c) and (d), sizeable variation, as evidenced by the CV covering the full five stress levels, appeared at the same points discussed in the last paragraph. The peak values were 16% above 1400 nm, 22% above 1900 nm, 21% above 2400 nm, 22% near 700 nm, and 19% near 590 nm. Looking only at the first four stress levels, only the peak above 1900 nm exceeded 10% (actual value, 11%). It can therefore be concluded that there was no significant variation in reflectance in the first four stress levels (representing leaves unwatered for one, two, three, and four days). Taking into account the very small variation, there does appear to be an increase in reflectance with increasing stress. But the change is almost imperceptible until stress levels correspond to four and five days without water.

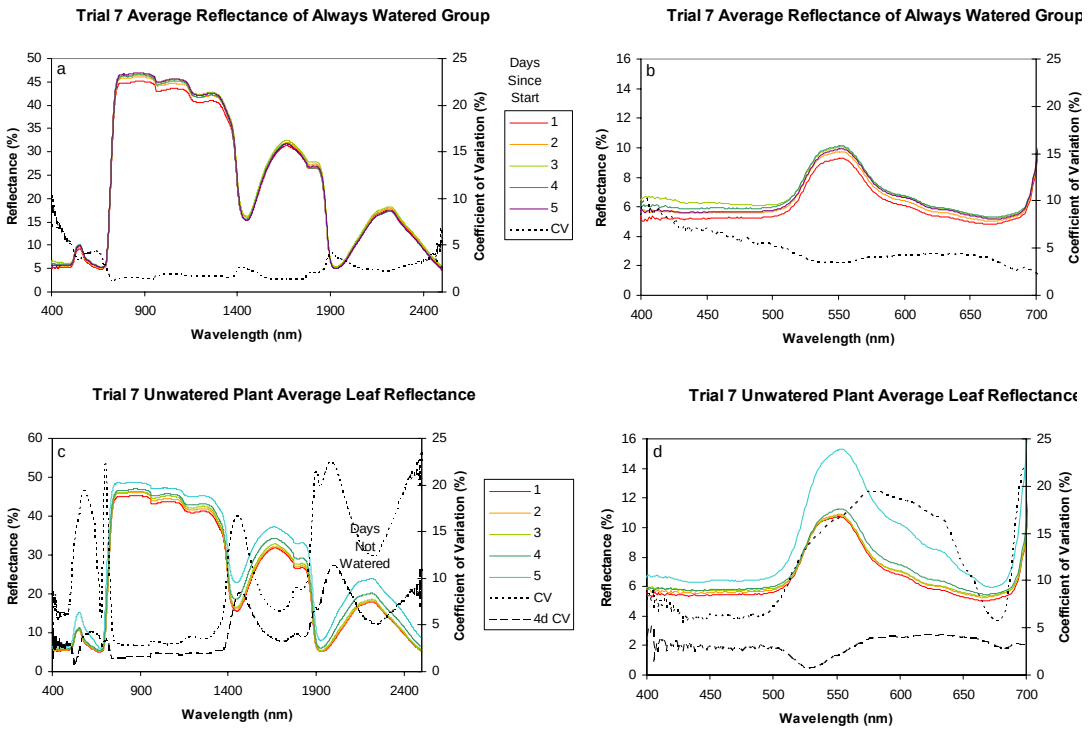

Figure 4-17. Trial 7 "control" and "test" leaf analogs to earlier Trials. Panels (a) and (b) depict reflectance from leaves watered every day. Panels (c) and (d) depict reflectance from leaves not watered since the first day of the experiment. The full spectrum is shown in panels (a) and (c). Only the PAR spectrum is shown in panels (b) and (d).

To increase the number of sample leaves, reflectance spectra were averaged over all leaves having the same number of days without water, e.g., the same stress level. For instance, in each line, the third plant was unwatered starting the third day. So on the third day, they had been unwatered for one day. These data were averaged with the first day for those leaves unwatered since day one, the second day of those plants unwatered since day two, the fourth day of plants not watered the fourth day, and so on. Obviously, the number of samples increased for each stress level since only eight plants were not watered after the fifth day (plants five and six in each line were watered up until the last day). The results, shown in Figure 4-18, indicated increasing reflectance for increasing stress levels, except for the reflectance for plants not watered for three days. CV over the whole range of stress levels were virtually identical to those described for the unwatered

plants in the previous paragraph. CV covering only the first four levels peaked over 10% only in the MIR. The peaks were 13% above 1900 nm and 14% above 2400 nm. As before, there was no significant variation in the NIR. One can again conclude that over the first four levels of stress variation in reflectance was very slight over most of the measured spectrum.

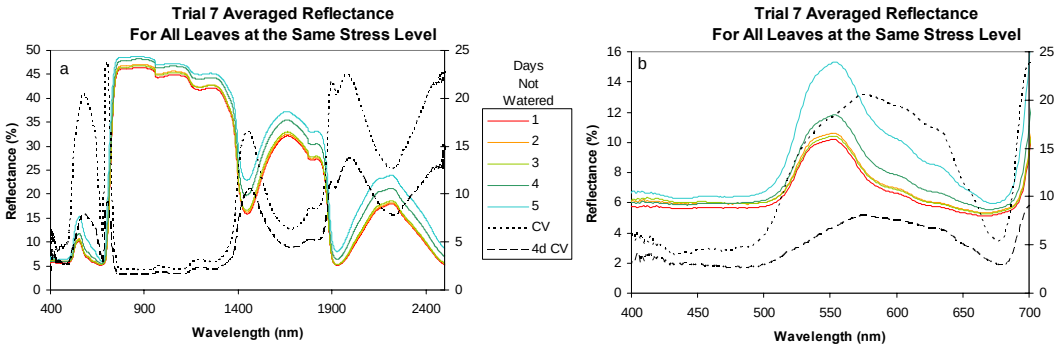

Figure 4-18. Trial 7 reflectance spectra averaged for all leaves at the same stress level. "CV" designates the coefficient of variation for all five stress levels (days without water). "4d-CV" designates the CV for the first four levels of stress (unwatered for one, two, three, or four days). Panel (a) covers the entire spectrum. Panel (b) shows only the PAR portion of the spectrum.

4.3.2.1.2 Information Content

Because the variability in the reflectance spectra was so slight, information content will be explored by using the averaged spectra in Figure 4-18. As before, R^2 was determined for reflectance across the spectrum compared to that at the seven characteristic wavelengths previously used. As can be seen in Figure 4-19, at wavelengths longer than about 500 nm, R^2 was greater than 0.8. Reflectance at each of the seven wavelengths correlated well with reflectance at all other wavelengths except blue (400 nm to500 nm). The different response of blue may result from the low variation in blue (CV at or below 5%) or the presence of interfering pigments such as flavonoids. The close relationship between MIR and red reflectance is apparent, just as in other trials. Based on the consistent and high levels of correlation, it can be concluded

that little information is available by comparing reflectance at different wavelengths (ignoring the blue region).

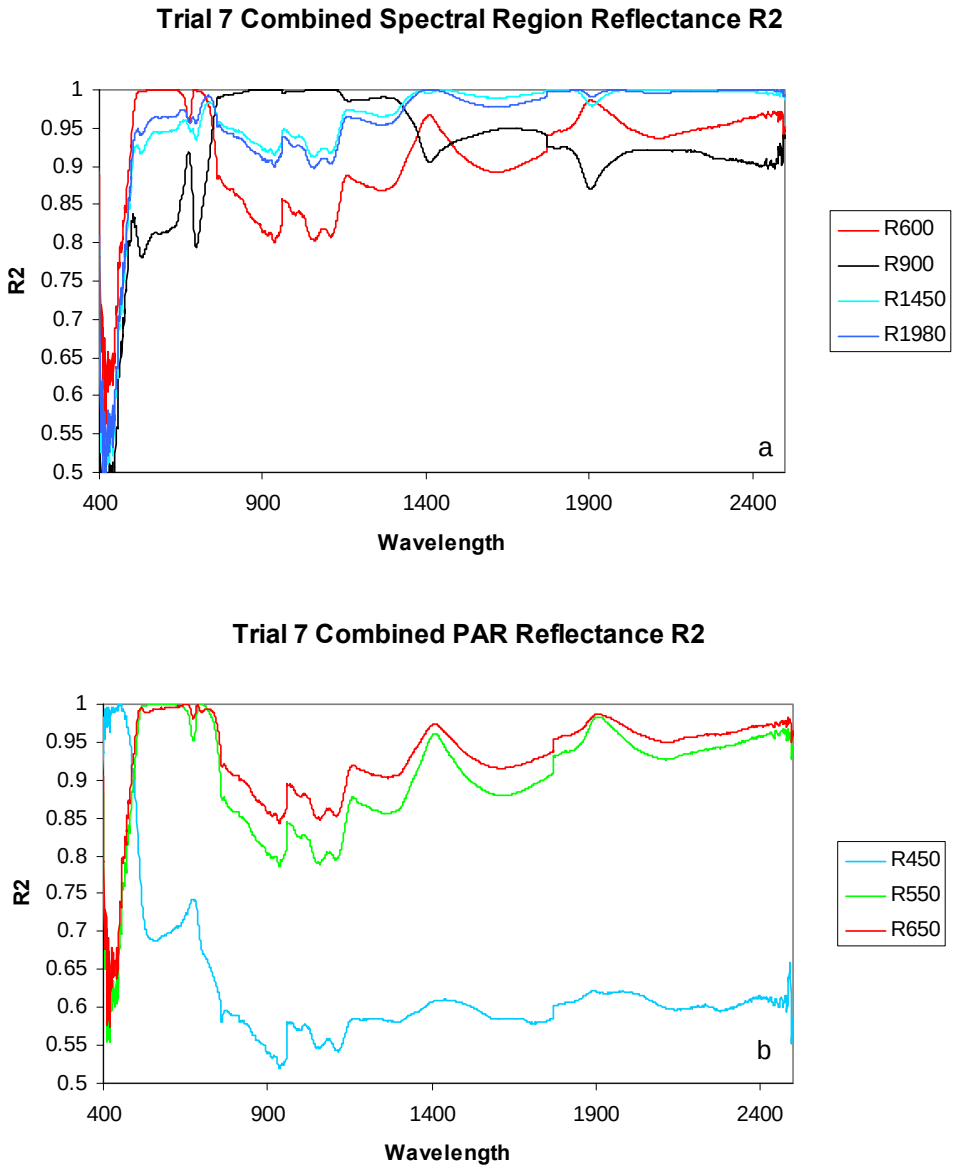

Figure 4-19. Trial 7 last day leaves strength of the relationships of changes in reflectance at specific characteristic wavelengths against all other measured wavelengths. Lines depict R^2 for major spectral regions, panel (a) and the PAR region, panel (b).

4.3.2.2 Transmittance

Trial 7 included measuring transmittance using a Shimadzu hyperspectral radiometer. Measurements were made on the last day of the experiment and used sample leaves from the ninth trifoliate on the plants from two lines. The transmittance, shown in Figures 4-20 and 4-21, is the average of three leaves on each plant (a total of six leaflets). Overall transmittance decreased, but not steadily, with increasing stress. At 550 nm, for example, transmittance decreased in leaves not watered from one to three days. The fourth day leaflets showed an increase in transmittance and then a decrease for the fifth day. Computed CV over the entire span of stress and over just the first four levels showed variation (>13%) at wavelengths shorter than about 710 nm. These results support the observations made for reflectance.

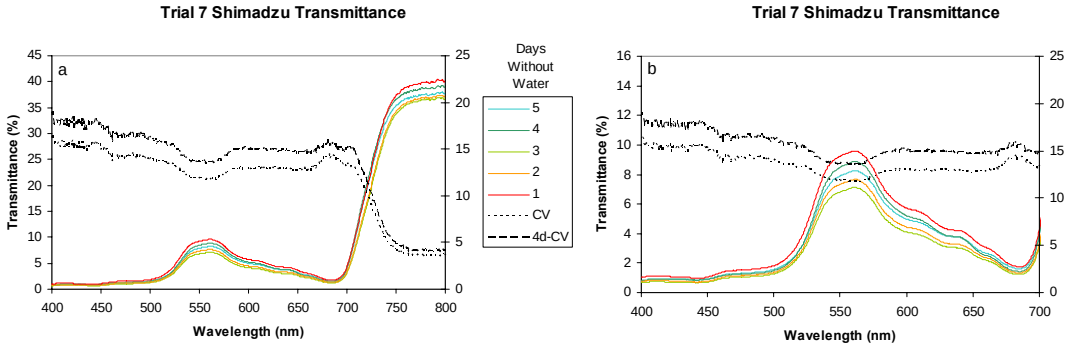

Figure 4-20. Trial 7 transmittance determined on the last day of the experiment. The transmittance value is the average transmittance measured for three leaflets from each of two plants (a total of six leaflets) at each stress level. "CV" designates the coefficient of variation for all five stress levels (days without water). "4d-CV" designates the CV for the first four levels of stress (unwatered for one, two, three, or four days). Panel (a) covers the entire spectrum. Panel (b) shows only the PAR portion of the spectrum.

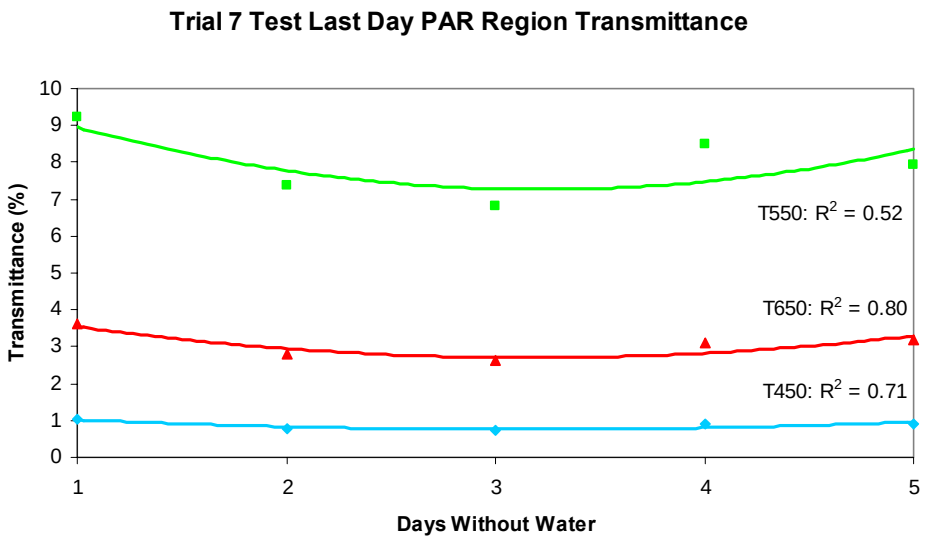

Figure 4-21. Trial 7 last day transmittance for selected PAR wavelengths. The lines are quadratic best-fit.

Figure 4-22 plots R^2 comparing the transmittance at the three characteristic PAR wavelengths (450 nm, 550 nm, and 650 nm) used earlier against the transmittance measured at all other measured wavelengths. R^2 values were, in general, above 0.9. There was, however, less correlation in the red edge for all three representative wavelengths, and in the blue and red regions for 550 nm. The 550 nm response once again corroborates the observation that the regions influenced by strong pigment absorption respond slightly differently to water stress than the green region which is influenced by both pigment absorption and structural scattering. The suggestion is that the PAR region response to water stress is manifested as a change in absorption rather than as a change in scattering.

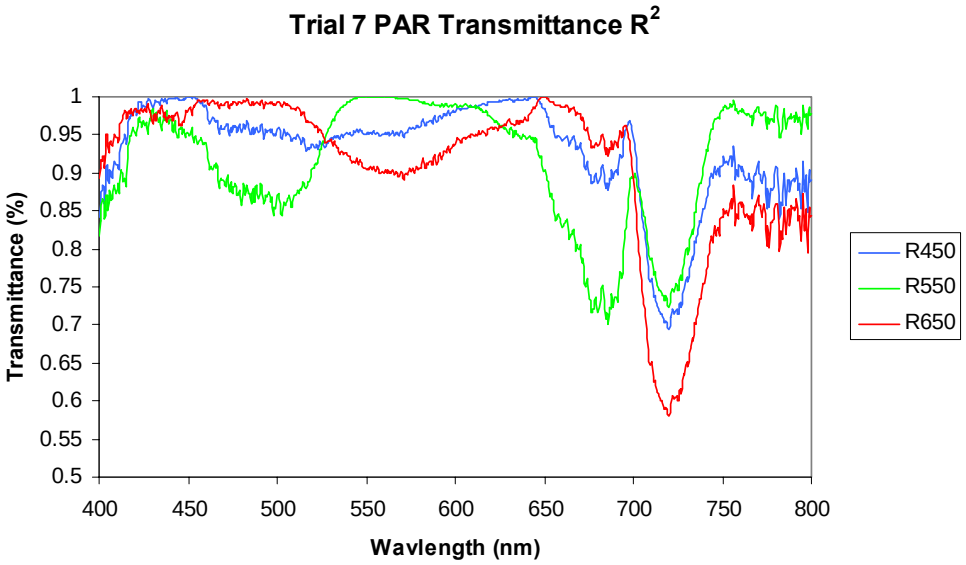

Figure 4-22. Trial 7 transmittance coefficients of determination (R^2) for the change in transmittance at specific wavelengths against all other measured wavelengths over all five levels of water stress.

4.4 Chapter Conclusions

The principal findings from the research summarized in this chapter are as follows:

1. Over two independent experiments, it was demonstrated that soy leaf reflectance in PAR and MIR, like maize leaf reflectance, increases over time for plants deprived of water. The reflectance response was not as strong as that seen in maize, especially for the early stages of stress. As with maize, there was slightly smaller response in green versus red and blue wavelengths, reinforcing the suggestion that the effects observed are more likely due to changes in light absorption than changes in scattering.
2. The two different experimental approaches employed for soy appeared to work. However, the test and control "sampled" design used in Trial 6 offers a clean history of leaf water status versus hyperspectral reflectance. Although daily

radiometric measurements were made during Trial 7, without concomitant RWC determination, it was difficult to understand what was driving the daily changes in reflectance. If RWC and/or water potential had been measured each day, it would be much easier to analyze and understand the differences between the two soy experiments. Given the destructive nature of these physical measurements, that would have required substantially more plants and a return to a sampled approach.

Chapter 5: Relationship of PAR Reflectance to Water Status

5.0 Chapter Contents

5.1 Chapter Introduction

The objectives of this chapter are to use the observations presented in Chapters 3 and 4 to derive an understanding of how changes in plant water status relate to changes in reflectance and to demonstrate that the changes in PAR reflectance can be used to estimate plant water status.

Observations reported in Chapters 3 and 4 indicated the existence of a consistent relationship in maize and corn between water status (RWC and water potential) and reflectance in PAR and MIR. While water molecules absorb strongly in MIR, there is little or no absorption by water molecules in PAR. The observed effects, increasing reflectance and decreasing transmittance concomitant with increasing water deficit must, therefore, result from some different process which changes the optical properties of leaves. That process seems to be related only indirectly to the amount of water in the plant.

Note that analysis of the relationships obtained thus far does not distinguish between reflectance and RWC versus reflectance and water potential. Because water

potential and RWC are closely related, RWC will be used as the indicator of water status in this chapter.

5.2 Relating PAR and MIR Reflectance

The strength of the coupling between PAR and MIR reflectance may easily be demonstrated by comparing MIR reflectance at 2100 nm with PAR reflectance in the blue at 450 nm and in the red at 670 nm. Figure 5-1 presents this comparison for maize and soy test leaves.

In all five trials, there was a strong correlation between PAR and MIR reflectance. Coefficients of determination (R^2) were near or above 0.9 except for Trial 7, 450 nm, where it was 0.70. R^2 for reflectance at 670 nm for Trial 7 was 0.87. The reason for the discrepancy at 450 nm is not known. However, the cause may relate to the anomaly observed in the control leaves in Trial 6. The presence of other pigments, such as flavonoids, may have caused the lower R^2. For comparison, the reflectance at 500 nm, a region less affected by flavonoids, was added to the chart for Trial 7. Note that R^2 has increased to 0.83.

Figure 5-1 also provides evidence that no other processes, such as varying amounts of pigments (e.g., chlorophyll) affect the relationship between PAR and MIR reflectance. Chlorophyll absorbs strongly at 450 nm and 670 nm and not at all at 2100 nm. If a decrease in chlorophyll had caused a substantial decrease in PAR absorption, the relationship between the PAR and MIR wavelengths would not have been so close. Given the R^2 values obtained and the lack of evidence of any divergence in the plotted points (even in the anomalous Trial 7 case), one can conclude that any changes in

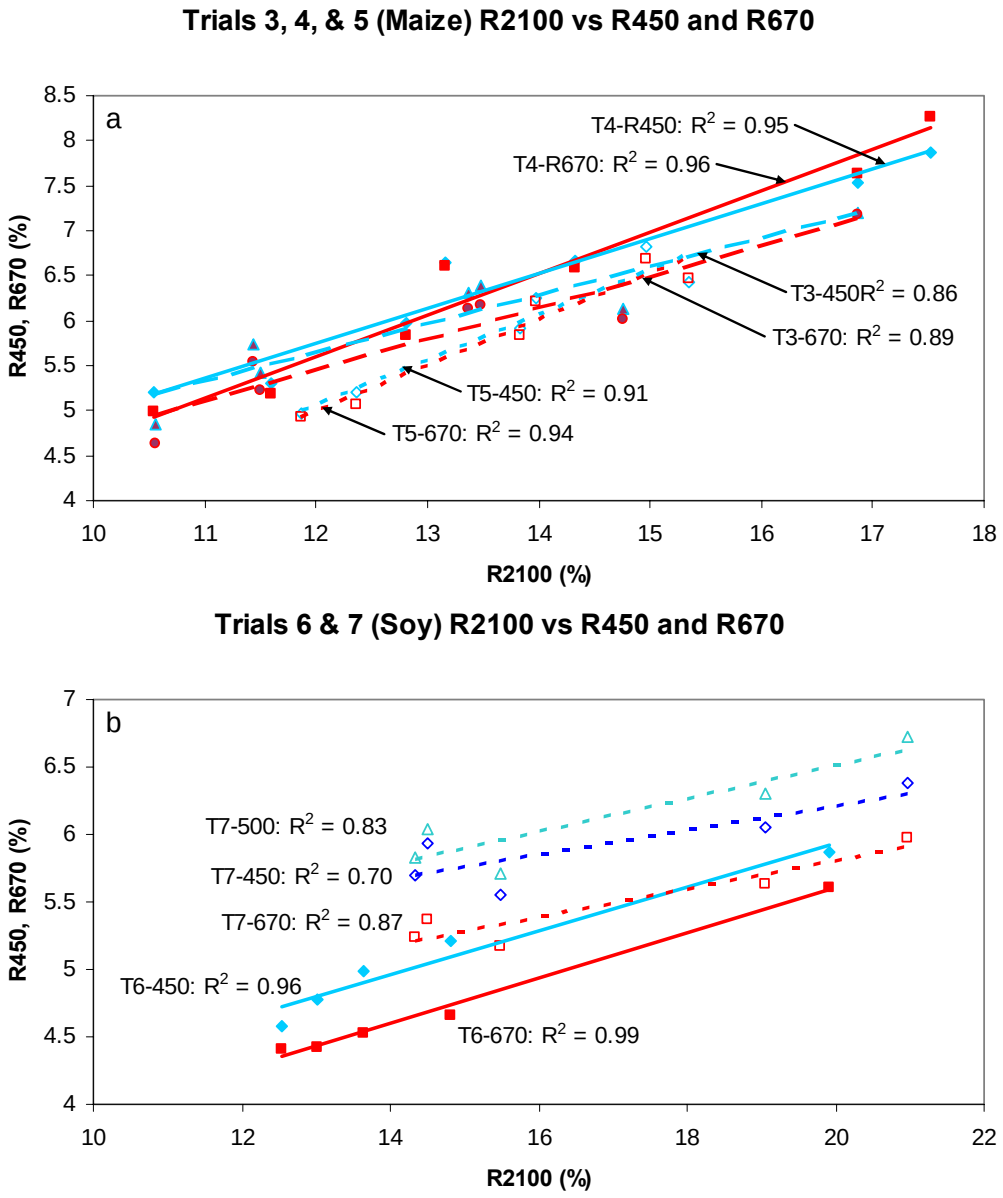

Figure 5-1. Reflectance at 2100 nm compared to reflectances at 450 nm and 670 nm for Trials 3, 4, and 5, panel (a) and Trials 6 and 7 panel (b). Reflectance at 500 nm has been added for Trial 7, as explained in the text. Data points for Trials 4 and 6 are denoted by solid symbols, and data points for Trials 5 and 7 are denoted by open symbols. Trial 3 data points are denoted by symbols filled with a contrasting color.

pigment amounts played little or no role in the in the behavior of PAR reflectance observed during the experiments conducted during this research.

The strong connection between reflectance at PAR and MIR wavelengths has been established.

5.3 Relating PAR Reflectance to RWC

5.3.1 Albedo

Five leaf albedo[4] spectral regions are designated as follows: PAR (400 nm to 700 nm), MIR (1300 nm to 2500 nm), blue (400 nm to 500 nm), green (500 nm to 600 nm), and red (600 nm to 700 nm). PAR albedo is strongly influenced by pigment absorption, especially chlorophylls and carotenoids; it is also affected by scattering in the green region. MIR albedo is influenced strongly by water content as well as leaf scattering. Red and blue region albedo is governed by pigment absorption. Green region albedo is influenced by both pigment absorption and structural scattering. (NIR albedo will not be discussed here because reflectance in this region was shown, in Chapters 3 and 4, to be only weakly related to water status.)

Albedo is examined for each trial. In maize, the middle leaf albedo is presented here. Top and bottom leaf albedo charts are included in Appendix A (Figures A-9 to A-11). While there are some differences among the leaf positions, the differences do not affect the conclusions and findings in this section.

In Figure 5-2, panels (a) and (c) contain graphs plotting the five albedos versus RWC for Trial 4. A quadratic best-fit line is shown for each set of points. Differentiating the equations of these lines yields straight lines depicting the slope of the relationship RWC versus albedo, as shown in panels (b) and (c) of Figure 5-2.

Albedo increases with decreasing RWC, Figure 5-2, panels (a) and (c). The increases in the albedo values, on the order of 3% to 6%, correspond to an RWC change of 95% to 44%. MIR and green ranges show the greatest amount of change.

---

[4] Albedo is the fraction of the incident light that is reflected. Here PAR albedo is defined as average reflectance over the PAR region of the spectrum (400 nm to 700 nm).

As shown in Figure 5-2 panels (b) and (d), slope or sensitivity of albedo to RWC increases with decreasing RWC in all albedos. MIR albedo shows the highest sensitivity to RWC among the major spectral regions. At maximum RWC, it shows a sensitivity magnitude of about 0.08 % change in albedo per % change in RWC. At the minimum RWC, the slope magnitude is much higher: 0.18. In PAR, green has the highest sensitivity overall, but with RWC below 85%. The green albedo sensitivity to RWC is very low, around 95% RWC, and reaches a magnitude of 0.24 at 44% RWC. (The ordinate axis has been inverted in these graphs to emphasize the magnitude of change.)

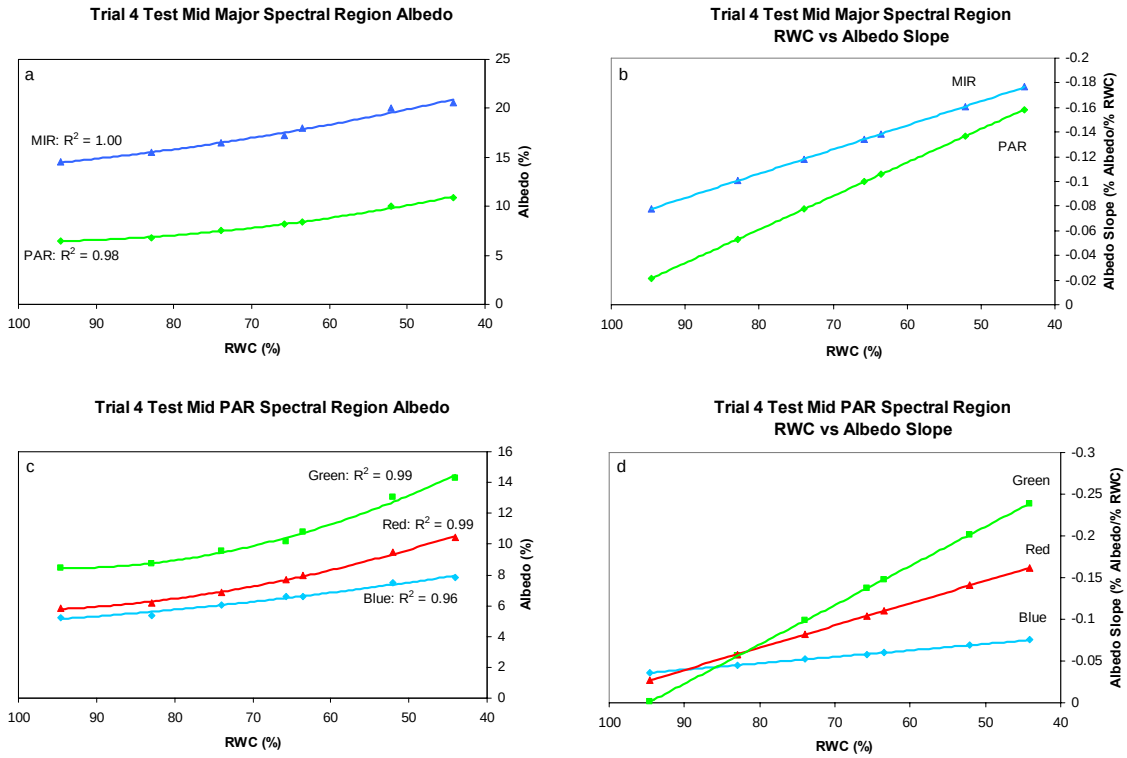

Figure 5-2. Trial 4 albedo versus RWC. Panels (a) and (c) show albedo versus RWC. Lines are quadratic best-fits to the points. Panels (b) and (d) show the first derivatives of the best-fit lines versus RWC. Albedos for major spectral regions are plotted in panels (a) and (b). Albedos for the PAR region are plotted in panels (c) and (d).

Albedo and slope graphs for Trial 5 are shown in Figure 5-3. The change in RWC was smaller in Trial 5 (99% to 57%) than in Trial 4 (95% to 44%). The changes in

albedo were also smaller but consistent with similar RWC ranges in Trial 4. In the major spectral regions identified above, the changes in albedo were 2% and 3% in PAR and MIR, respectively. Within PAR, albedos changed by 1% or 2%. As before, sensitivity increased with falling RWC. The MIR albedo was the most sensitive to RWC, showing a sensitivity magnitude starting at very small values around 95% RWC and increasing to 0.10 % albedo per % RWC. Green range albedo was the most sensitive in PAR. Sensitivity magnitude started at 0.05 and increased to 0.09.

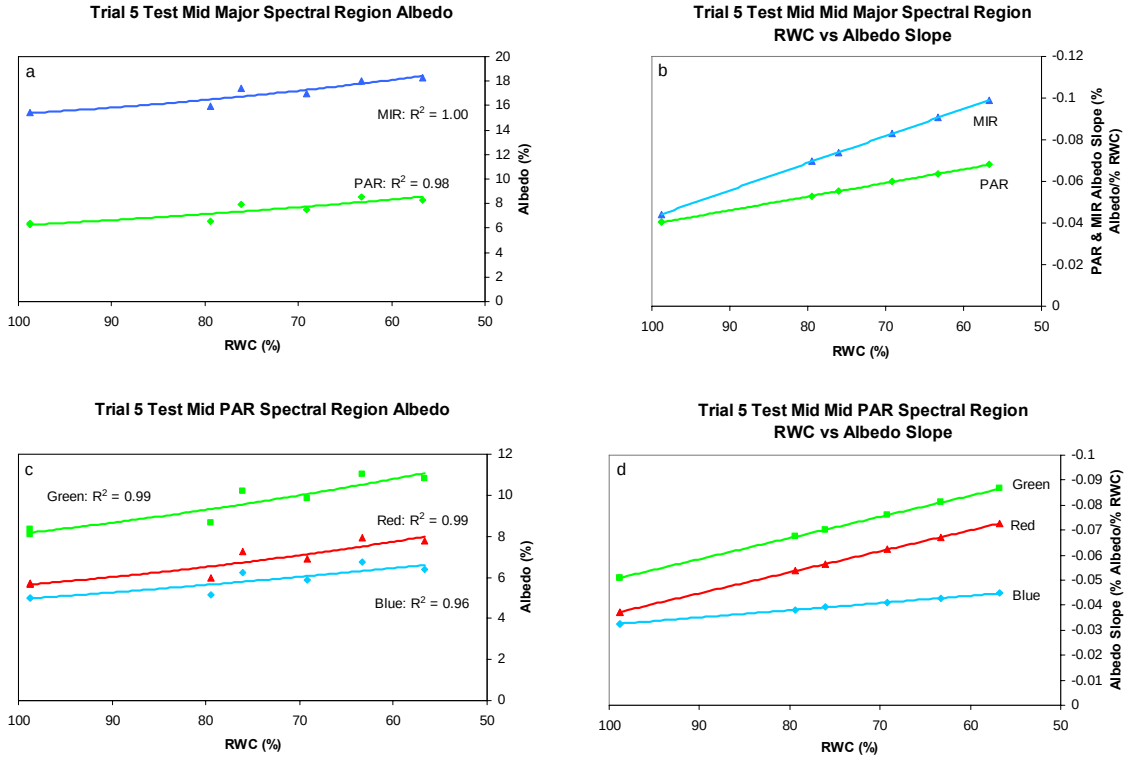

Figure 5-3. Trial 5 albedo versus RWC. Panels (a) and (c) compare albedo versus RWC. Lines are quadratic best-fits to the points. Panels (b) and (d) depict the first derivatives of the best-fit lines versus RWC. Albedos for major spectral regions are plotted in panels (a) and (b). PAR albedos are plotted in the panels (c) and (d).

Trial 6, the first of the soy experiments, also showed increasing PAR and MIR albedo with decreasing RWC (Figure 5-4). The overall change in albedo over the

experiment period was 2% in PAR and 6% in MIR, and 1%, 3%, and 2%, in blue, green, and red, respectively, as RWC changed from 93% to 66%.

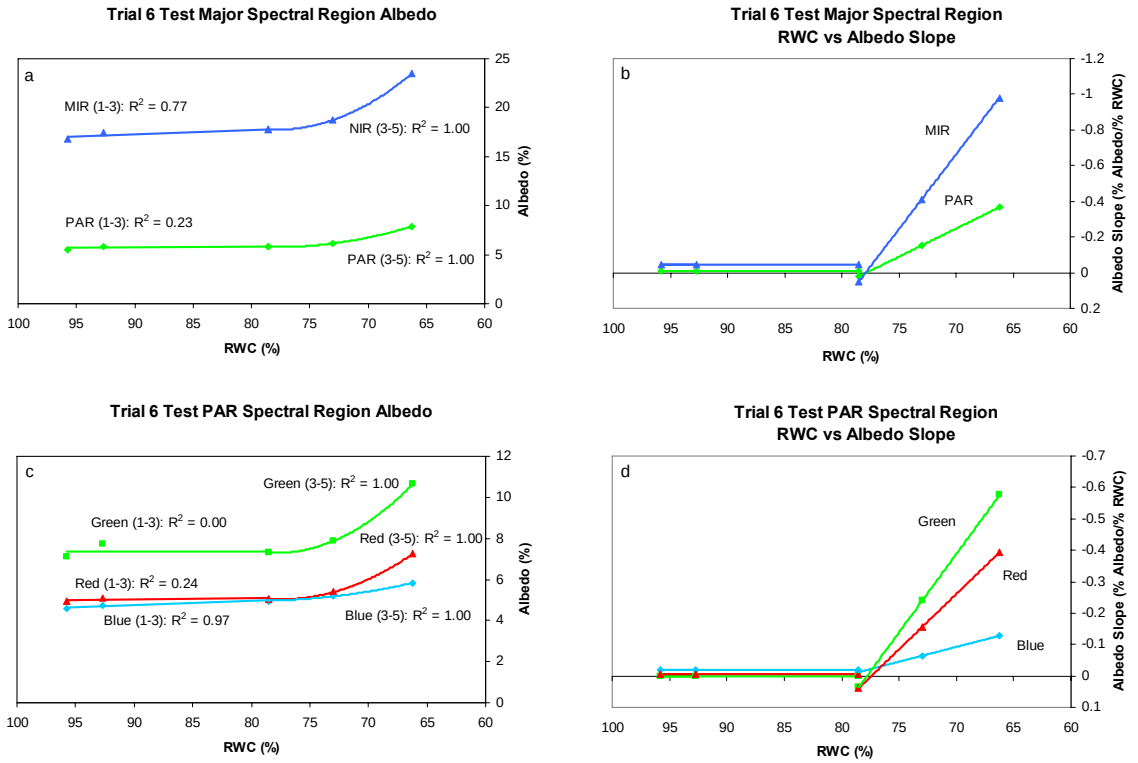

Figure 5-4. Trial 6 albedo versus RWC. Panels (a) and (c) show albedo versus RWC. Lines are linear best-fit to the first three points (RWC > 75%) and quadratic best-fits to the last three points (RWC<80%). Panels (b) and (d) show the first derivatives of the best-fit lines versus RWC. Albedos for major spectral regions are plotted in panels (a) and (b). Albedos for PAR albedos are plotted panels (c) and (d).

While albedo changes with RWC were similar in direction to those in earlier trials, sensitivity to RWC was much lower for soy than for maize, especially during the first three days of the trial. As can be observed in Figure 5-4, there was little or no change in PAR albedo when RWC decreased from 95% and 80%. To demonstrate this and to accommodate the limitations of polynomial best-fit regression, the plotted best-fit lines have been split into two; the first representing the points from days one to three and the second representing those from days three to five. A linear best-fit was applied to the first points and a quadratic fit to the last points. When RWC fell below 80%, sensitivity

in the most sensitive spectral region albedo, MIR, changed from 0.00 to about a magnitude of 1.00 % albedo per % RWC. The most sensitive albedo in the PAR was green albedo. Starting from 0.00, the sensitivity magnitude at the end of the experiment was about 0.60 % albedo per % RWC.

Trial 7 confirmed the findings of Trial 6 as shown in Figure 5-5. Although albedo increased with decreasing RWC, there was only a 0.2% change in PAR albedo until

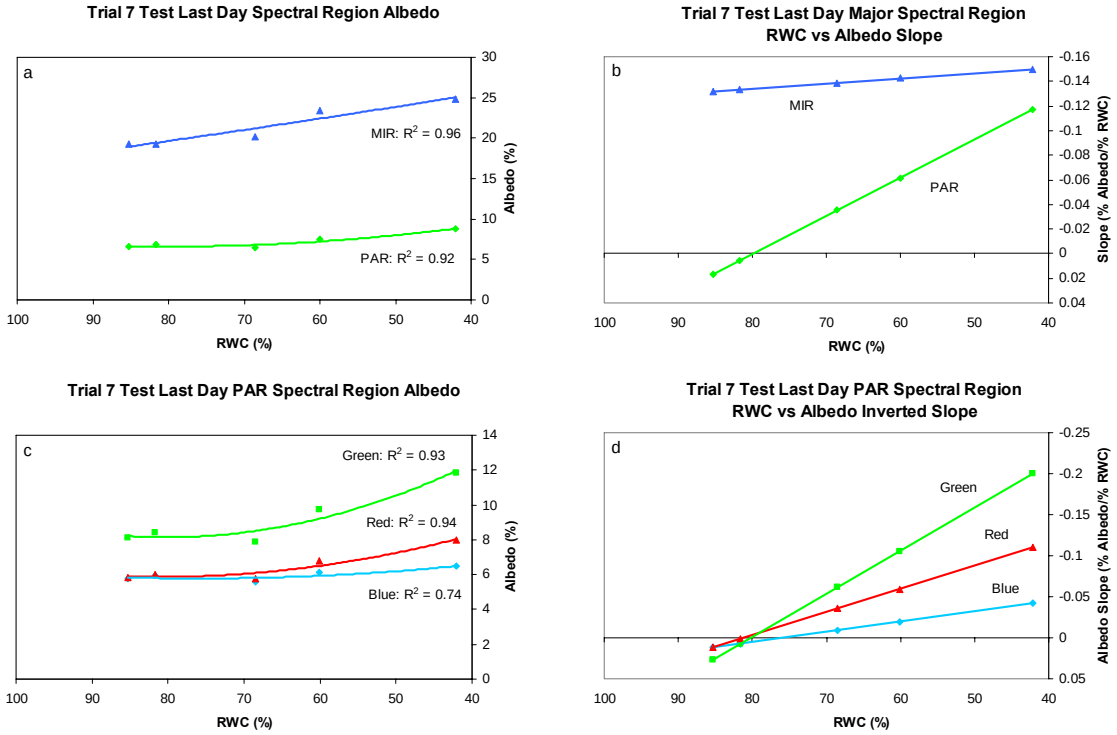

Figure 5-5. Trial 7 albedo versus RWC. Panels (a) and (c) show albedo versus RWC. Lines are quadratic best-fits to the points. Panels (b) and (d) show the first derivatives of the best-fit lines versus RWC. Albedos for major spectral regions are plotted in panels (a) and (b). Albedos for PAR albedos are plotted panels (c) and (d).

RWC dropped below 80%. RWC during this trial ranged from 85% to 42%. The change in albedo in PAR was 2% and in MIR was 6%. Within the PAR region, the change was 1% to 4%. The slope of the albedo vs. RWC relationship was increasing in magnitude as RWC decreased. MIR and green albedo again had the highest sensitivities. The slope for

the MIR albedo was nearly constant, changing in magnitude from 0.13 to 0.15. Green albedo sensitivity changed in magnitude from near 0.00 to 0.20.

In soy, PAR albedo does increase consistently with decreasing water status in all of the analyzed trials. However, the sensitivity of albedo to RWC appears much lower in soy than in maize (Figure 5-6). This figure combines both maize and both soy experiment PAR albedo measurements into one graph. The relationship between maize PAR albedo and RWC for Trials 4 and 5 had R^2 of 1.00 and 0.83, respectively.

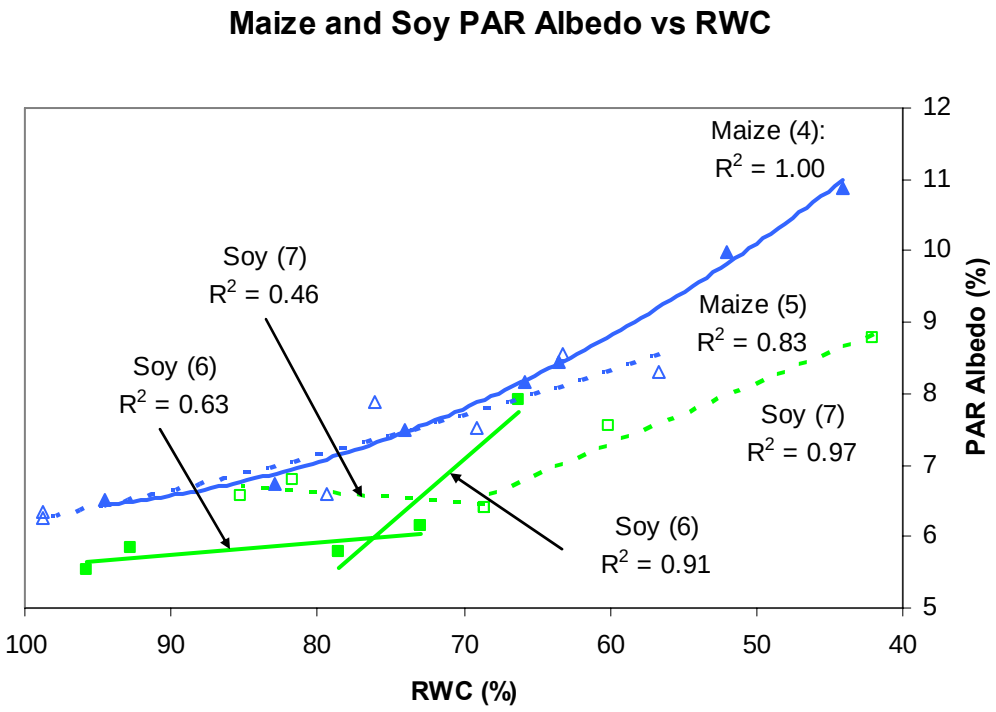

Figure 5-6. Maize and soy PAR albedo versus RW**C**. This graph displays all PAR albedo observations for maize in blue (Trials 4 and 5) and soy in green (Trials 6 and 7). Lines are quadratic and linear best-fit for maize and soy, respectively. Designations in parenthesis are the trial number.

To show the relative insensitivity for early stages of stress in soy, the lines for soy are shown in two parts. From 100% to 70% RWC, the lines for both trials are nearly horizontal. Below 70% RWC, both trials had R^2 values above 0.9. As was shown

earlier, soy albedo sensitivity to change in RWC is weak. The best-fit line does not correctly represent the relationship.

In Chapter 3, it was shown that the sampling technique used in Trials 4, 5, and 6, had an error limit on the order of 8% in maize. Assuming the number is the same for soy, there is a statistical error of that magnitude in using the sampled RWC measurements as proxies against which to compare hyperspectral measurements. That would explain a significant portion of the scatter in the data in Figure 5-6.

Earlier in this chapter, it was shown that MIR reflectance at 2100 nm was highly correlated with reflectance in the PAR. Further, as explained earlier, MIR reflectance is closely tied to water molecule absorption. Reciprocal reflectance ($1/\rho$), because of the nonlinear nature of inversion, provides a sensitive metric for spectral areas with very strong absorption features. Using the average hyperspectral measurements from each day to obtain both reciprocal reflectance at 2100 nm and albedo minimizes the sampling error. The results are shown in Figure 5-7.

In this figure, the R2 values for maize, Trials 4 and 5 are nearly identical at 0.97 and 0.98, respectively. The soy trial data sets are, again, broken into two parts. At the early stages of stress, RWC>70%, the lines are close to horizontal or even negative in slope. Below 70% RWC, the lines for both Trials 6 and 7 have nearly the same slope and show R2 values of 0.99 and 0.93, respectively. The insensitivity of PAR albedo at early stages of water stress is again confirmed. In comparison to Figure 5-6, R2 values are higher (ignoring the early-stage soy data) and the later-stage soy data have similar slopes. These features are probably manifestations of the RWC sampling error, especially when RWC falls below 60%.

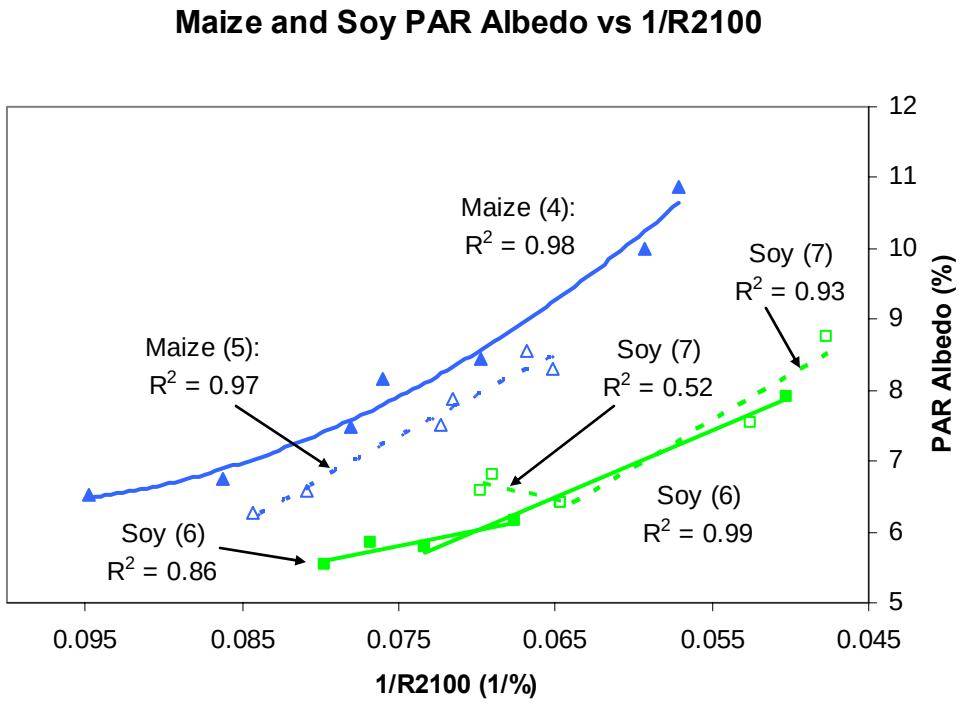

Figure 5-7. PAR albedo for maize and soy versus the reciprocal of reflectance at 2100 nm. This graph displays all PAR albedo observations for maize in blue (Trials 4 and 5) and soy in green (Trials 6 and 7). Lines are linear best-fit except for maize, Trial 6, where the line is quadratic best-fit. Numbers in parenthesis indicate the trial number.

It can definitively be said that PAR albedo increases with decreasing RWC in both species, which suggests that water status may be retrievable by observation of PAR reflectance. However, special consideration may be required to overcome the low sensitivity of PAR reflectance to RWC, especially at the early stages of water stress.

Albedo in the PAR region has been shown to be related to albedo in MIR and to RWC in both maize and soy. Therefore, it is appropriate to investigate whether PAR reflectance may be used to estimate RWC. That is the subject of the next section.

5.3.2 Example of a Model: Two Band Normalized Difference

Models based on reflectance provide indexes whose values relate to biophysical parameters. One example is the commonly used Normalized Differenced Vegetation Index (NDVI):

$$NDVI = \frac{\rho_{NIR} - \rho_{RED}}{\rho_{NIR} + \rho_{RED}}$$

where ρ_{NIR} indicates reflectance in the NIR spectral region and ρ_{RED} indicates reflectance in the red spectral region (Jensen, 2007). Other types of indices include two-band models such as a ratio of reflectances and the difference of two reciprocal reflectances, and three-band models such as those defined by Gitelson (Gitelson, et. al., 2003).

NDVI is a two-band model used as an indicator of the amount of vegetation in an observed area. It is a "normalized difference" index. NDVI works because vegetation reflects highly in NIR and less-so in red. Normalization by the sum of the two reflectances helps to make the index immune from error sources that cause both reflectances to change in common.

A normalized difference model is identified in the next section only to show the existence of a method to retrieve RWC from PAR reflectance. Selecting a so-called optimal model at this early stage of research is premature. Since there is no understanding of the physics, chemistry, or physiology underlying the observed changes in PAR reflectance, a model could be selected which works only within a restricted environmental regime or only for a small set of plants within a species. However, it is useful to explore an example.

5.3.2.1 Wavelength Selection

An "Index Analysis" software tool, developed by the author, was described in Chapter 2. That tool was used to identify the two wavelengths needed for a potential normalized difference model to retrieve RWC. In this section, the process used will be described. Only those data points representing 60% RWC and above, above the level of desiccation, will be included in the analysis.

Consider the image in Figure 5-8 which was generated by the Index Analysis tool for Trial 4 reflectance data. This figure is a matrix of determination coefficients (R^2) of the relationship between the index in the form

$$I_{i,j} = \frac{\rho_{\lambda_i} - \rho_{\lambda_j}}{\rho_{\lambda_i} + \rho_{\lambda_j}} \tag{5-1}$$

and relative water content, $R^2\{I_{i,j}\ vs\ RWC\}$, for all pairs of λ_i and λ_j in the region from 400 nm to 1000 nm.

Figure 5-8 shows show how normalized difference index values relate to RWC for every pair of wavelengths from 400 nm to 1000 nm. Bright regions indicate that R^2 is near one. Dark regions denote that R^2 is near zero. Ignoring, for the moment, the red line, observe that there is a fairly large bright region where both λ_1 and λ_2 range between 530 nm and 580 nm. An index using pairs of wavelengths within this region correlates very well with RWC.

To select an optimal pair of wavelengths, the tool generates a profile view which holds λ_1 constant and varies λ_2 through the whole range of measured wavelengths. For example, selecting λ_1 as 580 nm produces the profile depicted in Figure 5-9 (in this case limiting λ_2 to the PAR region) which corresponds to the red line in Figure 5-8.

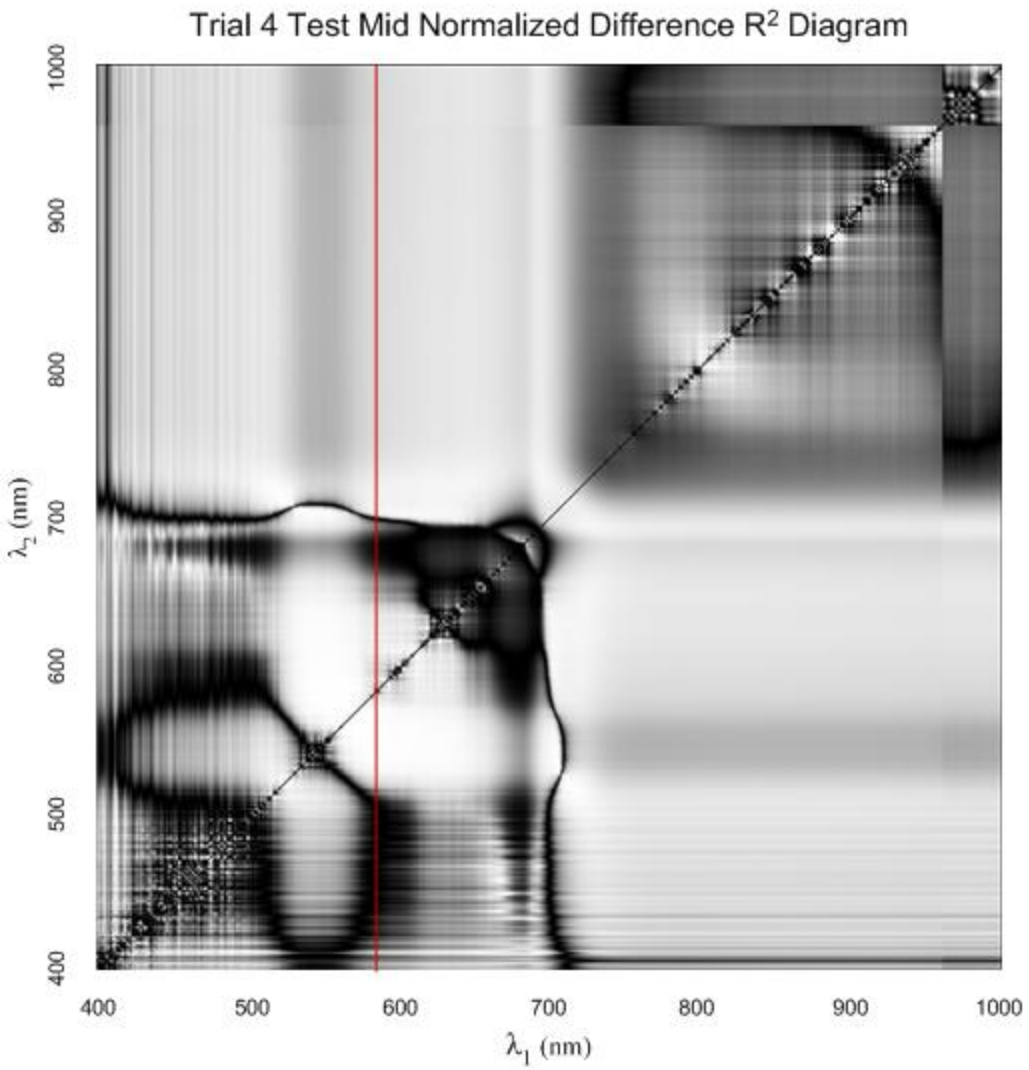

Figure 5-8. Trial 4 Test middle leaf R^2 chart comparing RWC (>60%) to the index generated by a normalized difference model. The red line indicates the location of the profile shown in Figure 5-9.

The second wavelength for the model, λ_2, can be selected from any value in the range from about 535 nm to 575 nm, where R^2 is near one. If, for instance, one were to pick 550 nm, then the index resulting from the following equation would have a high correlation with RWC:

$$Index = \frac{\rho_{580} - \rho_{550}}{\rho_{580} + \rho_{550}}$$

This particular model is "tuned" to the results of Trial 4.

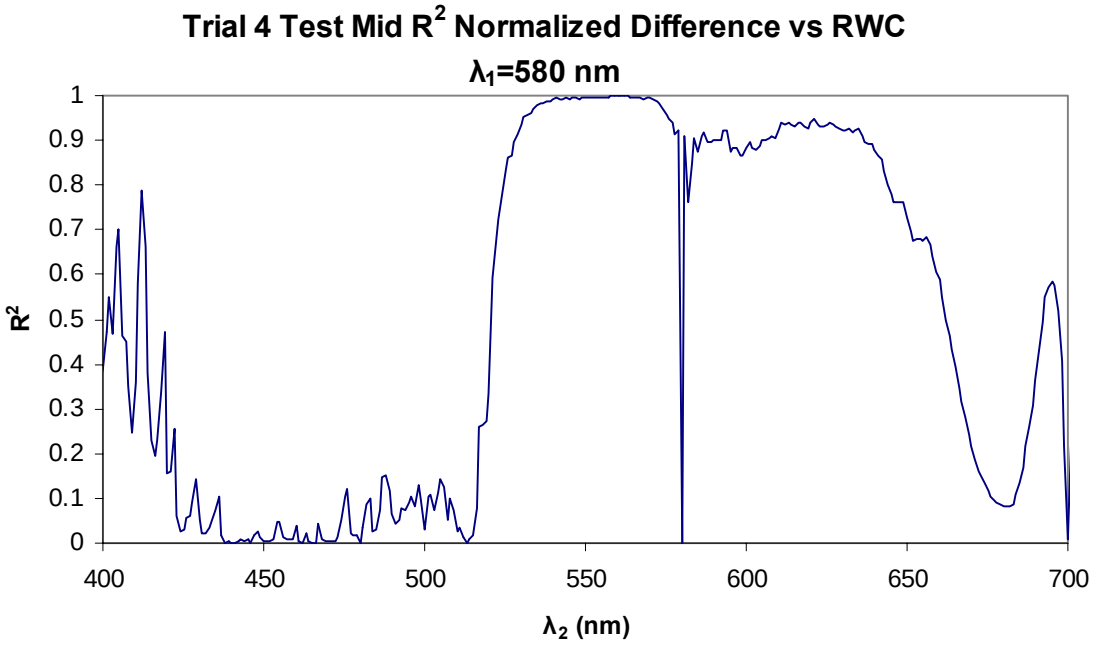

Figure 5-9. Coefficients of determination between RWC>60% and a Normalized Difference Model Index where λ1 is fixed at 580 nm and λ2 is varied from 400 nm to 700 nm. This profile is taken in the PAR region along the red line shown in Figure 5-8.

To find a general model that works for all data taken in Trials 4 through 7, R^2 diagrams and related profile charts were generated for each trial (Figure 5-10). Looking at the diagrams, λ_1=580 nm and λ_2 in the neighborhood of 550 nm were seen to have high R^2 for all four trials. The four profile charts are therefore based on λ_1=580 nm. Examination of the profile charts led to the selection of λ_2=540, since there was an R^2 peak for each trial at that wavelength. Hence, the example index is:

$$Example\ Index = \frac{\rho_{580} - \rho_{540}}{\rho_{580} + \rho_{540}} \tag{5-2}$$

The example model (Eq. 5-2) was tested by comparing RWC and index values in all four trials. Figure 5-11 contains two graphs with those results. Unlike other figures in this section, all data are included, not just those data points representing RWC>60%.

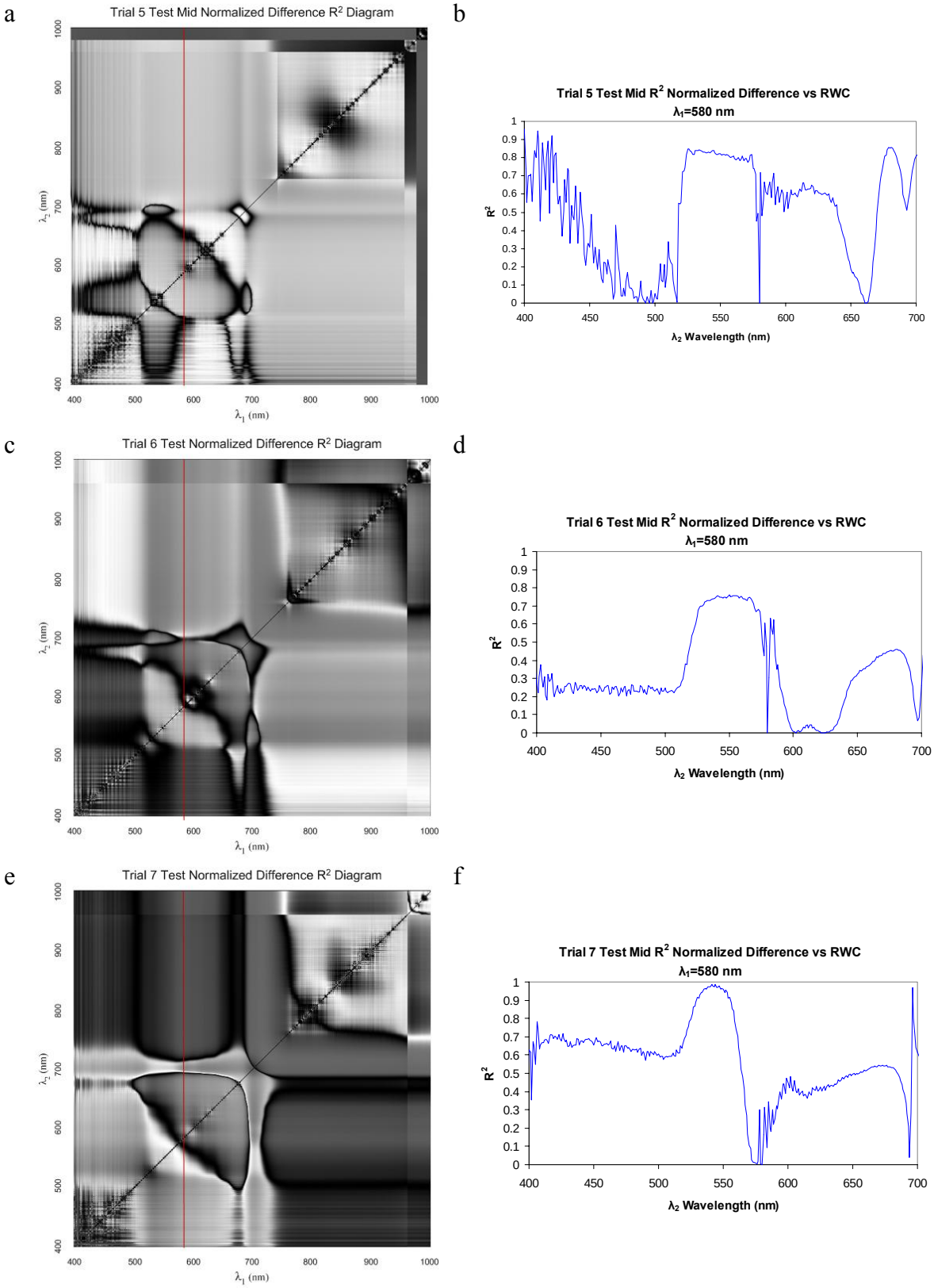

Figure 5-10. R^2 diagrams and related profile charts for Trials 5, 6, and 7. Data displayed are R^2 relating the example model to RWC>60%.

Panel (a) shows the results for Trials 4 and 5, maize, and panel (b) shows the results for Trials 6 and 7, soy. Linear best-fit lines are applied to all four datasets. The quality of the fits are high for Trials 4, 5, and 7 (R^2>0.88), and lower for Trial 6 (R^2=0.75).

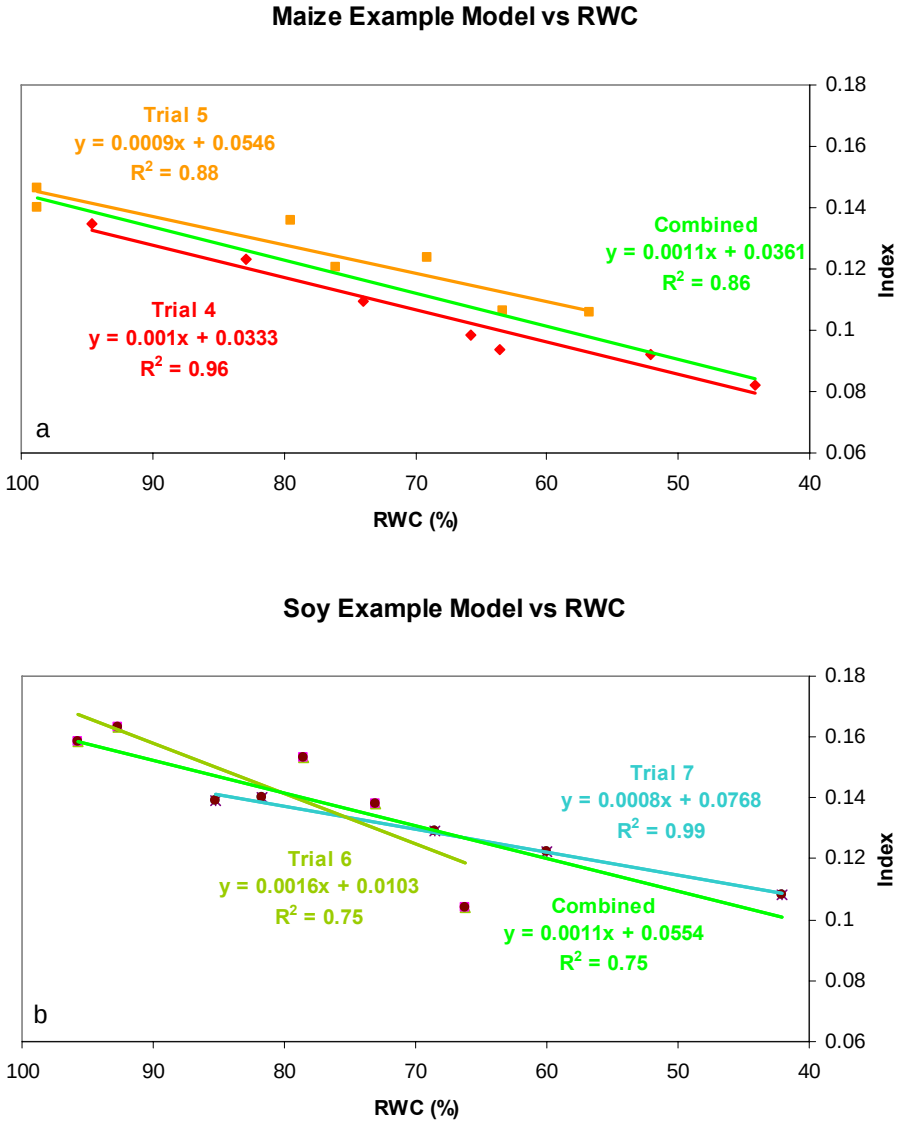

Figure 5-11. Comparison of example model to RWC. Panel (a) shows the results for Trials 4 and 5. Panel (b) shows the results for Trials 6 and 7. Lines are linear best-fit.

Trial 4, 5, and 7 best-fit lines had similar slopes. If all of the maize data points are combined into one dataset, the best-fit line has a slope of 0.0011 and intercepts or offsets of 0.0361. Likewise, if all of the soy data points are combined into one dataset,

the best-fit line also has a slope of 0.0011 and intercept of 0.0554. This is evidence that the example model sensitivity is similar for four independent experiments covering two different plant species despite varying environmental conditions. The slopes are quite small, however. The low sensitivity will need to be addressed in attempting use PAR reflectance to estimate RWC.

Figure 5-11 is optimistic and does a poor job of representing the early stages of water stress. For example, see Figure 5-12, which presents similar graphs, but where RWC is limited to the range above 60%. Notice that the slopes in the combined data sets are no longer identical and the similarity of slopes among the trials has disappeared.

As was done at the end of the previous section, one can use reciprocal reflectance at 2100 nm as a proxy for RWC. The resulting comparison charts appear in Figures 5-13 and 5-14. Note that R^2 values have improved overall. Qualitatively, the data points fit the line much better for the early stages of water stress.

The normalized difference model is effective, in the example here, for reasons different from the explanation presented earlier for NDVI. Within the region with high R^2 values, there is a close relationship between index values over a fairly large range of wavelengths. This suggests that within that range, the difference between the reflectances, the numerator in Eq. 5-1, remains almost invariant with changes in RWC. The sums of the reflectances, the denominator, increase with decreasing RWC. Thus, the ratio of an invariant numerator and increasing denominator results in a number which has a high correlation with RWC.

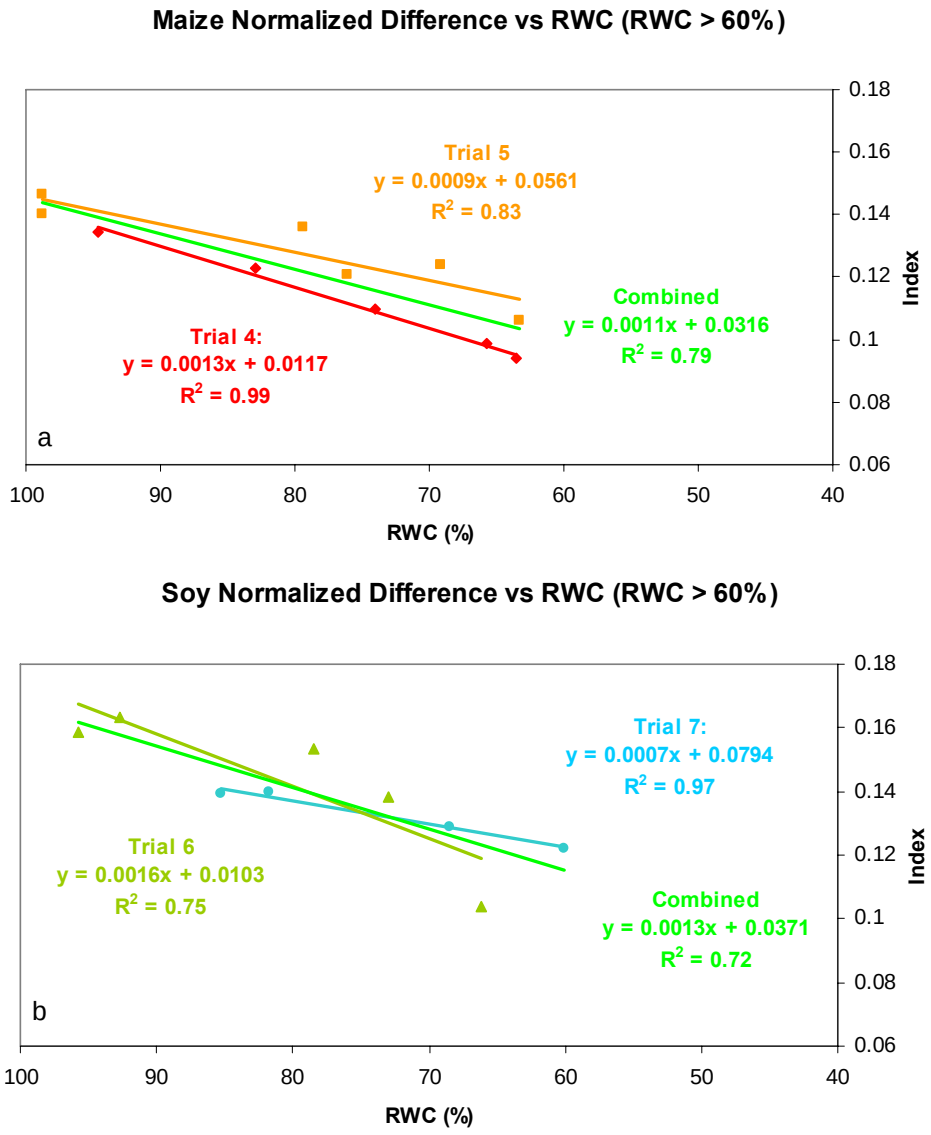

Figure 5-12. Comparison of example model to RWC for RWC > 60%. Panel (a) shows the results for Trials 4 and 5. Panel (b) shows the results for Trials 6 and 7. Lines are linear best-fit.

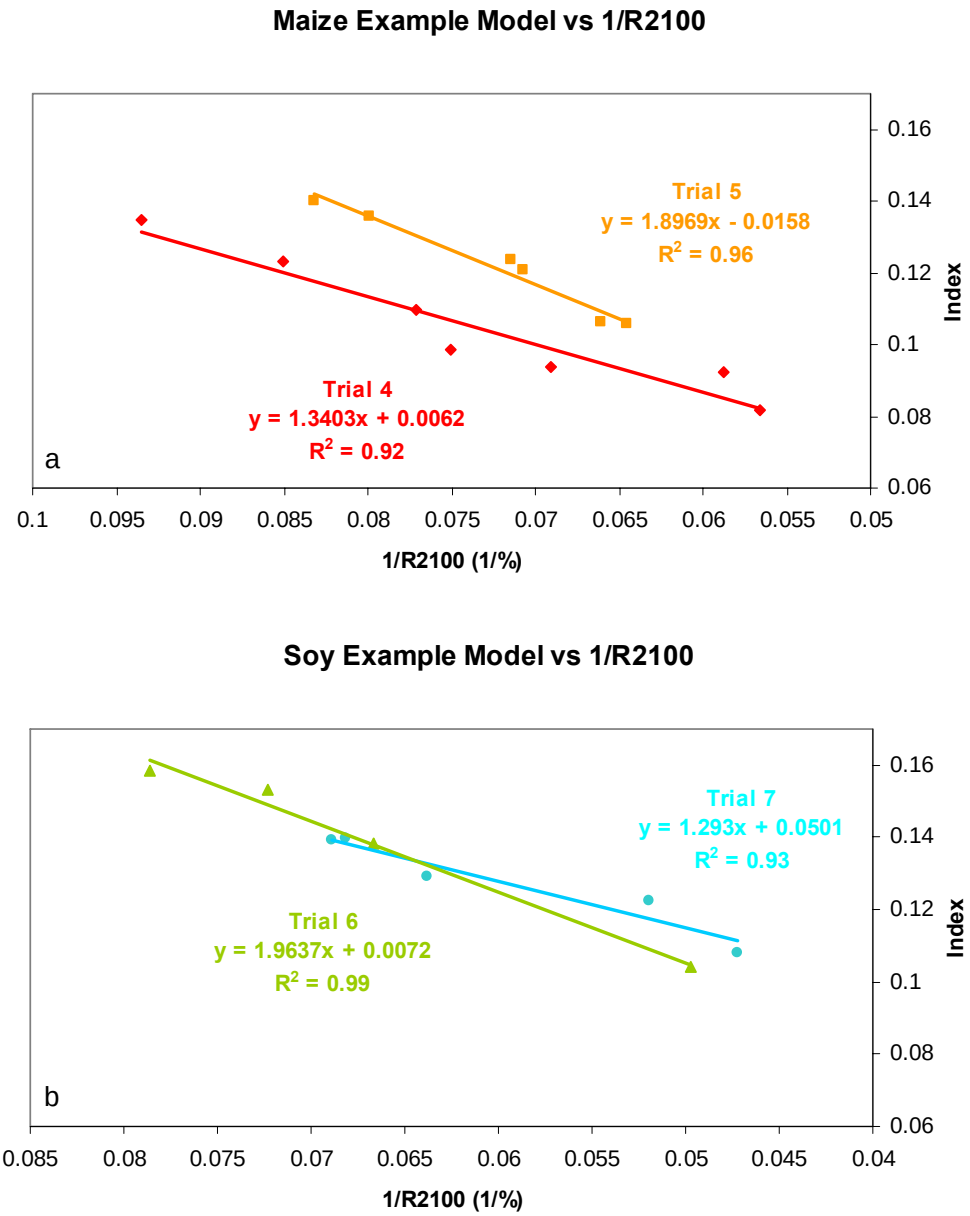

Figure 5-13. Comparison of example model to reciprocal reflectance at 2100 nm. Panel (a) shows the results for Trials 4 and 5. Panel (b) shows the results for Trials 6 and 7. Lines are linear best-fit.

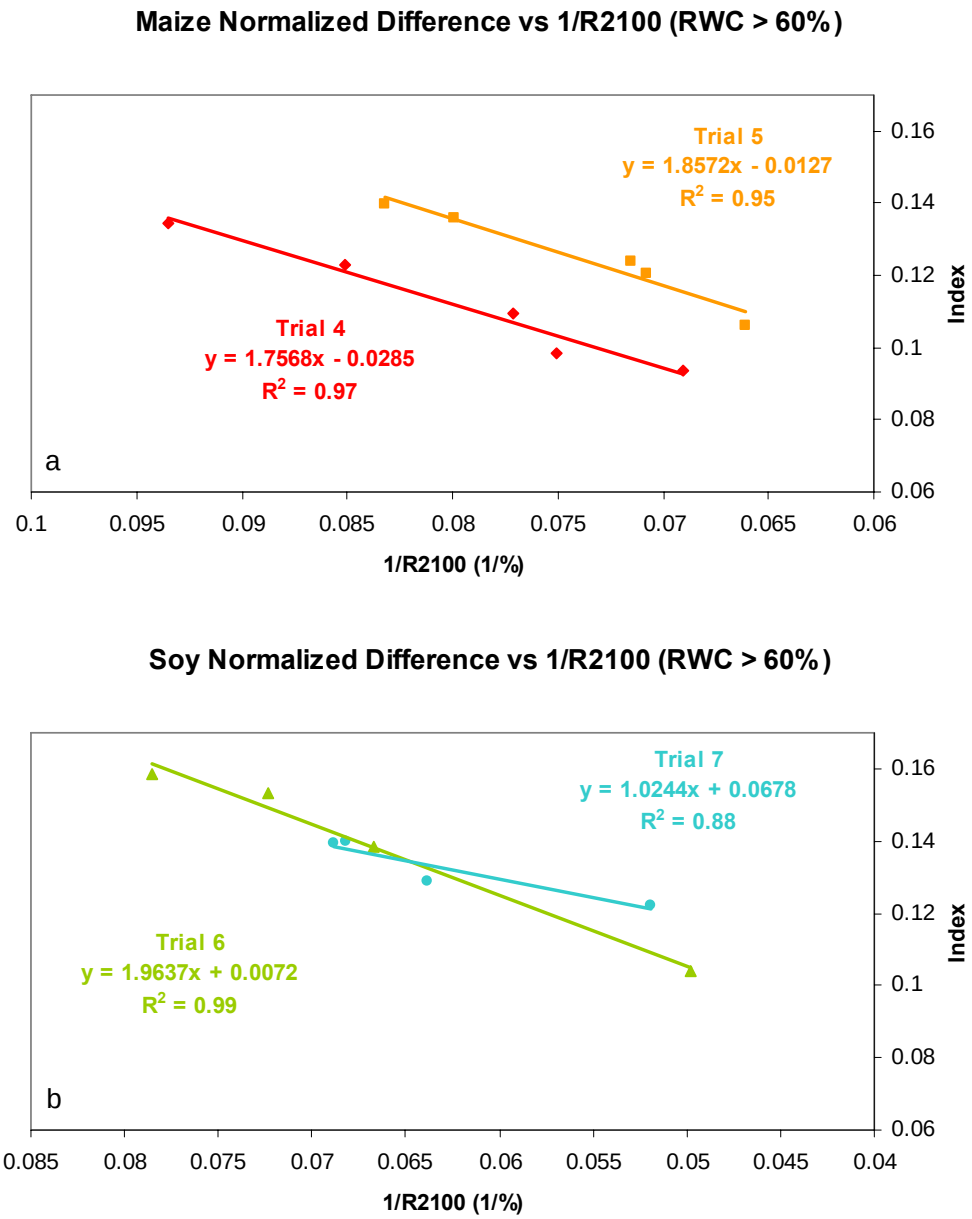

Figure 5-14. Comparison of example model to reciprocal reflectance at 2100 nm for RWC > 60%. Panel (a) shows the results for Trials 4 and 5. Panel (b) shows the results for Trials 6 and 7. Lines are linear best-fit.

5.3.2.3 Sensitivity of the model to Changes in Chlorophyll

Based on Figure 5-1, the first section of this chapter made the case that that PAR reflectance was observed to change in concert with changes in RWC and that there was no evidence of changes in reflectance due, for example, to changes in a pigment such as chlorophyll. In Chapter 3, it was shown that chlorophyll varied from about 400 mg/m^2 to 600 mg/m^2 during Trial 5 (Figure 3-18). To assure that the example model was not sensitive to changes in chlorophyll, a set of maize data, which included both hyperspectral and physical chlorophyll measurements, was obtained (Gitelson, 2009c). Applying the example model in Eq. 5.2 to the reflectance data in this data set, it was shown that as chlorophyll varied from 400 mg/m^2 to 600 mg/m^2, the index value changed by 0.001, or no more than 1% of the index values obtained in the previous section. The example model appears, therefore, insensitive to changes in chlorophyll.

5.4 Chapter Conclusions

The principal findings from the analysis presented in this chapter are as follows:

1. Reflectance in PAR and the water absorption bands in the MIR are strongly correlated.
2. In corn, a strong relationship exists between PAR albedo and RWC. In soy, sensitivity to relative water content is much lower when RWC > 70%.
3. A spectral model in the form of a normalized difference index was identified as an example for non-destructive estimation of RWC. Sensitivity of the model to RWC > 70% is considerably lower in soy than in corn probably due to different physiological mechanisms in each species for handling and reacting to water deficiency.

4. A previously unknown effect exists that changes the optical properties of leaves in concert with changes in water status. This effect is limited at moderate to high levels of water content in soy.

Chapter 6: Conclusions and Recommendations

6.0 Chapter Contents

6.1 Overview

The objectives of this chapter are to: 1) summarize research findings, innovations, and limitations, 2) suggest scientific implications and practical applications of the findings, 3) review how well this effort met the original research objectives, and 4) recommend future research.

A large body of data was collected in several greenhouse experiments. A new, and heretofore untested, experimental design was employed along with new software tools for data processing and analysis. This work resulted in findings not previously reported in the scientific literature. The findings have implications for future research in remote sensing and plant physiology as well as for the development of tools to estimate the water status of plants.

6.2 Major Findings

There has been considerable effort expended in attempting to remotely assess the water status of vegetation. Much of this work, as discussed in Chapter 1, involves measuring plant leaf reflectance in middle infrared wavelengths (MIR), which is logical because the MIR region of the spectrum contains strong water molecule absorption. The

amount of absorption is directly related to the number of molecules present. As discussed earlier, scientific literature over the past two decades has reported changes in photosynthetically active radiation (PAR) reflectance as well as in MIR reflectance when plants are subjected to water deficit. Except to attribute the effect to decreasing leaf turgor and pressure potential, no explanation or attention was applied to the phenomenon.

By using a large number of plants in controlled experiments conducted in a greenhouse, the present work established that PAR reflectance increases systematically with increasing water stress in maize and, when RWC is less than 70% in soy. Analysis of this observation identified the existence of quantitative relationships between RWC and both PAR reflectance and PAR albedo. These relationships were shown to be statistically reliable in maize as RWC ranged from near 100% to less than 50%. In soy, the relationship was statistically reliable only when RWC was below about 70%. Although PAR reflectance variation with RWC change has been reported in scientific papers for at least two decades, the research effort reported here appears to be the first to quantify the effect.

In concert with the above findings, examination of the reflectance spectra showed that reflectance in the visible range increases concomitantly with MIR reflectance as RWC decreases. The relationship is very strong, showing coefficients of determination between MIR reflectance and reflectance in blue and red better than 0.9 overall. Since RWC and MIR reflectance are closely correlated, this underscores the observation that PAR reflectance changes with a change in plant water status. The strong relationship is particularly intriguing because PAR reflectance and MIR reflectance are influenced by different plant constituents. PAR reflectance is the result of pigment absorption while

MIR reflectance is linked directly to the amount of water in the leaf. But, there is no pigment absorption in the MIR and there is no water molecule absorption in the PAR. Despite diligent literary searches, no reference to this effect has been found in the scientific literature. As of yet, no explanation based on a chemical or physical process has been identified.

In order to be useful in remote sensing, there must be a repeatable and accurate mathematical transform identified as a model to convert reflectance measurements to estimates of a biophysical parameter. For example, the well utilized Normalized Difference Vegetation Index (NDVI) provides an estimate of the health of vegetation at regional scales. NDVI is calculated using a normalized difference transform applied to reflectance in red and NIR to provide the index value. In the present work, a normalized difference index using two PAR spectral bands was developed and tested which closely relates PAR reflectance to RWC. Statistically significant correlations were found when the model was applied to maize, but not to soy when RWC was above 70%. This new index was developed as an example that such transforms exist. Until the physics, chemistry, and physiology behind the observed effect are established, practical application of this index cannot be recommended.

These four findings represent new knowledge and have the potential to influence not only procedures for remote sensing of stress conditions affecting terrestrial vegetation but also research in plant physiology itself. Before discussing the impact of this work, it is appropriate to review the intrinsic limitations that result from both the experimental design of the project and the environment within which the investigations occurred.

6.3 Limitations of Findings

The findings above must be considered within, and perhaps constrained by, the context of experiments that were conducted in the artificial environment of a greenhouse. The conditions were, by design, carefully controlled, and are therefore not necessarily representative of conditions in the field. For example total irradiance impinging upon the test and control plants was diminished by the glass roof of the building, and there was little air movement to encourage tissue growth in the plant stems. Additionally, the spacing of the plants in the greenhouse environment did not match the spacing of plants growing in a field setting. Thus, leaf shadowing, leaf orientation and possibly other light-climate phenomena were different than those found in large agricultural fields.

In sum, the findings reported here represent an initial stage of research. The effects discovered may not exist, or may be weaker or stronger, in plants growing in the field. Further research is required to corroborate the findings outside of the greenhouse setting.

6.4 Implications of Findings

Because the research effort was apparently the first to demonstrate a systematic relationship between PAR reflectance and water status in plants, there are no reference papers or text books available that explain the effect. Since it appears that the effect is manifested as a decrease in pigment absorption rather than an increase in light scattered, it is possible that the source of the effect lies within the chloroplasts themselves. In fact, it may lie within the thylakoids and/or grana, the chlorophyll bearing structures within the chloroplasts. In any case, the optics of the leaf appear to be changing with variations in

relative water content, and these changes lead to an increase in PAR reflectance with a moisture deficit.

The results also demonstrate that PAR reflectance responds differently to water stress in maize and soy. The reasons may be tied to these specific species, or, perhaps, to fundamental differences between C3 and C4 plants. It is interesting to speculate that changes internal to the leaf may modify leaf optics. The two plant types, as was shown in Chapters 3 and 4, have very different structures. For example, soy has less intricate bundle sheath cells compared to maize. It is also possible that the explanation is more subtle, and maybe more profound. Soy leaves track the sun daily and maize leaves do not. Soy and maize show different canopy level responses to water stress. The leaflets in each soy trifoliate will turn to shade each other if the plant is stressed. Maize leaves roll up with extreme stress. The maize mechanism is different than the stem movement in soy. Therefore, the PAR response in maize may result from some chemical protection mechanism required by a plant that is not as agile in adjusting the amount of leaf surface area exposed to light.

The findings are also interesting because they may influence the development of mathematical and software models of leaf spectra. One of the more popular models is called "Prospect" (Jacquemoud & Baret, 1990). Prospect generates a simulated leaf spectrum based on parameters such as pigment content, water content and leaf structure. If the water content parameter is changed in Prospect, there are expected changes in MIR and slight changes in NIR ranges. But, as the model exists today, there are no changes shown in PAR with water deficit. In other words, Prospect does not currently model the PAR reflectance changes due to variations in RWC.

The issue raised is important because Prospect and other models are used to generate sample spectra for comparison to real-world spectra. They may also be inverted to facilitate estimation of biophysical parameters based on real-world spectra. If the PAR reflectance effect is not included, Prospect and the other models may generate incorrect representations of actual spectra.

Along with research and mathematical modeling implications, it is possible that PAR reflectance is useful in the remote sensing of vegetation water status from canopy, aircraft, and satellite levels. However, it is difficult, at this stage of research, to know whether or not it is possible to remotely sense the discovered effect in canopies of maize or soy. Extension to canopy level and above requires that the physics, chemistry, or physiology causing the effect be understood to allow the response of a collection of leaves in a canopy to be reliably predicted and tested. It is also necessary to identify scattering and absorption processes (such as those involving non-leaf parts of plants and the ground) which may hide or distort the PAR reflectance effect. These must be filtered before reliable RWC estimation is to be possible. In addition, the weak nature of the effect may not be sufficient to allow remote sensing at a distance. Hence, extrapolation of sensors based on leaf-level transforms to canopy level, let alone airplane or satellite level, requires additional research.

6.5 Innovation

Several innovations were developed as a part of this research effort. These include the experimental design, a refined technique to physically measure RWC, and software used for data processing and analysis.

A new experimental design was developed to obtain daily reflectance data from plants and to determine their water status despite the destructive techniques used for RWC and water potential measurement. Ideally, to perform experiments such as those described, RWC, water potential, and radiometric measurements could be performed coincidently, on a daily or more frequent basis, on each of a number of plants. Such data could easily relate RWC and water status to reflectance spectra on the same leaves at the same time at frequent intervals over many days of an experiment. Unfortunately this is not possible because reliable RWC and water potential measurements currently involve a destructive process. To maintain a coherent reflectance record, the sampling design described in Chapter 2 utilizes a large number of plants. Several are used for daily reflectance measurements. A small number of the rest are sacrificed each day for destructive measurements. These measurements are then proxies for the water status of the remaining plants. In the design described here, 34 plants were sacrificed to provide RWC and water potential proxy measurements for the 16 plants used for daily reflectance measurements covering the entire experiment period.

In the past, the physical water content measurements were made using a whole leaf or leaf section that was wrapped in plastic or placed into a water-filled container to prevent the loss or gain of water from the atmosphere. It is difficult to assure a good seal if plastic is used and the water-filled container proved difficult because of the inadvertent loss of water during handling. A different technique was used in the experiments reported here. Discs were punched from the leaves of the sacrificed plants. These discs were sealed into vials in order to minimize loss or gain of water. The vials were easy to handle and small enough to be used in a field setting as well as in a greenhouse. The

technique produced reliable results and has now become a standard technique at this university.

The new methods and experimental design generated a significant amount of data. As many as 120 hyperspectral measurements were made each day for seven days. Software was written to process the daily data sets so that the data for any leaf could be followed through each day of the experiment. These programs also averaged the data and presented them in graphical form for analysis. The Index Analysis tool allowed the author to use the resulting processed data to quickly identify and test an example index for RWC estimation. The visualization component of the software provided a simple means to examine all combinations of wavelengths applied to a particular index. An optimum set of wavelengths could thereby be chosen. This avoided the sub-optimizations that can occur if incorrect initial conditions are selected when using an iterative algorithm.

6.6 Review of Original Objectives

The previous sections presented findings and innovations resulting from this research effort. The effort itself was based on one overall goal and two specific objectives enumerated as stated in Chapter 1. It is appropriate at this point to examine how well those objectives were met.

The overall goal was "…to study the optical properties of water-stressed and non-stressed maize and soy leaves using reflectance spectroscopy to establish the relationships among PAR, NIR, and MIR reflectance and water stress and to use those relationships as the basis for non-destructive retrieval of plant water status."

This goal was essentially met as reported in Chapter 5. Relationships among PAR, NIR, and MIR for maize and soy undergoing water stress were established. A model was identified to transform reflectance measurements into an estimate of RWC.

The two specific objectives will be discussed in turn.

1) Detect and quantify any systematic relationships between leaf-level PAR reflectance and water stress.

   The systematic increase in PAR reflectance with increasing water stress was detected and quantified in maize and for RWC less than 70% in soy, as described above.

2) Given the existence of such systematic relationships, use leaf-level PAR reflectance to develop techniques, in the form of spectral transformations, for accurately estimating plant water status.

   A spectral transform using PAR reflectance was identified, as an example, to estimate RWC. Coefficients of determination (R^2) between the resulting index and RWC were above 0.83 in maize and above 0.75 in soy for RWC greater than 60%. These numbers include the statistical variation due to the sampling error. If the index values are compared to a different RWC proxy, inverse reflectance at 2100 nm (within the same group of plants), R^2 values are near or above 0.9. There is evidence of very low sensitivity in soy when RWC is greater than 70%.

6.7 Recommendations for Future Research

Based on the results and limitations presented above, several key research questions can be raised as topics for future research. They are grouped into three subject areas: 1) understanding the underlying causes of the PAR reflectance change effect, 2) extending the work to canopy level, using close range, aircraft, and satellite remote sensing, and 3) developing better means of obtaining "ground-truth" data.

6.7.1 Underlying causes

Before this work can be reliably extended to differing environments and other vegetation species, it is necessary to understand what chemical, physical, physiological, or anatomical characteristics of plants cause PAR reflectance to change with water stress. Without such knowledge, measurements may be misinterpreted or important responses missed. Research to identify the underlying processes is vital.

One question that needs to be answered is whether the effect is caused by change in relative water content or change in water potential. Although the two are linked, the relationship is nonlinear and possibly distinguishable with respect to PAR reflectance. Knowing the answer to this question would influence the interpretation of measurements made by instruments using the PAR reflectance effect.

It is most interesting that PAR reflectance in soy and maize shows different response to stress. What distinguishes the anatomy or physiology of the two plants to cause such an effect? Is it a difference in mechanisms that attempt to protect the plant in case of stress? Or could it be a manifestation of the differing cellular arrangement and structure in the leaves of the two plants? It is very possible that the answer will give new

insight to understanding stress response in plants and the underlying physiology and anatomy involved.

Other issues must also be considered. For example, are there other aspects of plants, such as leaf surface characteristics or pigment distribution, that impact the level of response? Plant stress level is known to be a combination of the amount of light the leaves are exposed to and the water content in the leaves. Is this response a result of the current state of the plant or does it result from a particular pattern of change in the environment (humidity, temperature, light intensity, water deficiency etc.)? If so, the light climate inside the canopy could strongly influence the reflectance response seen from above the canopy.

It is rewarding that this research has raised so many questions.

6.7.2 Extending to canopy, aircraft, and satellite remote sensing

Understanding the cause of the water deficit induced PAR reflectance change may facilitate its use to detect and measure water stress from a canopy, aircraft, or satellite perspective. Several questions must first be answered. The most fundamental is whether there is sufficient strength of signal to allow detection at a distance (e.g., hundreds or thousands of meters). To answer this question, the signal must first be observed under field conditions, in a situation less ideal than that associated with a greenhouse.

Even given that sufficient signal strength is found, canopy observation is more challenging than near-leaf observation. Interfering signals may come from different parts of the plant, from the soil, or from other vegetation. Techniques to overcome such interference would be required before PAR reflectance can be used at other than near-leaf distances.

There may also be bidirectional reflectance effects that could prevent seeing the change in PAR reflectance under specific lighting conditions and leaf orientations. If the effect is caused by changes in leaf optics, it could very well be that the illumination and viewing angles will affect the strength of the signal.

The atmosphere is relatively more transparent in the visible optical region than in infrared. But there may be atmospheric absorption and scatter effects driven by water vapor concentration, particulates, or gases that would corrupt observation of the PAR reflectance effect. Significant interfering components need to be identified and filtered before aircraft or satellite observation using the effect is possible.

The utility of the findings in estimating vegetation water status awaits further research.

6.7.3 Obtaining ground-truth data

It must be noted that further research is dependent on the availability of physical water status measurements for comparison to radiometric measurements. The current state of technology requires that destructive tests are used to obtain these ground-truth data, i.e., large numbers of plants, and significant time and effort are required to compensate for the loss of plants. Creating or adapting non-destructive technologies for laboratory instruments based on, for example, microwave absorption or Raman scattering would minimize time, effort, and resources required. It would also improve reliability and accuracy. The result would be the opportunity for more accurate and more frequent measurements. This would raise the quality and reliability of research into plant water stress. Such an instrument would, by its nature, be expensive. However, its use in conducting research could speed the development of a multi-band spectral reflectance

instrument that would, by its nature, be inexpensive. Such an instrument would find ready application in both the laboratory and the field.

6.8 Final Remarks

The results from this research have potential to improve understanding of plant physiology, leaf optics, and plant chemistry as well as to provide new techniques to nondestructively and remotely assess the water status of vegetation. It has been a rewarding effort from the standpoint of the outcomes obtained, and even more so, because the work resulted in questions that will require new research to answer.

The true value and utility of what was presented here cannot be assessed from the current vantage. The author is appreciative, however, for the chance to perform cutting-edge research with supportive professors and colleagues in an environment that encouraged good science and good understanding.

References

Aldakheel, Y.Y. and F.M. Danson, 1997. Spectral reflectance of dehydrating leaves: measurements and modeling. *Int. J. Remote Sensing*, 18: 3683-3690.

Acevedo, E., E. Fereres, T.C. Hsiao, and D.W. Henderson, 1979. Diurnal growth trends, water potential, and osmotic adjustment of maize and sorghum leaves in the field. *Plant Physiol,* 64: 476-480.

Barrs, H.D., 1968. Determination of water deficits in plant tissues. in: T.T. Kozlowski, ed., *Water Deficits and Plant Growth, Vol. 1*, pp 235-368, Academic Press, New York.

Björkman, O., and S.B. Powles, 1984. Inhibition of photosynthetic reactions under water stress: interaction with light level. *Planta,* 161: 490-504.

Boyer, J.S., 1995. Measuring the water status of plants and soils. Academic Press, Inc., http://dspace.udel.edu:8080/dspace/handle/19716/2828.

Carter, G.A., 1991. Primary and secondary effects of water content on the spectral reflectance of leaves. *American Journal of Botany*, 78: 916-924.

Carter, A.C., 1993. Responses of leaf spectral reflectance to plant stress. *American Journal of Botany,* 80(3): 239-243.

Ceccato, P., S. Flasse, S. Tarantola, S. Jacquemoud, and J. Gregoire, 2001. Detecting vegetation leaf water content using reflectance in the optical domain. *Remote Sens. Environ.,* 77: 22-33.

Ciganda, V., A. Gitelson, and J. Schepers, 2008. Non-destructive determination of maize leaf and canopy chlorophyll content, *Journal of Plant Physiology*, 166: 157-167.

Claudio, H.C., Y. Cheng, D.A. Fuentes, J.A. Gamon, H. Luo, W. Oechel, H. Qiu, A.F. Rahman, and D.A. Sims, 2005. Monitoring drought effects on vegetation water content and fluxes in chaparral with 970 nm water band index. *Remote Sensing of Environment*, 103: 304-311.

Dekker, S.C., M. Rietkerk, and M.F.P. Bierkens, 2007. Coupling microscale vegetation – soil water and macroscale vegetation – precipitation feedbacks in semiarid ecosystems. *Global Change Biology*, 13: 671-678.

Diaz-Perez, J.C., K.A. Shackel, and E.G. Sutter, 1995. Relative water content and water potential of tissue-cultured apple shoots under water deficits. *Journal of Experimental Botany*, 46: 111-118.

Gamon, J.A., C.B. Field, D.A. Roberts, S.L. Ustin, and R. Valentini, 1993. Functional patterns in an annual grassland during an AVIRIS overflight. Remote Sens. Environ., 44: 239-253.

Gamon, J. A., J. Penuelas, and C. B. Field, 1992. A narrow waveband spectral index that tracks diurnal changes in photosynthetic efficiency. *Remote Sens. Environ*., 4: 35–44.

Gates, D.M., H.J. Keegan, J.C. Schleter, V.R. Weidner, 1965. Spectral Properties of Plants. *Applied Optics*, 4: 11-20.

Gitelson, A.A., Y. Gritz, and M.N. Merzlyak, 2003. Relationships between leaf chlorophyll content and spectral reflectance and algorithms for non-destructive chlorophyll assessment in higher plant leaves. *J. Plant Physiol.,* 160: 271-282.

Gitelson A., and M.N. Merzlyak, 1996. Signature analysis of leaf reflectance spectra: algorithm development for remote sensing of chlorophyll. *J. Plant Physiol.,* 148: 494-500.

Gitelson, A.A., 2009a. Personal communication, June 16, 2009.

Gitelson, A.A., 2009b. Personal communication, July 24, 2009.

Gitelson, A.A., 2009c. Personal communication, November 11, 2009.

Hsiao, T.C., 1973. Plant Responses to Water Stress. *Ann Rev. Plant Physiol*, 24: 519-70.

Hunt, E.R. and B.N. Rock, 1989. Detection of changes in leaf water content using near- and middle-infrared reflectances. *Remote Sens. Environ*, 30: 43-54.

Jacquemoud, S. and F. Baret, 1990. PROSPECT: a model of leaf optical properties spectra. *Remote Sensing of Environment*, 34: 75-91.

Jacquemoud, S. and S.L. Ustin, 2001. Leaf optical properties: a state of the art. *Proc. 8th International Symposium Physical Measurements & Signatures in Remote Sensing*, Aussois (France), pp. 223-232.

Jensen, J.R., 2007. *Remote Sensing of the Environment: An Earth Resource Perspective,* 2nd Ed., Prentice Hall, Upper Saddle River, NJ.

Jones, H.G., 2006. Monitoring plant and soil water status: established and novel methods revisited and their relevance to studies of drought tolerance. *Journal of Experimental Botany*, 58: 119–130.

Jones, H.G., M. Stoll, T. Santos, C. de Sousa, M.M. Chaves and O.M. Grant, 2002. Use of infrared thermography for monitoring stomatal closure in the field: application to grapevine. *Journal of Experimental Botany*, 53: 2249-2260.

Jones, M.M., and N. Turner, 1978. Osmotic Adjustment in Leaves of Sorghum in Response to Water Deficits. *Plant Physiol*., 61: 122-126.

Kasahara, M., T. Kagawa, K. Oikawa, N. Suetsugu, M. Miyao, and M. Wada, 2002. Chloroplast avoidance movement reduces photodamage in plants. *Nature* 420: 829-832.

Kaufmann, M.R., 1976. Stomatal Response of Engelmann Spruce to Humidity, Light, and Water Stress. *Plant Physiol.*, 57: 898-901.

Kuester, M., K. Thome, K. Rause, K. Canham, and E. Whittington, 2001. Comparison of surface reflectance measurements from three ASD FieldSpec FR spectroradiometers and one ASD FieldSpec VNIR spectroradiometer. *Geoscience and Remote Sensing Symposium, 2001, Sydney, Australia. IGARSS '01. IEEE 2001 International*, Volume 1, pp. 72–74.

Lichtenthaler, H. K., 1987. Chlorophylls and carotenoids: pigments of photosynthetic biomembranes. *Methods in Enzymology,* 148: 350–382.

Long, S.P., S. Humphries, and P.G. Falkowski, 1994. Photoinhibition of photosynthesis in nature. *Annu. Rev. Plant Physiol. Plant Mol. Biol.,* 45: 633-62.

Maxwell, K. and N.J. Giles, 2000. Chlorophyll fluorescence – a practical guide. *Journal of Experimental Botany*, 51: 659-668.

McDonald, M.S., 2003. *Photobiology of Higher Plants*, Wiley and Sons, Chichester (United Kingdom).

Milburn, J.A., 1979. *Water Flow in Plants*, Longman Group Ltd., New York.

Morgan, J.M., 1984. Osmoregulation and water stress in higher plants. *Ann. Rev. Plant Physiol.*, 35:299-319.

Munns, R., J. B. Passioura, J. Guo, O. Chazen, and G.R. Cramer, 2000. Water Relations and leaf expansion: importance of time scale. *Journal of Experimental Botany*, 51: 1495-1504.

Nobel, P.S., 1983. *Biophysical Plant Physiology and Ecology*, W.H. Freeman and Company, San Francisco .

Pederson, P., 2004. *Soybean Growth and Development*, University Extension PM1945, Iowa State University, Ames, IA.

Porra, R. J., W.A. Thompson, and P.E. Kriedemann, 1989. Determination of accurate extinction coefficients and simultaneous equations for assaying chlorophylls a and b extracted with four different solvents: Verification of the concentration of chlorophyll standards by atomic absorption spectroscopy. *Biochimica et Biophysica Acta,* 975: 384-394.

Ristic, Z. and D.D. Cass, 1992. Chloroplast structure after water and high-temperature stress in two lines of maize that differ in endogenous levels of abscisic acid. *Int. J. Plant Sci.,* 153(2): 186-196.

Ritchie, S.W., J.J. Hanway, and G.O. Benson, 1997. *How a Corn Plant Develops*, Iowa State University of Science and Technology Cooperative Extension Service, Special Report No. 48., Iowa State University, Ames, IA.

Serrano, L., S.L. Ustin, D.A. Roberts, J.A. Gamon, and J. Peñuelas, 2000. Deriving Water Content of Chaparral Vegetation from AVIRIS Data. *Remote Sens. Environ*., 74: 570–581.

Taiz, L., and E. Zeiger, 2006a. *Plant Physiology*, Fourth Edition, Sinauer Associates, Sunderland, MA.

Taiz, L., and E. Zeiger, 2006b. Measuring Water Potential, *Plant Physiology*, Fourth Edition, Companion Website Topic 3.6, http://www.plantphys.net, Sinauer Associates, Sunderland, MA.

Thenot, F., M. Methy, and T. Winkel, 2002. The Photochemical Reflectance Index (PRI) as a water-stress index. *Int. J. Remote Sensing*, 32: 5135-5139.

Utrillas, M.J. and L. Alegre, 1997. Impact of water stress on leaf anatomy and ultrastructure in *Cynodon dactylon* (L.) Pers. under natural conditions. *Int. J. Plant Sci.,* 158(3): 313-324.

Weatherley, P.E., 1966. A porometer for use in the field, *New Phytologist*, 65: 376-387.

Woolley, J.T., 1971. Reflectance and Transmittance of Light by Leaves. *Plant Physiol*., (1971) 47: 656-662.

World Economic Forum (2008), *Managing our Future Water Needs for Agriculture, Industry, Human Health and the Environment, Discussion Document for the World Economic Forum Annual Meeting 2008*, Geneva, Switzerland.

Yu, G-R., T. Miwa, K. Nakayama, N. Matsuoka and H. Kon, 2000. A proposal for universal formulas for estimating leaf water status of herbaceous and woody plants based on spectral reflectance properties. *Plant and Soil,* 227: 47–58.

Zygielbaum, A.I., A.A. Gitelson, T.J. Arkebauer, and D.C. Rundquist, 2009. Non-destructive detection of water stress and estimation of relative water content in maize. *Geophysical Research Letters*, Vol. 36, L12403, doi: 10.1029/2009GL038906.

Appendix A: Supplementary Figures and Tables

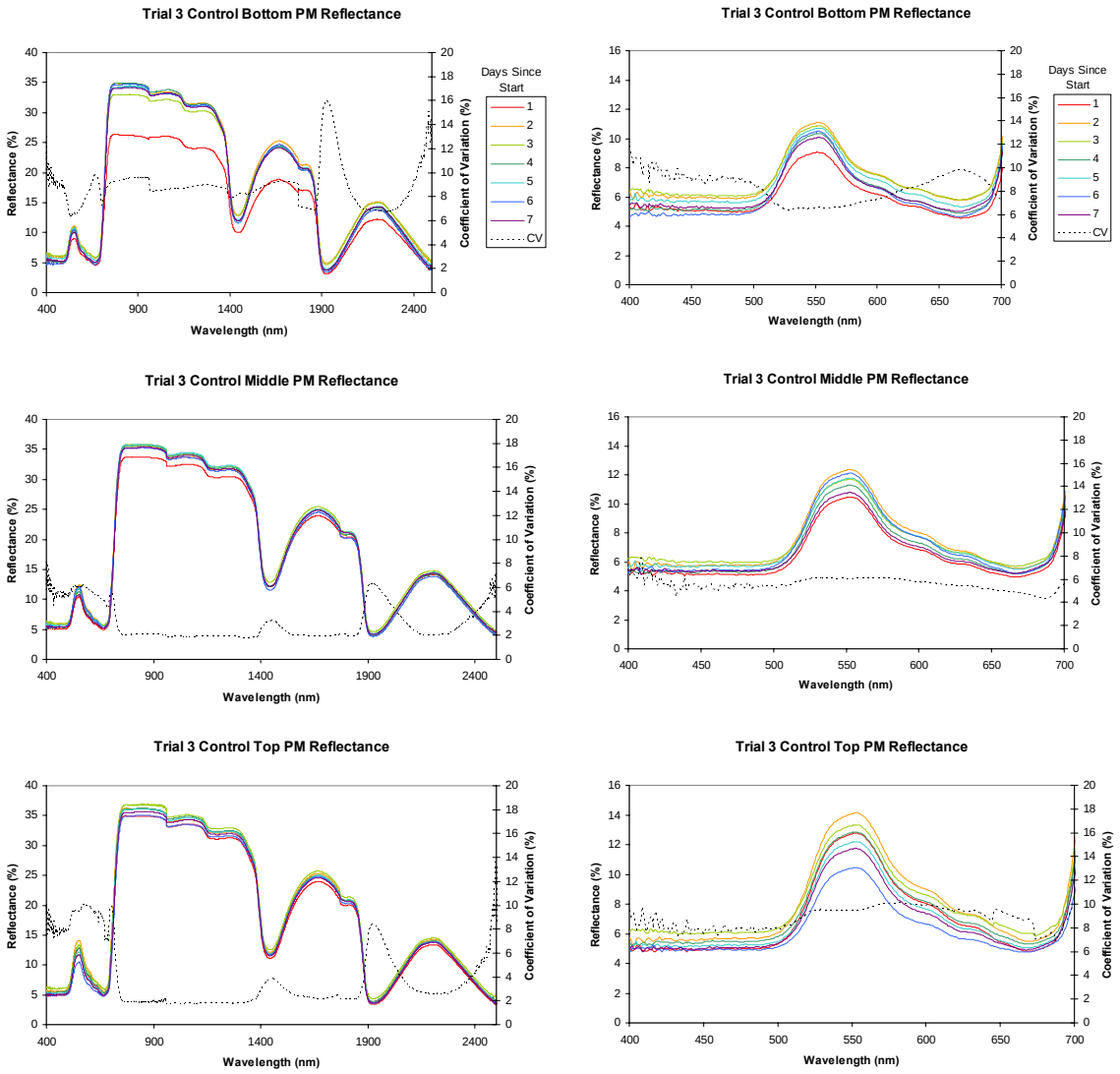

Figure A-1. Trial 3 daily control leaf average reflectance spectra. Panels on the left show the full spectrum. Panels on the right show only the PAR spectrum. The panels in each column contain the bottom, middle, and top leaf spectra, respectively.

Trial 4 Control Plants		Day 1	2	3	4	5	6
Top	Max	97.27626	99.39966	97.95918	95.47135	94.40267	96.74419
	Min	96.97266	98.07187	95.28746	92.56435	93.40055	94.78338
	Average	97.12446	98.73576	96.62332	94.01785	93.90161	95.76378
	Difference	0.303608	1.32779	2.671719	2.907002	1.002123	1.960809
Middle	Max	97.2167	99.68153	95.36946	100.5935	94.97041	97.43346
	Min	94.95718	97.45348	94.61078	93.83886	94.70135	97.17411
	Average	96.08694	98.5675	94.99012	97.21617	94.83588	97.30379
	Difference	2.259516	2.228052	0.75868	6.754609	0.269065	0.259349
Bottom	Max	95.98326	98.90311	92.67399	98.9071	96.53979	97.37274
	Min	86.03448	89.5288	85.22427	93.45392	92.87926	92.23301
	Average	91.00887	94.21595	88.94913	96.18051	94.70952	94.80288
	Difference	9.948781	9.374312	7.449718	5.453185	3.660535	5.139732

Table A-1. Trial 4 Control Leaf Relative Water Content

Trial 4 Test Plants		Day 1	2	3	4	5	6
Top	Max	94.39853	83.17266	76.53142	67.98354	59.80392	56.02504
	Min	92.99242	77.10168	66.33416	56.88817	59.1224	48.60197
	Average	93.69548	80.13717	71.43279	62.43585	59.46316	52.31351
	Difference	1.406107	6.070974	10.19726	11.09537	0.68152	7.423065
Middle	Max	94.87427	84.62214	74.66555	72.59149	63.76186	54.14552
	Min	94.28571	81.20438	73.28708	58.94454	63.29234	49.95844
	Average	94.57999	82.91326	73.97631	65.76802	63.5271	52.05198
	Difference	0.58856	3.417765	1.378475	13.64694	0.469527	4.187079
Bottom	Max	91.71875	81.67539	76.295	72.25296	54.64567	42.45211
	Min	90.6383	80.86304	63.0898	50.95541	51.34731	26.91057
	Average	91.17852	81.26922	69.6924	61.60419	52.99649	34.68134
	Difference	1.080452	0.812353	13.20519	21.29755	3.298364	15.54154

Table A-2. Trial 4 Test Leaf Relative Water Content

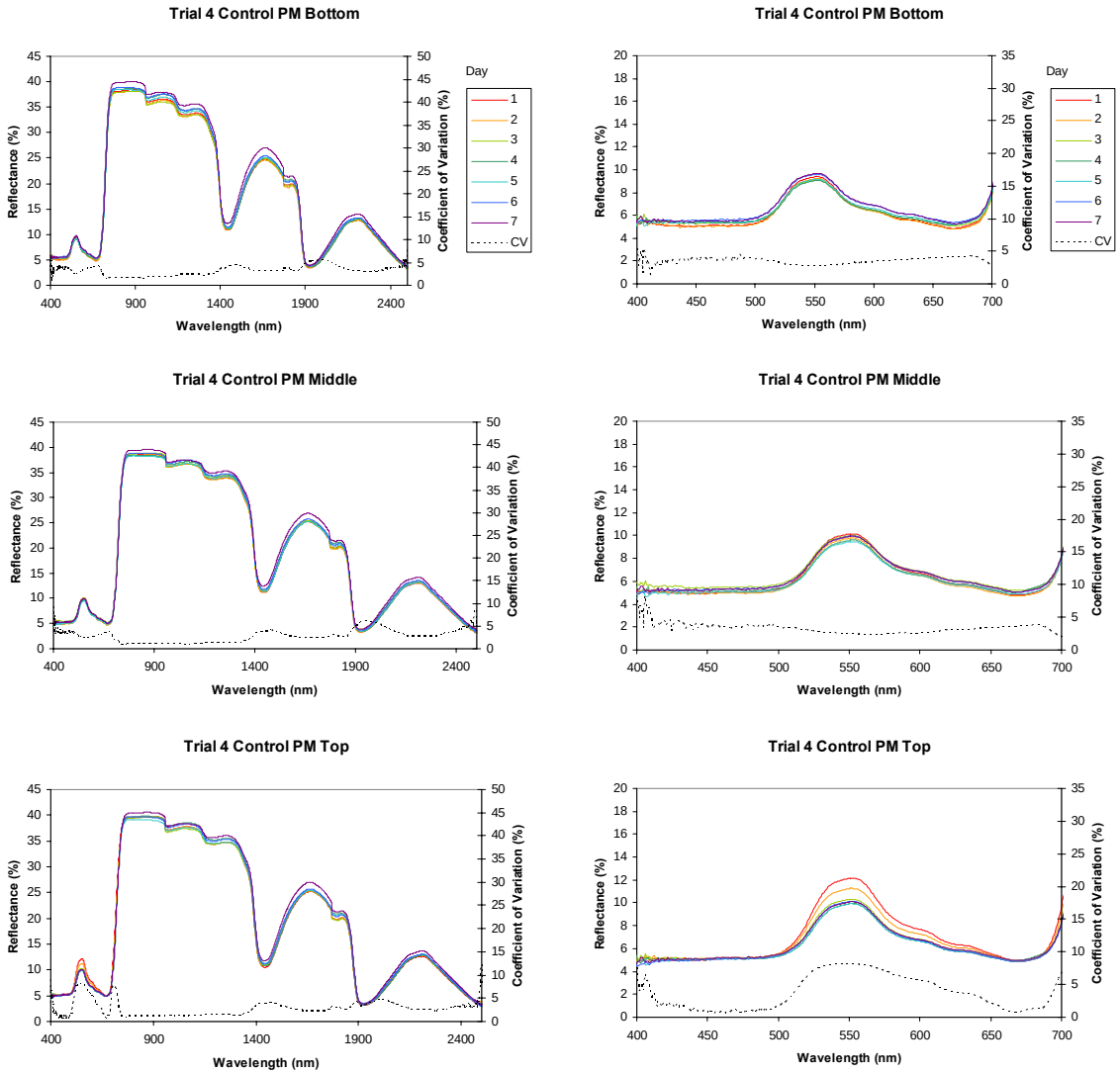

Figure A-2. Trial 4 daily control leaf average reflectance spectra. Panels on the left show the full spectrum. Panels on the right show only the PAR spectrum. The panels in each column contain the bottom, middle, and top leaf spectra, respectively.

Trial 5 Control Plants		Day						
		1	2	3	4	5	6	7
Top	Max	96.9419	97.28601	98.74638	97.75281	101.9007	98.19149	97.95427
	Min	96.68803	94.84083	98.62434	96.07635	101.8626	95.82339	97.1831
	Average	96.81497	96.06342	98.68536	96.91458	101.8817	97.00744	97.56869
	Difference	0.253862	2.445178	0.122045	1.676457	0.038108	2.3681	0.771173
Middle	Max	94.71503	99.47753	100.5107	100.7946		98.46491	97.25209
	Min	94.68439	97.41468	100.5107	94.87179		97.2619	95.95051
	Average	94.69971	98.44611	100.5107	97.83317		97.86341	96.6013
	Difference	0.030641	2.062849	0	5.922757	0	1.203008	1.301585
Bottom	Max	95.53191	98.55247	100.4566	100.5875	101.5432	97.49702	99.52996
	Min	95	96.14112	96.36929	90.10638	101.2917	95.67901	98.37297
	Average	95.26596	97.3468	98.41296	95.34696	101.4175	96.58802	98.95147
	Difference	0.531915	2.411348	4.087326	10.48116	0.251498	1.818008	1.156999

Table A-3. Trial 5 Control Leaf Relative Water Content

Trial 5 Test Plants		Day						
		1	2	3	4	5	6	7
Top	Max	96.66667	96.99666	82.34043	79.97763	70.33639	66.05081	62.7409
	Min	96.66667	96.99666	78.4141	78.77508	67.9368	63.31828	54.69388
	Average	96.66667	96.99666	80.37726	79.37635	69.1366	64.68455	58.71739
	Difference	0	0	3.926329	1.202549	2.399588	2.732524	8.047022
Middle	Max	98.79518	98.78935	79.80022	79.51669	70.33639	63.36516	57.63052
	Min	98.79518	98.78935	79.03044	72.64325	67.9368	63.21608	55.78947
	Average	98.79518	98.78935	79.41533	76.07997	69.1366	63.29062	56.71
	Difference	0	0	0.769782	6.873433	2.399588	0.149075	1.841048
Bottom	Max			77.42279	70.24793	60	54.67626	52.39107
	Min			77.24551	68.45238	57.94669	54.19933	49.43123
	Average			77.33415	69.35016	58.97335	54.43779	50.91115
	Difference			0.177281	1.795553	2.053307	0.476931	2.959843

Table A-4. Trial 5 Test Leaf Relative Water Content

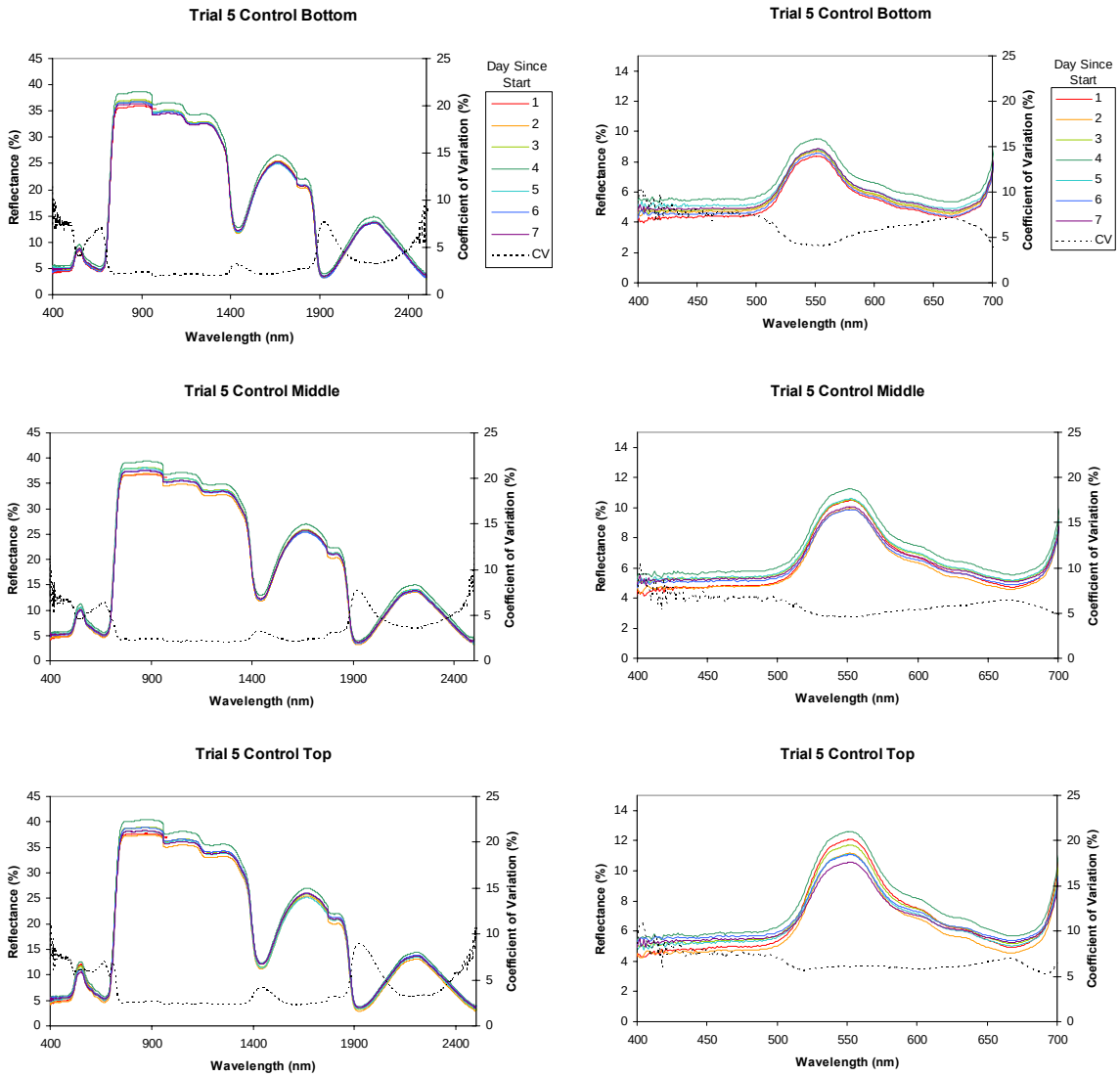

Figure A-3. Trial 5 daily control leaf average reflectance spectra. Panels on the left show the full spectrum. Panels on the right show only the PAR spectrum. The top three panels in each column contain the bottom, middle, and top leaf spectra, respectively.

Trial 6 Control	Day				
	1	2	3	4	5
Max	89.08228	97.97101	93.98601	91.05866	90.07937
Min	88.84326	96.75793	92.5116	90.14276	86.73863
Average	88.96277	97.36447	93.24881	90.60071	88.409
Difference	0.23902	1.213089	1.474417	0.915895	3.340737

Table A-5. Trial 6 Control Leaf Relative Water Content.

Trial 6 Test	Day 1	2	3	4	5
Max	94.02046	97.32342	89.12387	77.54777	67.85206
Min	91.37168	94.2029	67.89555	68.4368	64.55285
Average	92.69607	95.76316	78.50971	72.99228	66.20245
Difference	2.648775	3.120522	21.22832	9.110972	3.299217

Table A-6. Trial 6 Test Leaf Relative Water Content.

Trial 7	Days Without Water 1	2	3	4	5
Max	87.53709199	84.11927878	69.9602122	66.87898089	44.42934783
Min	80.14134276	79.25278219	67.07566462	53.21154979	39.78300181
Average	85.2532627	81.68603049	68.51793841	60.04526534	42.10617482
Difference	7.395749232	4.866496586	2.88454758	13.6674311	4.646346018

Table A-7. Trial 7 Leaf Relative Water Content

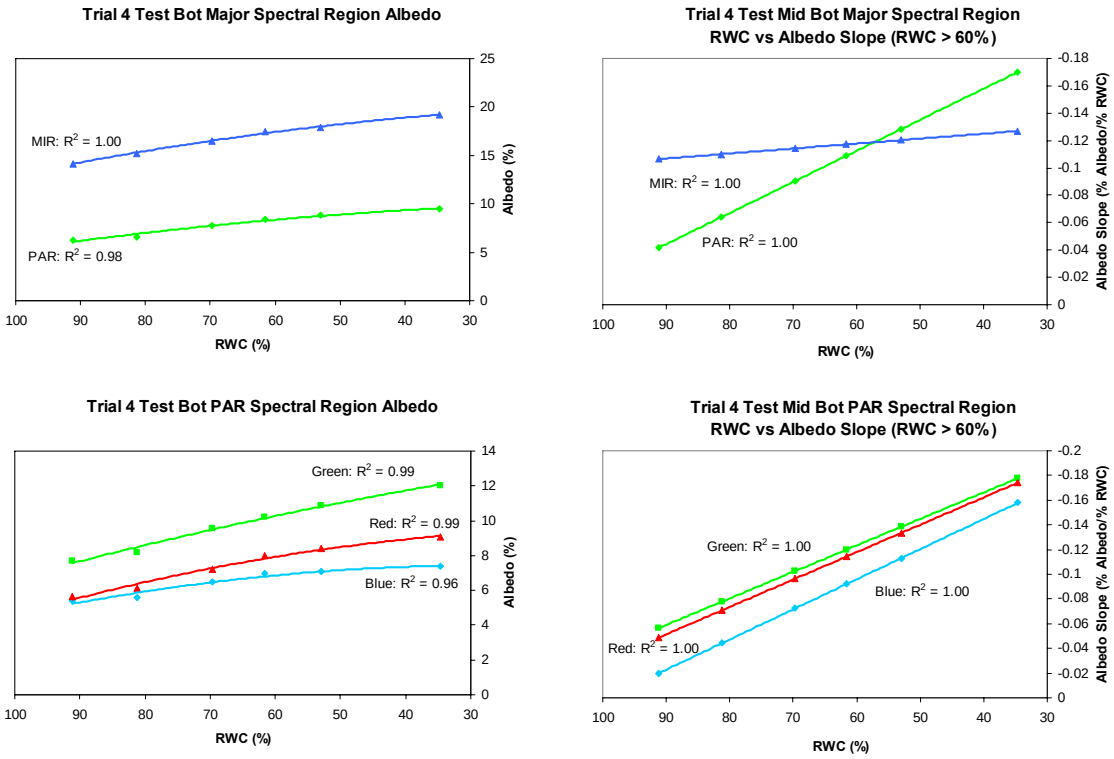

Figure A-4. Trial 4 bottom leaf albedo versus RWC. Panels on left show albedo versus RWC. Lines are quadratic best-fits to the points. Panels on right show the first derivatives of the best-fit lines versus RWC. Albedos for major spectral regions are plotted in the upper panels. Albedos for PAR region are plotted in the lower panels.

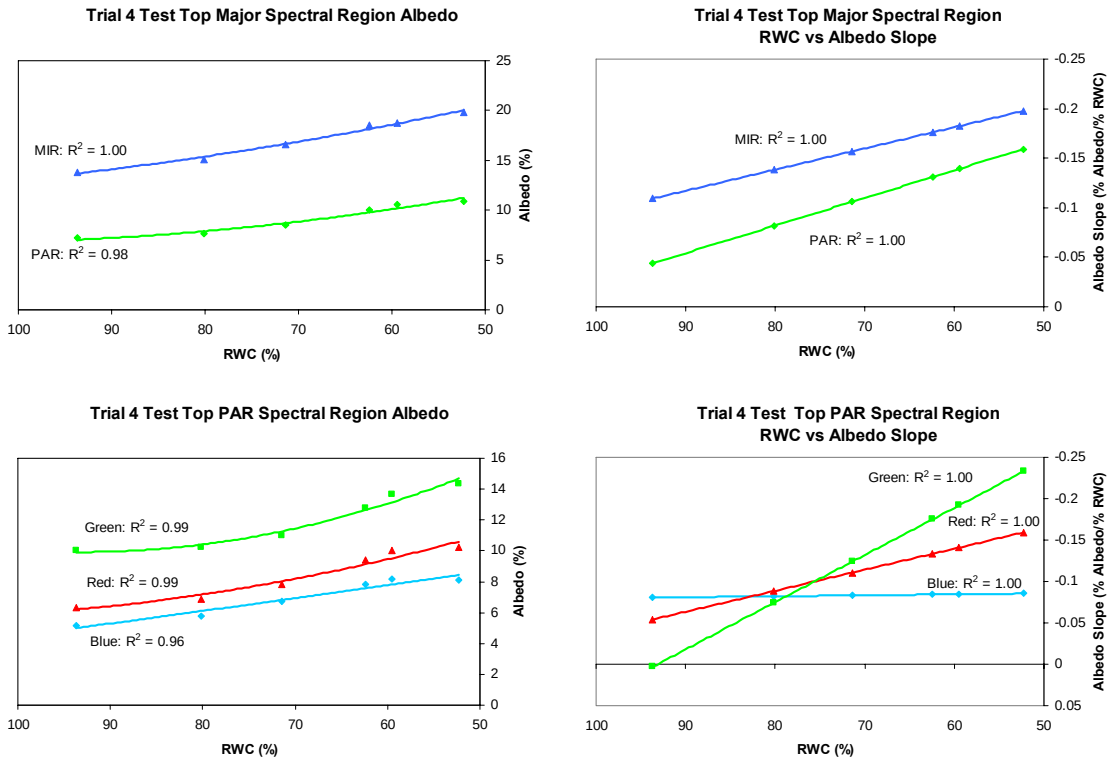

Figure A-5. Trial 4 top leaf albedo versus RWC. Panels on left show albedo versus RWC. Lines are quadratic best-fits to the points. Panels on right show the first derivatives of the best-fit lines versus RWC. Albedos for major spectral regions are plotted in the upper panels. Albedos for PAR region are plotted in the lower panels.

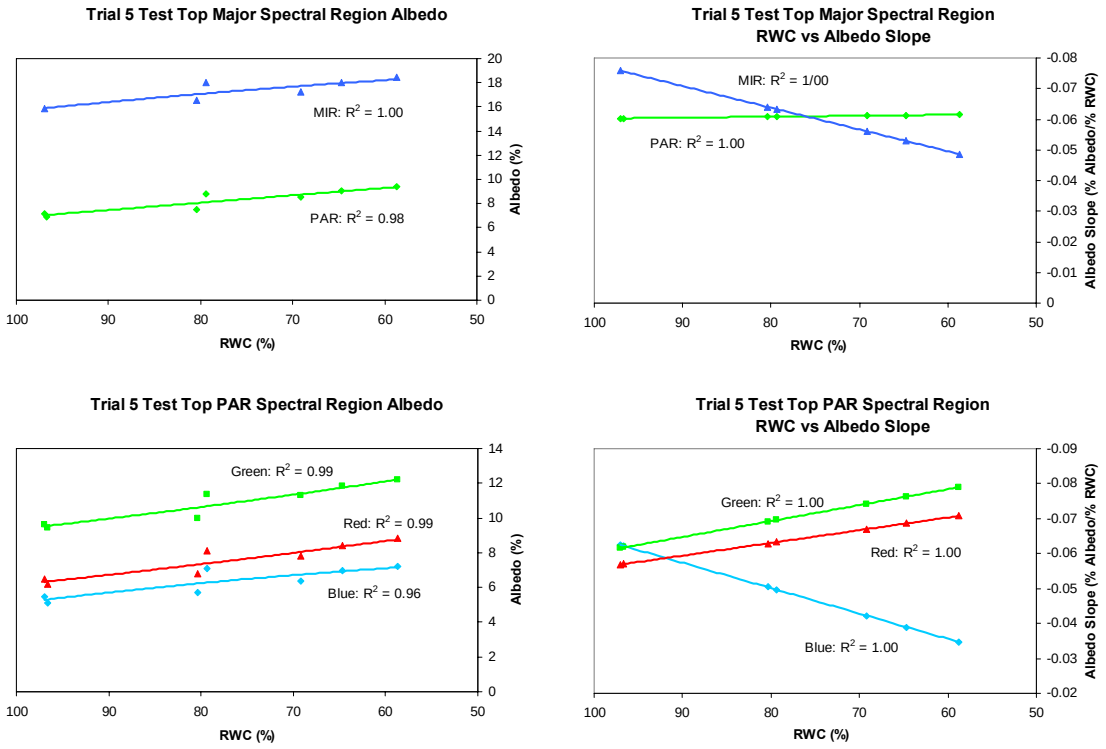

Figure A-6. Trial 5 top leaf albedo versus RWC. Panels on left show albedo versus RWC. Lines are quadratic best-fits to the points. Panels on right show the first derivatives of the best-fit lines versus RWC. Albedos for major spectral regions are plotted in the upper panels. Albedos for PAR region are plotted in the lower panels. The decreasing magnitude of the slopes in blue and MIR appears to be related to increased reflectance seen on day four of the experiment (corresponding to RWC=79.4%, for all albedos measurements. The cause is not yet known.